UCRL-11986

University of California

Ernest O. Lawrence Radiation Laboratory

THE KINETICS OF THE CHLORINATION OF UCl_4 BY Cl_2

TWO-WEEK LOAN COPY

This is a Library Circulating Copy which may be borrowed for two weeks. For a personal retention copy, call Tech. Info. Division, Ext. 5545

Berkeley, California

DISCLAIMER

This document was prepared as an account of work sponsored by the United States Government. While this document is believed to contain correct information, neither the United States Government nor any agency thereof, nor the Regents of the University of California, nor any of their employees, makes any warranty, express or implied, or assumes any legal responsibility for the accuracy, completeness, or usefulness of any information, apparatus, product, or process disclosed, or represents that its use would not infringe privately owned rights. Reference herein to any specific commercial product, process, or service by its trade name, trademark, manufacturer, or otherwise, does not necessarily constitute or imply its endorsement, recommendation, or favoring by the United States Government or any agency thereof, or the Regents of the University of California. The views and opinions of authors expressed herein do not necessarily state or reflect those of the United States Government or any agency thereof or the Regents of the University of California.

UCRL-11986

UNIVERSITY OF CALIFORNIA

Lawrence Radiation Laboratory
Berkeley, California

AEC Contract No. W-7405-eng-48

THE KINETICS OF THE CHLORINATION OF UCl_4 BY Cl_2

José Luis Camahort
(Ph.D. Thesis)

20 May 1965

Contents

Abstract v

I. INTRODUCTION 1

II. FUSED SALTS 7

A. Structure of Fused Salts 7

1. Structure of Molten Alkali Halides 8

2. Interaction in Molten Alkali Halides 12

B. Diffusion in Fused Salts 14

III. THEORY OF THE HYDRODYNAMICS AND DIFFUSION IN FILM FLOW DOWN A ROD 20

A. Simultaneous Diffusion and Chemical Reaction 20

B. Gas Phase 22

1. Hydrodynamics 22

2. Diffusion in the Gas Phase 27

C. The Liquid Phase 31

1. Hydrodynamics 31

2. Hydrodynamic Stability at Low Reynolds Number 36

3. Diffusion in Liquid Film 38

D. Comparison of Gas and Liquid Phase Resistances 47

IV. EXPERIMENTAL WORK 49

A. Handling of Fused LiCl-KCl Eutectic 49

B. Solubility Studies 50

1. Previous Work 50

2. Solubility of Cl_2 in Fused LiCl-KCl Eutectic 51

C. Absorption of CO_2 in Water 57

D. The Chlorination of UCl_4 61

V. DISCUSSION OF RESULTS 87

VI. CONCLUSIONS 90

Acknowledgments 91

Appendices 92

A. Physical Properties of Fused LiCl-KCl Eutectic 92

B. Chemistry of Uranium Chlorides 95

C. Chemical Reactions and Equilibria of Analytical Methods 105

References 107

Figure Captions 111

THE KINETICS OF THE CHLORINATION OF UCl_4 BY Cl_2

José Luis Camahort

Inorganic Materials Research Division
Lawrence Radiation Laboratory
University of California
Berkeley, California

20 May 1965

ABSTRACT

The kinetics of the chlorination by Cl_2 gas of UCl_4 dissolved in the LiCl-KCl eutectic melt was studied. The objective of the study was the determination of the mechanism of the overall process, i.e. the location of the reaction zone, the type of reaction (reversible or irreversible) and its order with respect to each reactant, the effect of the gas and liquid phase resistances, the relative importance of the diffusion and chemical reaction steps, and the disposition of the reaction products.

The solubility of Cl_2 gas in the uranium-free salt was measured with the same technique used at Oak Ridge for the solubilities of gases in molten fluorides. The results showed that Cl_2 is essentially insoluble in the LiCl-KCl melt. Henry's Law constants at 400 and 500°C are less than 4×10^{-9} moles/(cm^3) (atm).

The equilibrium of the reaction $UCl_4(\ell) + Cl_2(g) = UCl_6(\ell)$ in the fused salt was studied by sparging a 2 wt.% UCl_4 solution with pure Cl_2 gas at 400-600°C. The reaction was found to be reversible and endothermic, with a heat of reaction of 5.4 kcal/mole.

The kinetics of the reaction was investigated using a wetted-rod apparatus at 400-700°C. The performance of the set-up was tested with

preliminary runs using the well-known CO_2-water system. Theoretical and experimental results show that the chlorination reaction is essentially a liquid phase process, with diffusion-chemical equilibrium control. The experimental rates at 400 and 450°C are greater than the predicted values for an infinitely fast reaction, but at the higher temperatures ($\geq$ 500°C) the experimental values become less than the theoretical predictions. This uncommon behavior tends to rule out any reaction rate control of the overall process. It may be caused by an unknown interfacial resistance, a much lower diffusivity of UCl_6 than UCl_4 in the salt or a sudden shift in the equilibrium during the sample collection. The latter two seem to be more plausible.

I. INTRODUCTION

High temperature non-aqueous reprocessing of nuclear fuels has received considerable attention in recent years.[19,58,61] Development work at Argonne, Brookhaven, Oak Ridge, Batelle, Atomics International, and Iowa State College points to the possibility that such processes will eventually compete with, if not supplant the now standard aqueous methods.

One of the main incentives for the use of high temperature reprocessing in decontaminating spent nuclear fuels is the significant reduction in the number of steps involved. Other major advantages are the considera le decrease in the volume of material handled and the elimination of criticallity problems during processing due to the absence of low molecular weight moderating materials. Lower decontaminating factors, severe corrosion problems in handling uranium and salts as liquids, and little technological background are disadvantages of high temperature reprocessing.

Volatility processing[14,25,55,29] is a promising non-aqueous method which yields high decontamination factors for the recovery of uranium from irradiated reactor fuel . These separation processes depend upon differences in volatility of the appropriate halides. Processes utilizing the fluoride, chloride, and iodide systems have been seriously considered. Of these three, the fluoride system is in the most advanced state of development.

The various processes in which a gas phase and a constituent of a molten salt or liquid metal phase react at the interphase can be classified into three types, depending upon the nature of the reaction product:

(a) Gaseous reaction product. The best known example of this type is the fluorination of UF_4 in ZrF_4-LiF fused salt mixtures, using fluorine gas to produce gaseous UF_6. In this example, not all of the gaseous product need appear in the gas phase since UF_6 is appreciably soluble in the fluoride melt. Another example, of no commercial value, but which is of interest because it involves a liquid metal instead of a molten salt, is the chlorination of Gadolinium by gaseous Cl_2 to produce the volatile trichloride. This reaction product is quantitatively released to the gas phase.

(b) Non-volatile reaction product insoluble in the liquid phase. Typical examples in this class are the hydrogenation of molten Th-U alloys to produce the insoluble solid hydride of thorium, and the precipitation of UO_2 from a fused fluoride salt by reaction with steam. The non-volatile, insoluble reaction products form a third phase at the interphase, or are dispersed in the liquid.

(c) Non-volatile reaction product soluble in the liquid phase. An example in this category is the fluorination of ZrF_2 in an inert solvent (e.g. NaF-LiF eutectic) to produce ZrF_4. There appears to be no commercially useful example of this type of gas-molten salt reaction.

In each of these cases, the overall process involves the combination of diffusional transport of the reactants to the phase boundary, chemical reaction, and the removal of the reaction product. The overall kinetics will depend upon the relative rates of the diffusion and reaction steps, which may involve intermediate compounds. A kinetic investigation requires some knowledge of the disposition of the reaction product, i.e. whether it diffuses towards the liquid or gas or whether it forms a

third phase. One characteristic of these gas-luqiid reactions which is generally absent from the analogous low temperature aqueous processes (e.g. the absorption of CO_2 by NaOH solutions) is the large heat release due to the chemical reaction. This may result in a large temperature rise in the neighborhood of the interphase, thus imposing a heat transfer restriction on the system. The chemical reaction may resemble a combustion reaction, in that an ignition temperature may separate regions of moderately slow and extremely rapid rates.

Object and Outline of Approach. The object of this investigation is to study both experimentally and theoretically the gas-liquid reactions that occur in the chlorination of UCl_4 by gaseous Cl_2 to produce UCl_6. Although the corresponding fluoride volatility reaction is more interesting from an application standpoint, the corrosion and toxicity problems were felt to be too severe to handle. As a substitute, the chlorine-based system was chosen, since chlorine is more manageable than fluorine. The kinetics of this system should resemble those of the analogous fluorine system.

The kinetics of the absorption of chlorine into UCl_4-LiCl-KCl melts was studied. The overall reaction was assumed to be:

$$UCl_4(\ell) + Cl_2(g) \longrightarrow UCl_6(g \text{ or } \ell)$$

The product is actually a mixture of UCl_5 and UCl_6 but in this work it is called UCl_6. The absorption rate is a function of the equilibria, chemical kinetics, diffusion rates and the hydrodynamics of the system.

There are no data in the literature on the solubility or chlorine and uranium hexachloride or F_2 and UF_6 in uranium-free molten salt systems. No methods for predicting diffusion coefficients of dissolved gas in these fused salt systems are available. The chemical kinetics of the process are completely unknown.

The first part of this investigation was therefore devoted to the measurement of the solubilities and the estimation of the diffusivities of chlorine and uranium tetrachloride in the uranium-free solvent salt. The apparatus chosen for chlorine solubility was similar to that used at Oak Ridge for salts. The technique consisted in the saturation of the fused salt with the gas, transfer of the solution to an isolated section of the apparatus, recovery of the dissolved gas by sparging with an inert gas, and subsequent determination.

An experimental correlation was derived for the diffusivities of different solutes in ionic liquids. The log-log plots of the group $\left(\frac{D\mu}{T}\right)$ versus $\left(V_2^{2/3}/V_1\right)$ were found to be straight lines - the slopes and intercepts varying with the degree of ionization and association of the solvent. The diffusivity of UCl_4 in the fused LiCl-KCl eutectic could therefore be estimated.*

The absorption apparatus chosen for the determination of absorption rates was designed for simplicity and reproducibility of the hydrodynamic patterns of the two phases: A film of the molten salt flows through an orifice in the bottom of a holding tank down a rod in an absorption chamber containing the gas at one atmosphere and at the melt temperature (400-700°C). After passing through a predetermined length of absorption chamber, the molten salt is collected in a sampling cup.

By choosing a wetted-rod apparatus, in which the liquid flow conditions are quite simple, the fluid mechanical part of the unsteady-state diffusion-reaction theory could be formulated very completely,

---

*Towards the end of this work, measured diffusivities of U^{+4} in the LiCl-KCl eutectic were reported by Thalmayer et al.[58]

and reliable values of unknown quantities such as chamical reaction rates could be derived from the measured overall rates. The area of the interphase and the contact time between the gas and liquid are known accurately. Molecular diffusion is the only transport process operating within the liquid which is in laminar flow.

The wetted-rod apparatus was chosen after attempts to perform laminar jet experiments with the molten salts were unsuccessful. The high surface tension of the eutectic melt prevented the formation of rod-like jet flow through a small orifice. The wetted-rod was found to have other advantages over a laminar jet or a wetted-wall column, namely:

(a) Less material is needed. The surface area of the rod is smaller than that of a typical wetted-wall column. The wetted rod is essentially a laminar jet with its center replaced with a solid bar.

(b) Contact times are greater. The surface velocity for film flow is slower than that of a free-falling jet because of viscous drag of the rod.

(c) % Conversion is increased. Higher % conversion is obtained with the wetted-rod because there is less material to saturate or react with and the contact times are greater.

A preliminary study using the well-known CO_2-water system was undertaken to determine the accuracy of the falling film technique. Preliminary runs were previously made using n-propyl alcohol (the kinematic viscosity of which is about the same as that of the UCl_4 - LiCl-KCl melts) to obtain a reasonable design of the all-quartz apparatus for the actual absorption studies.

The rates of absorption of chlorine in UCl_4-LiCl-KCl melts were studied at several temperature levels, where the reaction with UCl_4 might increase the absorption rate. As a result of such work, it was hoped that the basic physical and chemical phenomena upon which the overall process depends could be clarified.

II. FUSED SALTS

A. Structure of Fused Salts[8,24,38]

Two liquid models are under consideration for fused salts:[32,60]

(a) The quasi-lattice model. In this model the structure of a liquid is described by a solid-like framework in which the atoms are situated at certain positions or near these points. The essential difference between the solid and liquid salt is the presence in the liquid of large numbers of holes accompanied by the disappearance of long range order. Transport properties are analyzed in terms of jumps of cations and anions into the cavities; these being controlled by the energy to form a hole and that needed to jump into it. This model over-emphasizes the similarity between the solid and the liquid and, therefore, is expected to be less applicable far from the melting point and close to the critical temperature. It has been applied with good results to the estimation of thermodynamic properties.[9,10] Calculation of transport properties with this model has not been as successful. This model will be assumed throughout this section.

(b) The quasi-random model. This model has not been explicitly described for fused salts, but it has been implied in a recent consideration of transport phenomena.[35] Perturbations in interatomic distance, which result from the introduction of holes into the system upon melting, allow micro (1Å) movements, by which transport occurs.

It is now generally accepted that pure molten salts consist mainly of ions. They are the only group of pure liquids in which positively and negatively charged particles coexist. They could therefore logically be called "liquid electrolytes" or "ionic melts".

Due to the strong interaction between the charged particles (attractive forces between ions of like sign and repulsive forces between ions of opposite sign), and the fluid nature of molten salts, it is reasonable to assume that positive ions are surrounded almost exclusively by negative ions as nearest neighbors, and vice versa. Ions of like signs arrange themselves as far as possible from each other. Thus, cations and anions would not exchange positions, and in the lattice model the fused salt is considered to have two interlocking frameworks, one for cations and one for anions. This results in molten salts having rather more open structures than other liquids. The melting of solid salts therefore usually leads to a considerably greater increase in volume. Table I shows that alkali halides expand in volume by about 20% on melting, whereas, metals expand little and sometimes contract.

Table II shows that the average distances between ions of like sign are usually greater than in the solid, while the average distances of ions of unlike sign are less. The volume expansion of salts on fusion plus the changes on interionic distances, lead to the creation of empty space or "free volume", in the melt.

1. Structure of Molten Alkali Halides

Among the simplest and most typical ionic liquids are the molten alkali halides. Seventeen of the twenty alkali halides, crystallize in the NaCl structure (Table III), two (CsBr and CsI) in the CsCl structure, and one (CsCl) has the CsCl structure at ordinary temperatures, but changes to NaCl structure at higher temperatures. It may be concluded that in the liquid state the local arrangement of atoms will be similar to the NaCl structure, i.e. in a molten alkali halide $A^+ X^-$ each anion

Table I. Change of molar volume on melting of salts and metals

Substance	% Increase in Volume	Reference
NaF	24	36
KCl	21	36
KBr	22	36
Bi	4.75	41
Cd	4.7	41
Pb	4.8	41

Table II. Inter-ionic distance for some molten salts

	SOLID		LIQUID	
salt	cation-anion distance, Å	cation-cation or anion-anion distance, Å	cation-anion distance, Å	cation-cation or anion-anion distance, Å
LiCl	2.47	3.85	2.66	3.76
CsCl	3.53	4.87	3.57	5.05
LiI	2.85	4.45	3.12	4.41
NaI	3.15	4.80	3.35	4.74

Table III. Atom arrangements in NaCl type structure

coordination shell	1	2	3	4
ion pair	C-A	C-C or A-A	C-A	C-C or A-A
distance (r_i/r_1)	1	$(2)^{\frac{1}{2}} = 1.41$	$(3)^{\frac{1}{2}} = 1.73$	2.00
coordination number	6	12	8	6

has as its nearest neighbors six cations situated approximately at the ends of each of three mutually perpendicular diameters of a sphere of radius r_{AX}, where r_{AX} is the $A^+ X^-$ interionic distance.

2. Interaction in Molten Alkali-Halide Mixtures

In a molten mixture of two alkali-halides with common anions, $A^+ X^-$ and $B^+ X^-$, each cation has as its nearest neighbors six anions, or three mutually perpendicular axes, at distances r_{AX} and r_{BX}, respectively. The immediate arrangement in the solution is the same as in the pure melts.

There is no change of energy on mixing due to simple interaction between nearest neighbors. Interaction between farther neighbors are of two kinds - the London forces between cations and the polarizing forces due to different cations being in contact with the same anions.

a. London Forces. The non-polar London forces contribute the energy term:

$$E_L = - C/r^6 \qquad \text{(II-1)}$$

Since this function decreases so rapidly with interionic distance and since there is a common anion in the mixture, the only important non-polar interactions are between nearest cations. Any cation is surrounded by 12 cations, so that in x moles of $A^+ X^-$ (containing Nx cations, where N is Avogardro's number) there are 6Nx pairs of A^+ cations interacting 1.41 r_{AX} apart, and in y moles of $B^+ X^-$ there are 6Ny pairs 1.41 r_{BX} apart. Mixing both gives $6Nx^2/(x + y)$ A-A pairs, $6Ny^2/(x + y)$ B-B pairs, and 12 $Nxy/(x + y)$ A-B pairs. The A-B pairs are $(r_{AX}^2 + r_{BX}^2)^{0.5}$ apart. The change of potential energy on mixing due to London forces is:

$$E_L = C_L xy/(x + y) \qquad \text{(II-2)}$$

where

$$C_L = 6N\left[C_{AA}/(2r_{AX}^2)^3 + C_{BB}/(2r_{BX}^2)^3 - 2C_{AB}/(r_{AX}^2 + r_{BX}^2)^3\right] \qquad \text{(II-3)}$$

The London constants for like cations are given by Mayer[40] are:

$Li^+ - Li^+$, 0.11; $Na^+ - Na^+$, 2.68; $K^+ - K^+$, 38.6; $Rb^+ - Rb^+$, 94.3; $C_s{}^+ - C_s{}^+$, 247 eV - $Å^6$

The London interaction constant between two unlike cations is assumed to be:

$$C_{AB} = \sqrt{C_{AA} \cdot C_{BB}} \qquad \text{(II-4)}$$

b. Polarization energy. An X^- anion in contact with A^+ and B^+ cations at diametrically opposite positions is subjected to an electric field

$$Fo = e(1/r_{AX}{}^2 - 1/r_{BX}{}^2) \qquad \text{(II-5)}$$

It will also have X^- anions at distances $2r_{AX}$ and $2r_{BX}$, these producing an electric field,

$$F1 = -e(1/r_{AX}{}^2 - 1/r_{BX}{}^2)/4 \qquad \text{(II-6)}$$

It is assumed that other contributions would be terms in a geometric series with Fo and F1 as the first two terms. The field is then

$$F = \frac{4e}{5} (1/r_{AX}{}^2 - 1/r_{BX}{}^2) \qquad \text{(II-7)}$$

If α is the polarizability of the anion, the resultant polarization energy is

$$\alpha F^2 = -0.64\ \alpha e^2 (1/r_{AX}{}^2 - 1/r_{BX}{}^2) \qquad \text{(II-8)}$$

In the mixture of $A^+ X^-$ and $B^+ X^-$, it becomes

$$E_p = C_p\ xy/(x + y) \qquad \text{(II-9)}$$

where

$$C_p = 1.92\ N\alpha e^2 (1/r_{AX}{}^2 - 1/r_{BX}{}^2) \qquad \text{(II-10)}$$

Molar polarizabilities $N\alpha$ (α = polarizability per ion) given by

Kordes[34] for halide anions are:

$$F^-,\ 0.462;\ Cl^-,\ 1.63;\ Br^-,\ 2.29;\ I^-, 3.56\ cm^3.$$

The London and polarizing forces are usually applied to derive thermodynamic, thermochemical, and transport properties of fused salts and their mixtures.

B. Diffusion in Fused Salts

Incomplete pictures of the liquid state have led to a less than satisfactory theory of diffusion in liquids. Frenkel[23] gives a survey of kinetic theories of liquids, but stresses their limitations. More recently Bernal[3,4,5] has proposed a rather elaborate concept of the kinetic theory of liquids. So far his rigorous theory has not found practical applications in the treatment of diffusion phenomena.

The classical treatment of diffusion in liquids is based on the Stokes-Einstein equation:

$$\frac{D\mu}{T} = k/6\pi r \qquad \text{(II-11)}$$

where:

D is the diffusion coefficient defined in the equation:

$$N = -D\frac{\partial C}{\partial Y} \qquad \text{(II-12)}$$

and

r = radius of diffusing particles

k = Boltzmann constant

μ = viscosity

T = temperature

A more satisfactory approach to diffusion in solutions is by means of Eyring's theory of absolute reaction rates.[21,22] The Eyring theory treats the diffusion process as a viscous flow of the solute molecule

into holes in the medium. The diffusion coefficient may be given in the form:

$$\frac{D\mu}{T} = \frac{\lambda_1}{\lambda_2 \lambda_3} \frac{k}{\xi} \exp \frac{\Delta F_\mu^* - \Delta F_D^*}{RT} \qquad \text{(II-13)}$$

The parameter ξ was taken as unity in the original Eyring equation. However, a value of 5.6 has been obtained from am empirical evaluation of mutual diffusion data.[37] Olander[44] gives an approximate method for estimating the difference between the free energies of activation of the viscous and diffusional processes in dilute binary system.

Empirical correlations of diffusion coefficients in liquids abound in the literature.[1,45,51,63,64] None of these, however, are applicable to ionic liquids, such as molten salts. The following correlation was found to apply to fused salts:

$$\left(\frac{D\mu_2}{T}\right)^m = A \frac{V_2^{2/3}}{V_1} \qquad \text{(II-14)}$$

where:

D = diffusivity, cm^2/sec

μ = viscosity, cp.

T = temperature, °K

V = molar volume, cc/mole

A,m = constants depending on solvent studied.

Subscripts: 1 - solute; 2 - solvent

Values of A and m for the solvents examined are shown in Table IV. The data found for fused salts are summarized in Table V and plotted in Fig. 1.

It was found that m decreases as the degree of ionization increases,

Table IV. Constants for Different Solvents

Solvent	$A \times 10^7$	m
KNO_3	4.65	1
$NaNO_3$	7.38	1
LiCl-KCl	7280	0.53

Table V. Diffusion in Molten Salts[39,57,59]

Solute	T, °K	Dobs. x 10^5	Dcalc. x 10^5 (Eq'n.(14))
		Solvent - KNO_3	
Ag^+	663	4.80	5.35
Ag^+	633	4.56	4.35
Tl^+	618	3.17	3.18
Tl^+	653	3.40	4.07
Na^+	633	5.22	4.51
Ba^{+2}	643	2.06	2.30
Sr^{+2}	633	2.81	2.39
		Solvent - $NaNO_3$	
Ag^+	603	4.57	5.41
Ba^{+2}	633	3.71	3.16
Sr^{+2}	618	4.17	3.29
		Solvent - LiCl-KCl Eutectic	
Ag^+	753	4.60	6.16
	723	2.60	4.83
Cu^+	773	6.70	6.10
	723	3.50	4.12
Cd^{++}	773	2.70	2.47
	723	1.70	1.65
	723	2.08	1.65
Co^{++}	673	1.2 ± 0.2	1.08
	723	2.42	2.25
Ni^{++}	773	4.00	3.69
	723	4.14	2.50
Pb^{++}	723	2.18	1.51
	723	1.70	1.51
	673	0.89 ± 0.2	0.97
Bi^{+3}	723	0.60	0.81
	673	0.63 ± 0.1	0.52
U^{+4}	723	0.49	0.39

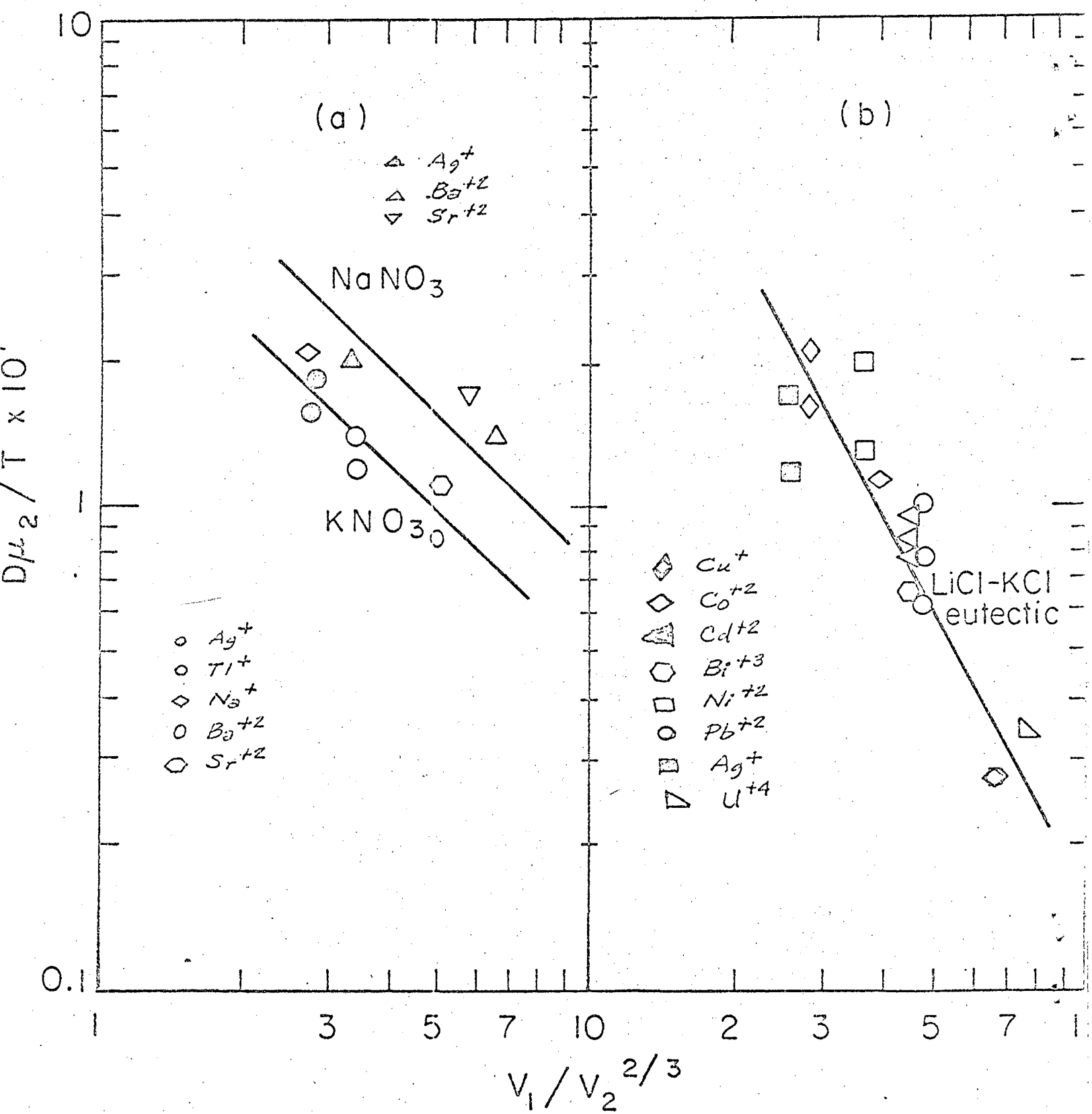
10
1
0.1
(a)
(b)
Ag+
Ba+2
Sr+2
NaNO3
KNO3
Ag+
Tl+
Na+
Ba+2
Sr+2
Cu+
Co+2
Cd+2
Bi+3
Ni+2
Pb+2
Ag+
U+4
LiCl-KCl
eutectic
Dμ2 / T x 10
1
3
5
7
10
2
3
5
7
1
V1 / V2 2/3

Figure 1

and that for a given m, A increases with increasing degree of association.

The diffusivity of U^{+4} in the LiCl-KCl eutectic was recently reported as[59]

$$D_T = 1.06 \times 10^{-3} \left(e^{-7700/RT}\right) \qquad \text{(II-15)}$$

III. THEORY OF THE HYDRODYNAMICS AND DIFFUSION IN THE FILM FLOW DOWN A ROD

A. Simultaneous Diffusion and Chemical Reaction

No clear dividing line exists between pure physical absorption and absorption controlled by the rate of a chemical reaction. Most cases belong to an intermediate group, the rate of absorption being controlled by both the diffusional resistance and the finite reaction velocity. Some advances have been made in recent years in the theory that can be applied in these cases.[15,16,30,31,54] Unless the chemical kinetics and the hydrodynamics are known, it is not feasible to determine beforehand whether a given case is controlled by diffusional or chemical resistance. Usually each case has to be studied experimentally.

The mechanism of processes in which gas absorption is accompanied by chemical reaction with a constituent of the liquid is one of physical solution followed by a reaction. The chemical reaction may take place in any of the following ways:[6,65]

(a) At the gas-liquid interface: this case applies when the gas is relatively insoluble in the liquid. It can be controlled by either the reaction rate or the diffusion of the reactants to the gas-liquid interface.

(b) In a narrow zone within the liquid: this mechanism applies when the reaction can take place rapidly compared to the diffusional rates of reactants and products. The rate of absorption is then controlled by the diffusion in the liquid.

(c) During the diffusion of the dissolved gas through the liquid film: the rate of absorption is then a function of both reaction velocity and rates of diffusion.

(d) In the main body of the liquid: this occurs with slow reactions. With moderately slow reactions, the concentration of free dissolved gas then takes up a value such that its rate of removal by reaction is balanced by the rate of diffusion through the film. If reaction is very slow, the liquid always may be practically saturated relative to the gas phase, and absorption is entirely controlled by the velocity of the reaction.

Four characteristics of diffusion-controlled reactions are:

(a) The chemical reaction occurs with a relatively great velocity;

(b) The degree of agitation of the reactants influences the speed of the observed reaction;

(c) The overall rate obeys the equation for first-order kinetics, since diffusion is a first-order process;

(d) The activation energy should be about the same as that of diffusion, i.e. about 3 kcal/mole.

The characteristics of reaction-controlled absorption are to a certain extent the converse of those that are controlled by diffusion:

(a) The order of such a reaction will be 1, 2 or an intermediate value;

(b) The activation energy should be similar to that of the ordinary homogeneous chemical reaction, i.e. in the order of 15-40 kcal/mole;

(c) The observed rate of reaction of this class is not influenced by the degree of agitation or turbulence of the system; and

(d) The velocity of the chemical reaction is much smaller in magnitude than the diffusion rate.

When the absorption rate is a function of both diffusion and chemical reaction, the diffusion and reaction rates are comparable. Subsequent theory concerns diffusion coupled with a reaction of the interface.

B. Gas Phase

1. Hydrodynamics.

Steady, two-dimensional, incompressible flow around a continuous cylindrical surface moving in a stationary fluid medium produces a boundary layer which grows in the direction of motion of the surface as shown in Figure 2. At the surface the fluid velocity in the z direction (u component) is equal to the surface velocity (u_s). At increasing distance from the surface the fluid velocity in the z direction approaches zero asymptotically. The velocity of the fluid in the r direction (v component) varies from zero at the surface to some finite value at the edge of the boundary layer.

The boundary layer equations for steady, laminar incompressible flow on a continuous cylindrical surface or circular jet with no pressure gradient are:

$$u \frac{\partial u}{\partial z} + v \frac{\partial u}{\partial r} = \nu \frac{1}{r} \frac{\partial}{\partial r} \left(r \frac{\partial u}{\partial r}\right) \qquad \text{(III-1)}$$

and

$$\frac{\partial u}{\partial z} + \frac{1}{r} \frac{\partial}{\partial r} (rv) = 0 \qquad \text{(III-2)}$$

The boundary conditions are:

$$u = u_s, \; v = 0; \text{ at } r = b \qquad \text{(III-3a)}$$

where b is the radius of the cylinder

$$u \longrightarrow 0 \quad \text{as } r \longrightarrow \infty \qquad \text{(III-3b)}$$

and

$$u = 0 \quad \text{at} \quad z = 0 \qquad \text{(III-3c)}$$

the auxiliary condition:

$$\left(\frac{\partial u}{\partial r}\right)_{r = \infty} = 0 \qquad \text{(III-3d)}$$

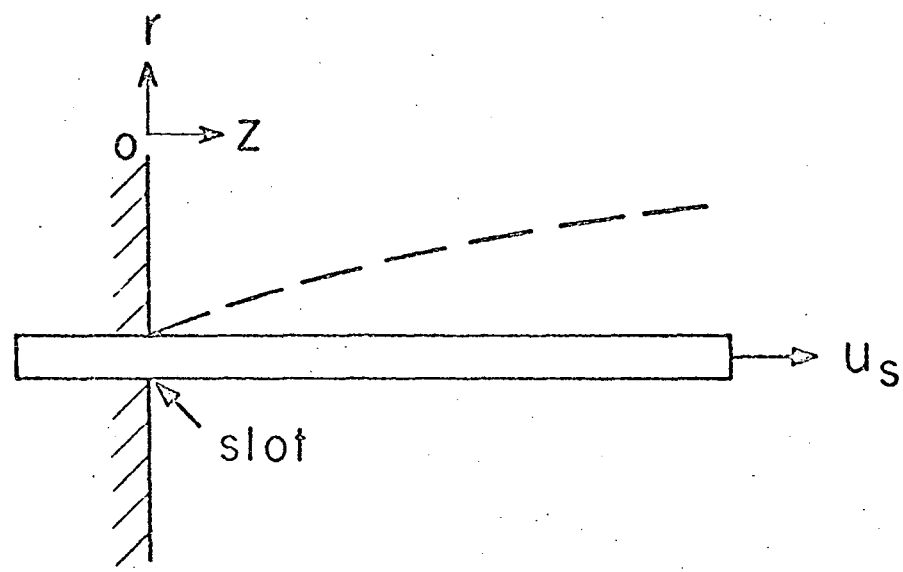

Figure 2

is needed for the solution of the equations of motion by the von Karman Integral Method.[52]

The momentum integral is obtained by multiplying equation (III-1) by rdr and integrating from $r = b$ to $r = b + \delta_v$, where δ_v is the thickness of the velocity boundary layer (according to equation (III-3b) and (III-3d), u and $\frac{\partial u}{\partial r}$ are assumed to vanish at $r = b + \delta_v$). The second term on the left of equation (III-1) is integrated by parts and use is made of equation (III-2). The result is:

$$\frac{\partial}{\partial z}\int_b^{b+\delta_v} u^2\, r dr = -\nu b \left(\frac{\partial u}{\partial r}\right)_b \qquad \text{(III-4)}$$

Equation (III-4) can be cast in dimensionless form by the transformations:

$$z^* = 4\left(\frac{\nu z}{u_s b^2}\right)^{1/2}$$

$$y = \frac{r}{b} - 1 \qquad \text{(III-5)}$$

$$u^* = u/u_s$$

This yields:

$$\frac{8}{z^*}\frac{\partial}{\partial z^*}\int_0^{\delta_v^*} u^{*2}(1+y)\,dy = -\left(\frac{\partial u^*}{\partial y}\right)_0 \qquad \text{(III-6)}$$

where δ_v^* is the dimensionless flow boundary layer thickness:

$$\delta_v^* = \frac{\delta_v}{b} \qquad \text{(III-7)}$$

The functional dependence of u^* on y is assumed to be:

$$u^*(y) = A_o + A_1\frac{y}{\delta_v^*} + A_2\left(\frac{y}{\delta_v^*}\right)^2 + A_3\left(\frac{y}{\delta_v^*}\right)^3 \qquad \text{(III-8)}$$

The four constants are evaluated from the conditions:

$$u^*(o) = 1$$

$$\left(\frac{d^2 u^*}{d y^2}\right)_o + \left(\frac{du^*}{dy}\right)_o = 0 \qquad \text{(III-9)}$$

$$u^* (\delta_v^*) = 0$$

$$\left(\frac{du^*}{dy}\right)_{\delta_v^*} = 0$$

The first, third and fourth of these conditions are obtained from the original boundary conditions (III-3). The second condition is obtained from equation (III-1) at r = b. The result is:

$$u^*(y) = 1 - \frac{3}{2}\left[\frac{1}{1 - \delta_v^*/4}\right]\left(\frac{y}{\delta_v^*}\right) + \frac{3}{4}\left[\frac{\delta_v^*}{1 - \delta_v^*/4}\right]\left(\frac{y}{\delta_v^*}\right)^2 + \frac{1}{2}\left[\frac{1 - \delta_v^*}{1 - \delta_v^*/4}\right]\left(\frac{y}{\delta_v^*}\right)^3 \qquad \text{(III-10)}$$

Substituting equation (III-10) into equation (III-6) and solving yields:

$$\frac{105z^*}{16} = 1080\ell n\left(\frac{4}{4 - \delta_v^*}\right) + 2108\left(\frac{\delta_v^*}{4 - \delta_v^*}\right) - 790\,\delta_v^* - 157\,\delta_v^{*2} - \frac{118}{3}\,\delta_v^{*3} - \frac{3}{4}\,\delta_v^{*4} \qquad \text{(III-11)}$$

Figure 3 shows a plot of δ_v^* as a function of z^* according to equation (III-11). Also shown is the result obtained by Sakiadis.[49,50] Sakiadis assumed a logarithmic velocity profile which satisfies the boundary conditions at y = 0 exactly, but not the boundary conditions at $y = \delta_v$.

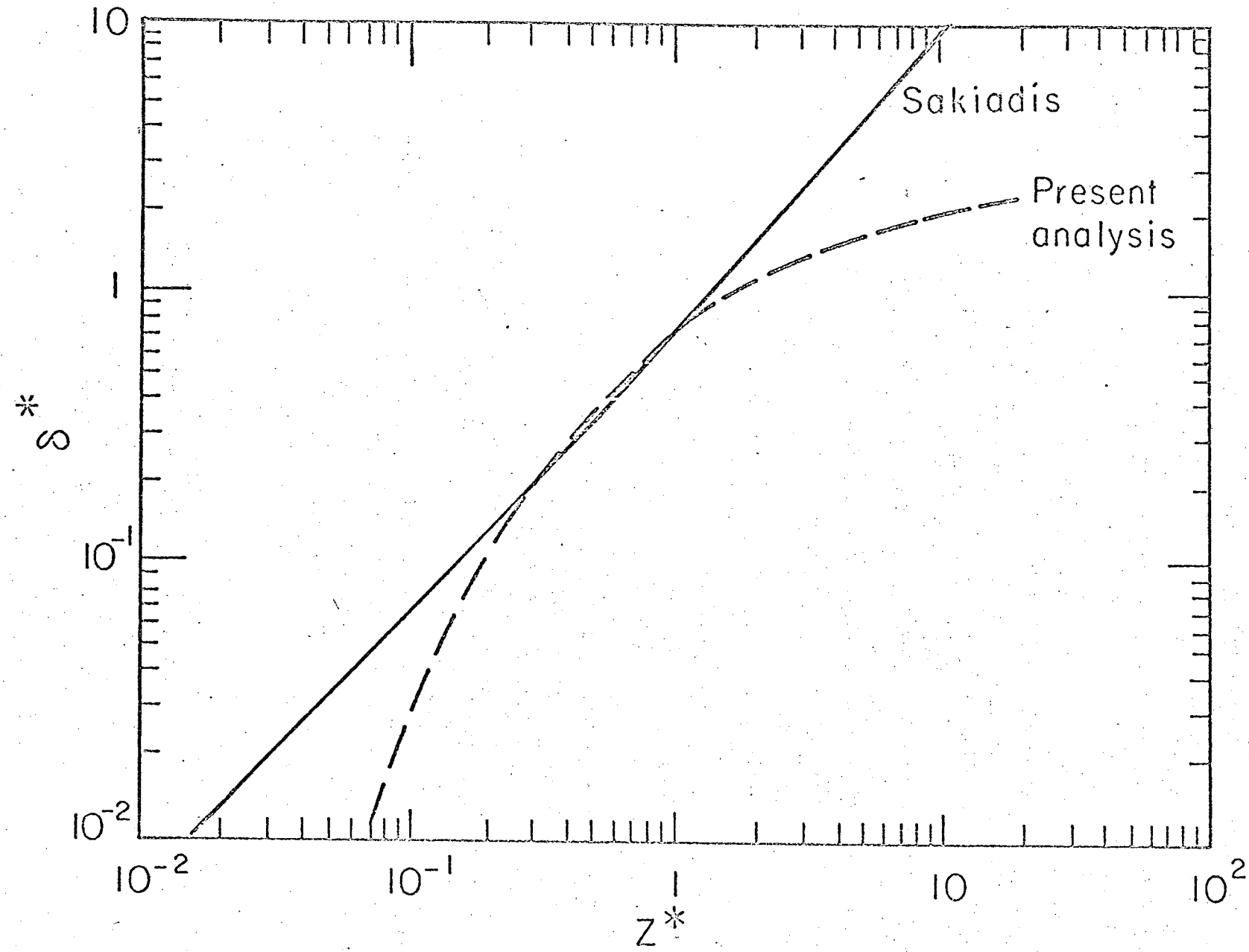
10
1
10^{-1}
10^{-2}
δ^*
10^{-2}
10^{-1}
1
10
10^2
Z^*
Sakiadis
Present analysis

Figure 3

The velocity profile derived above (Figure 4) satisfies all boundary conditions. Note that for $\delta_v^* \ll 1$, equation (III-10) reduces to:

$$\lim_{\delta_v^* \to 0} u^*(y) = 1 - \frac{3}{2}\left(\frac{y}{\delta_v^*}\right) + \frac{1}{2}\left(\frac{y}{\delta_v^*}\right)^3 \qquad \text{(III-12)}$$

This is the profile for the plane case, for which the radius of curvature (b) is much larger than the boundary layer thickness. In the limit of small δ_v^*, equation (III-11) becomes:

$$\delta_v^* = \sqrt{\frac{35}{44}}\, z^* \qquad \text{(III-13)}$$

Typical values for z^* for the CO_2 and fused salt experiments were ≤ 1.4 and ≤ 2.1, respectively.

2. Diffusion in the Gas Phase.

The concentration profile in the gas phase outside of the moving cylinder is:

$$u \frac{\partial C^*}{\partial z} + v \frac{\partial C^*}{\partial r} = D \frac{1}{r} \frac{\partial}{\partial r} \left(r \frac{\partial C^*}{\partial r}\right) \qquad \text{(III-14)}$$

where $C^* = \dfrac{C - C_o}{C_i - C_o}$

C_i is the interfacial concentration (independent of z) and C_o is the bulk concentration in the gas phase. The boundary conditions are:

$$\begin{aligned} &\text{at } z = 0,\ C^* = 0 \\ &\text{at } r = b,\ C^* = 1 \\ &\text{at } r = \infty,\ C^* = 0 \end{aligned} \qquad \text{(III-15)}$$

Applying the momentum integral method to equation (III-14), there results:

$$\frac{8}{z^*} \frac{\partial}{\partial z^*} \int_0^{\delta_c^*} C^* u^* (1 + y)\, dy = -\frac{1}{S_c} \left(\frac{\partial C^*}{\partial y}\right)_o \qquad \text{(III-16)}$$

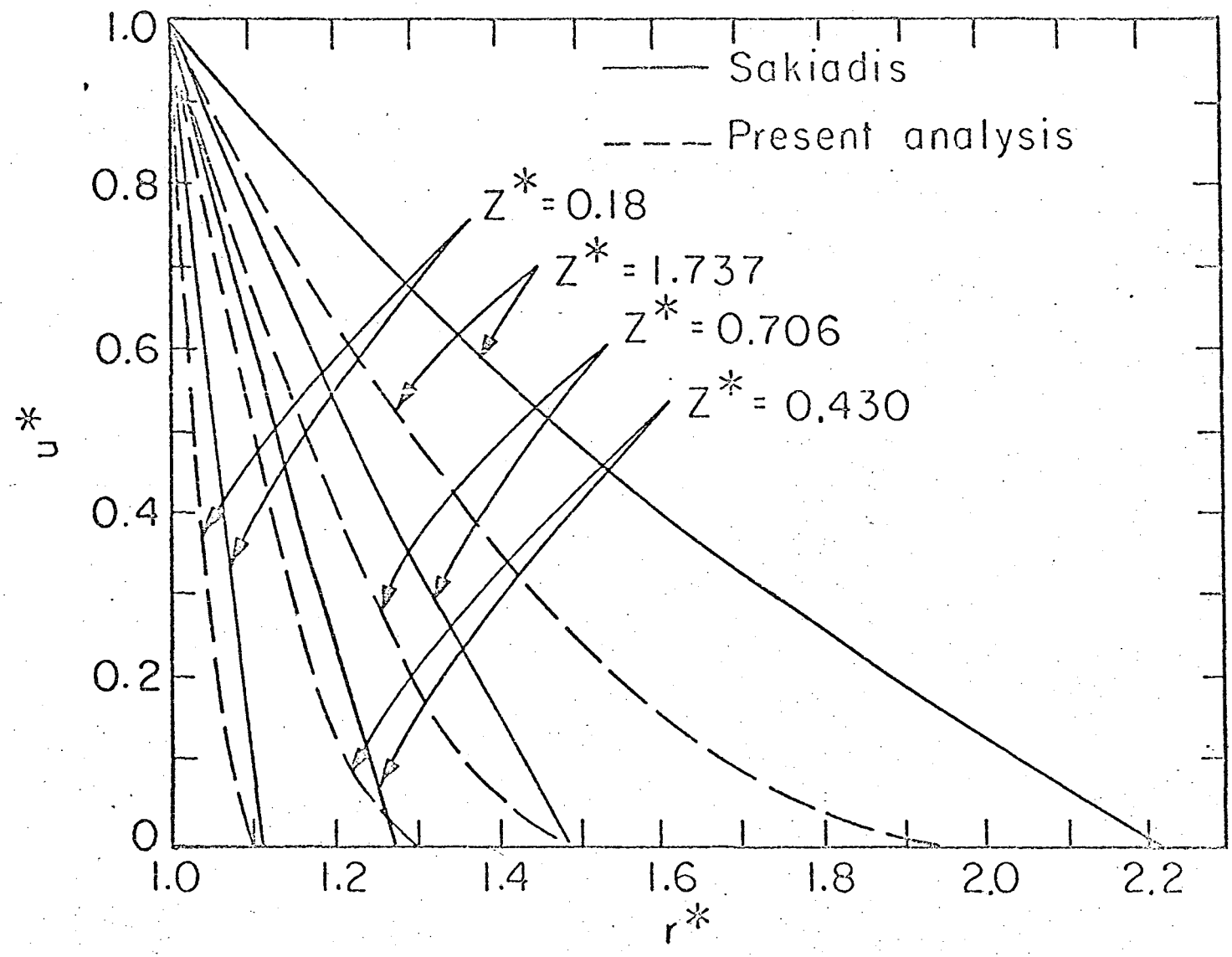
Sakiadis
Present analysis
Z* = 0.18
Z* = 1.737
Z* = 0.706
Z* = 0.430
1.0
0.8
0.6
0.4
0.2
0
1.0
1.2
1.4
1.6
1.8
2.0
2.2
r*

Figure 4

where the dimensionless variables of equation (III-5) have been introduced and the dimensionless concentration boundary layer thickness is

$$\delta_c^* = \frac{\delta_c}{b} \qquad \text{(III-17)}$$

Sc is the Schmidt number, ν/D.

A cubic approximation to C^* is obtained in the same manner as for u^*, using restraints analogous to equation (III-9). The result is an expression for $C^*(y)$ identical in form to equation (III-10), with u^* replaced by C^* and δ_v^* replaced by δ_c^*. In order to develop an expression for δ_c^* as a function of z^*, we would need to substitute C^* and u^* (as functions of y) into equation (III-16), and perform the indicated differentiation and integration. This cannot be accomplished analytically because of the complex behavior of δ_v^* as a function of z^* [(equation III-11)]. Before examining limiting cases which are amenable to analytical treatment, the expression for the average mass transfer rate will be developed.

The average mass transfer coefficient in the region $0 \leq z \leq \ell$, where ℓ is the length of the rod, is defined by:

$$\bar{N}_A = \bar{k}\,(C_i - C_o) \qquad \text{(III-18)}$$

The local mass transfer coefficient is

$$k(z) = \frac{N_A(z)}{C_i - C_o} = -D\left(\frac{\partial C^*}{\partial r}\right)_b = -\frac{D}{b}\left(\frac{\partial C^*}{\partial y}\right)_o = \frac{3}{2}\frac{D}{b}\,\frac{1}{\delta_c^*(1 - \delta_c^*/4)} \qquad \text{(III-19)}$$

where $\bar{k} = \frac{1}{\ell}\int_o^\ell k(z)\,dz$ (III-20)

Combining:

$$\frac{\bar{k}b}{D} = \frac{3}{\ell^{*2}}\int_o^\ell \frac{z^*\,dz^*}{\delta_c^*(1 - \delta_c^*/4)} \qquad \text{(III-21)}$$

where $\ell^* = 4\sqrt{\frac{\nu \ell}{u_s b^2}}$ (III-22)

If δ_c^* is known as a function of z^*, equation (III-21) can be integrated. For Sc = 1, δ_c^* is equal to δ_v^*, and is given by equation (III-11). Even in this case, however, the integration of equation (III-21) could only be accomplished numerically.

An approximate analytical solution, however, can be obtained for the limiting case of δ_v^* and $\delta_c^* \ll 1$ (corresponding to the case of a moving plane). In this instance, u^* is given by equation (III-12) and C^* by:

$$\lim_{\delta_c^* \longrightarrow 0} C^*(y) = 1 - \frac{3}{2}\left(\frac{y}{\delta_c^*}\right) + \frac{1}{2}\left(\frac{y}{\delta_c^*}\right)^3 \qquad \text{(III-23)}$$

The dependence of u^* upon y and z^* is obtained by combining equations (III-12) and (III-13). If this and equation (III-23) are inserted into equation (III-16) (wherein $1 + y \approx 1$), there results:

$$\frac{\delta_c^*}{z^*} \frac{d}{dz^*}\left\{\delta_c^*\left[1 - \frac{2}{5}\sqrt{\frac{44}{35}}\left(\frac{\delta_c^*}{z^*}\right) + \frac{1}{35}\left(\frac{44}{35}\right)^{3/2}\left(\frac{\delta_c^*}{z^*}\right)^3\right]\right\} = \frac{1}{2\,Sc} \qquad \text{(III-24)}$$

subject to

$$\delta_c^* = 0 \quad \text{at} \quad z^* = 0 \qquad \text{(III-25)}$$

The solution to equation (III-24) which satisfies equation (III-25) is:

$$\delta_c^* = mz^* \qquad \text{(III-26)}$$

A solution of this type satisfies both the differential equation and the initial condition, and must therefore be unique. The constant m is

given by a solution of:

$$m^2 \left[1 - \frac{2}{5} \sqrt{\frac{44}{35}}\ m + \frac{1}{35} \left(\frac{44}{35}\right)^{3/2} m^3 \right] = \frac{1}{2\ Sc} \qquad \text{(III-27)}$$

m is plotted as a function of Sc on Figure 5. Note that at Sc = 1, m = 0.89, which is equal to the constant in equation (III-13). At Sc = 1, the two boundary layers are equal. Between $1 \leq Sc \leq 2$, m can be represented by a simple power law, and δ_c^* is:

$$\delta_c^* = 0.89\ Sc^{-5/8}\ z^* \qquad \text{(III-28)}$$

Inserting equation (III-28) into equation (III-21), setting $1 - \left(\frac{\delta_c^*}{4}\right) \approx 1$, and using equation (III-22), gives

$$\bar{k} = 0.843\ Sc^{1/8} \sqrt{\frac{u_s D}{\ell}} \qquad \text{(III-29)}$$

C. The Liquid Phase

1. Hydrodynamics

The falling film model (Figure 6) simplifies the theoretical work considerably because of its idealized fluid mechanics, known interfacial area and easily estimated contact time.

The axial momentum equation in the liquid film flowing down the rod is:

$$u \frac{\partial u}{\partial z} = g - \frac{1}{p} \frac{\partial p}{\partial z} + \nu \left[\frac{\partial^2 u}{\partial r^2} + \frac{1}{r} \frac{\partial u}{\partial r} + \frac{\partial^2 u}{\partial z^2} \right] \qquad \text{(III-30)}$$

For steady flow, $\frac{\partial u}{\partial z} = 0$ and $\frac{\partial p}{\partial z} = 0$; therefore, equation (III-30) becomes:

$$\frac{1}{r} \frac{d}{dr} \left(r \frac{du}{dr}\right) = - \frac{g}{z} \qquad \text{(III-31)}$$

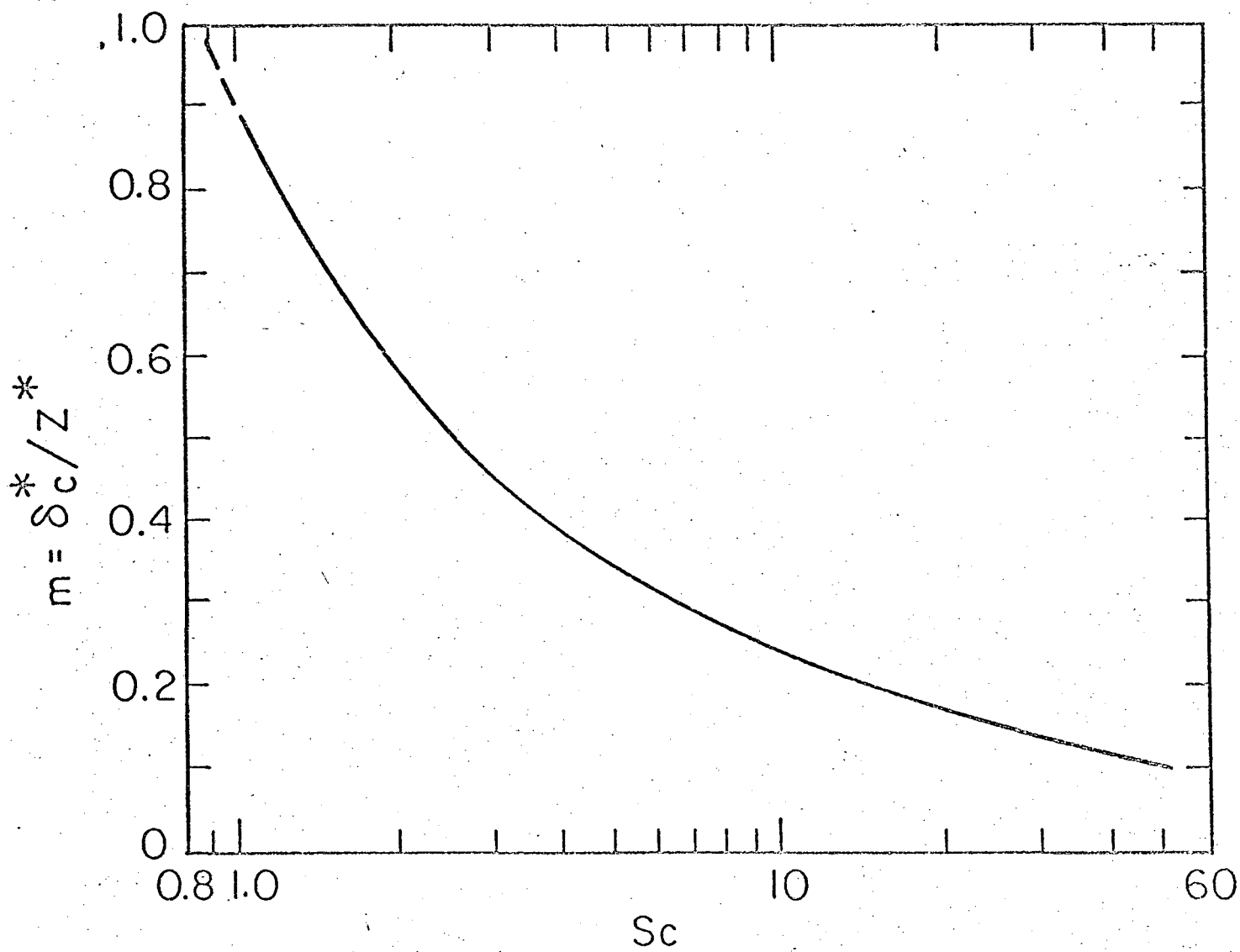

Figure 5

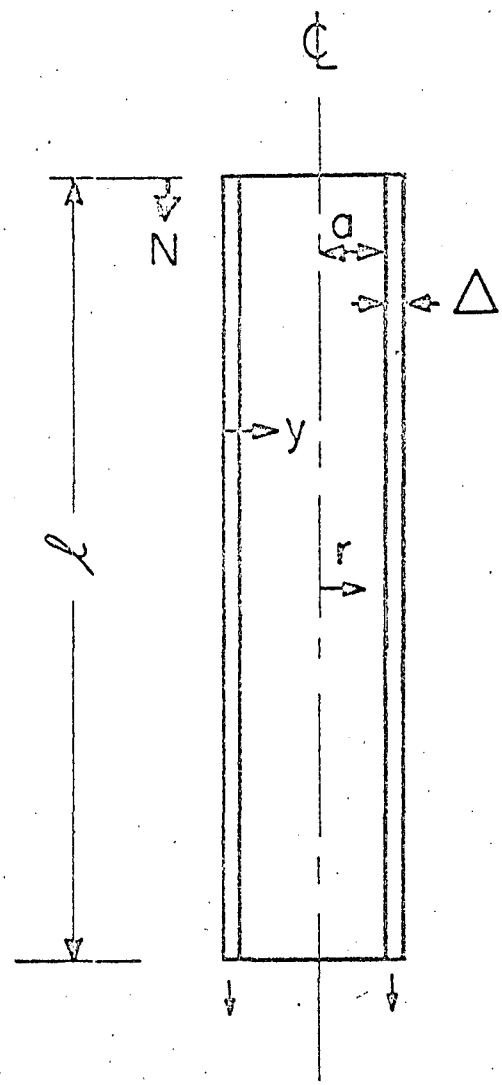

Figure 6

with boundary conditions

$$\text{at } r = a,\ u = 0$$
$$\text{at } r = a + \Delta,\ \partial u/\partial r = 0 \qquad \text{(III-32)}$$

Δ is the film thickness and a the radius of the rod. The cylinder radius used in the previous section is $(a + \Delta) = b$.

Integrating equation (III-31) gives

$$u^* = \frac{1}{\Delta^{*2}} \left\{ (1 + \Delta^*)^2 \ln [1 + \Delta^* (1 - y^*)] - \Delta^*(1 - y^*) - \frac{1}{2} \Delta^{*2}(1 - y^*)^2 \right\} \qquad \text{(III-33)}$$

where

$$u^* = \frac{u}{u_s} \qquad \text{(III-34)}$$

$$u_s = \left(\frac{ga^2}{z\nu}\right) \Delta^{*2} \qquad \text{(III-35)}$$

and

$$\Delta^* = \Delta/a \qquad \text{(III-36)}$$

The dimensionless distance measured from the interface in terms of the film thickness Δ is:

$$y^* = \frac{y}{\Delta} = \frac{a + \Delta - r}{\Delta} \qquad \text{(III-37)}$$

Expanding the logarithmic term in a Taylor series, we obtain a form valid for small Δ^*:

$$u^* = 1 - y^{*2} + \Delta^* y^* (1 - y^*) + \ldots\ldots \qquad \text{(III-38)}$$

The case of film flow down a plane wall is recoveres if $a \longrightarrow \infty$, $\Delta^* \longrightarrow 0$:

$$u^* = 1 - y^{*2} \qquad \text{(III-39)}$$

Equations (III-33) and (III-39) are plotted on Figure 7. It is common practice in treating diffusion into a falling film to assume penetrations

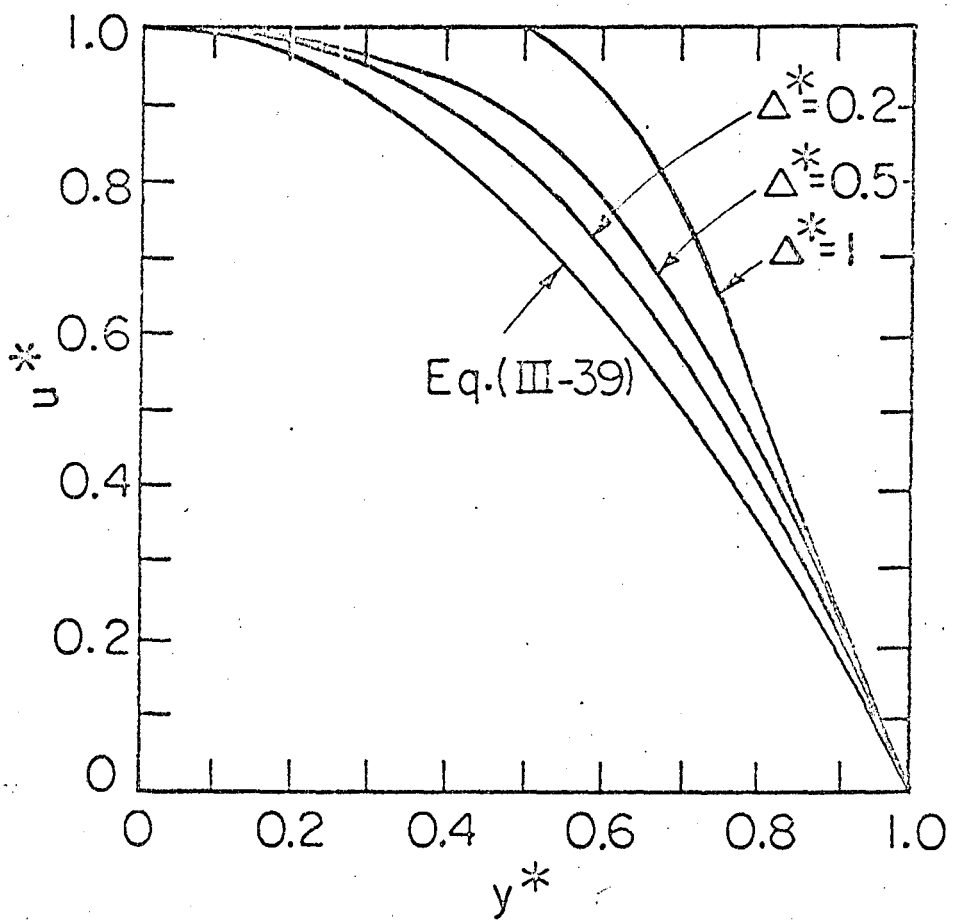
1.0
0.8
0.6
0.4
0.2
0
0
0.2
0.4
0.6
0.8
1.0
η^*
y^*
$\Delta^*=0.2$
$\Delta^*=0.5$
$\Delta^*=1$
Eq.(III-39)

Figure 7

sufficiently small to permit the approximation $u^* = 1$ in the convective term of the diffusion equation. As shown in Figure 7, this simplification is better for cylindrical film (where the velocity profile remains closer to $u^* = 1$ for greater penetration depths) than in the plane film case.

In our experiments the dimensionless film thickness Δ^* was on the order of 0.1 or less. The maximum deviation of the velocity profile from that for the plane case occurs when $y^* = 0.5$, at which portion equation (III-38) shows that the corrective factor is ~ 0.025. The fractional deviation from the plane profile is on the order of 3%. We have therefore employed the equation for flow down a plane wall in all calculations. In particular, the film thickness can be calculated by

$$Q = 2\pi a \int_0^{\Delta} u\,(y')\,dy' \qquad \text{(III-40)}$$

with $y = y^*\Delta$ and $u(y')$ given by equation (III-39), this gives:

$$\Delta^* = \frac{\Delta}{a} = \left(\frac{3\nu Q}{2\pi a^4 g}\right)^{1/3} \qquad \text{(III-41)}$$

The surface velocity is equal to u_s of equation (III-35) and the average velocity is 2/3 of the surface velocity.

2. Hydrodynamic Stability at Low Reynolds Number.[26]

A stagnant coating of liquid on a rod is unstable because the surface area is not a minimum. Infinitesimal disturbances will grow exponentially in amplitude, e^{qt}, where q is a function of the wave number, $\alpha = 2\pi\,(a + \Delta)\lambda$, of the disturbance, a geometrical factor, $a/(a + \Delta)$, and the physical properties of the liquid. When film is very thin, i.e., $[1 - a/(a + \Delta)] \ll 1$, inertial forces are unimportant and q is given by:

$$q = \frac{\mu}{\rho a^2} \cdot \mathcal{S} \cdot \phi_{visc.} \left(\alpha, \frac{a}{\Delta + a}\right)$$
$$\approx \frac{1}{3} (1 - \alpha^2)\, \alpha^2 \left[1 - \left(\frac{a}{\Delta + a}\right)\right]^3 \frac{\sigma}{\mu(a + \Delta)} \qquad \text{(III-42)}$$

A reasonable approximation for q at very low Reynolds number might be given by equation (III-42) with $\frac{a}{a + \Delta}$ now determined by the flow rate and physical properties instead of being arbitrary. At low Reynolds numbers the film will be thin compared to the rod diameter and the plane approximation can be used. The expression for q becomes

$$q \approx \frac{2}{3^{2/3}} (1 - \alpha^2)\, \alpha^2 \frac{\sigma\, \nu^{2/3} Re^{1/3}}{\rho g^{4/3} (a + \Delta)^3} \qquad \text{(III-43)}$$

where

$$Re = \frac{Q}{2\pi a \nu} \qquad \text{(III-44)}$$

For the most rapidly growing disturbance ($\alpha \approx 1/\sqrt{2}$), the amplitude increase in a length $u_s t = \ell$ is given by:

$$\exp\left\{\frac{1}{(2)3^{2/3}} \frac{\ell \sigma \nu^{2/3}\, Re^{1/3}}{\rho g^{4/3} (a + \Delta)^4}\right\} \qquad \text{(III-45)}$$

For the water - CO_2 experiment we have the following typical values:

$Q \approx 0.2$ cm^2/sec.	$\sigma \approx 70$ dynes/cm
$(a + \Delta) \approx 0.15$ cm	$\rho \approx 1$ gm/cm^3
$\nu \approx 0.01$ poise	$g \approx 980$ cm^2/sec

The Reynolds number is therefore

$$Re \approx \frac{0.2}{2\pi\ (0.15)\ (0.01)} \approx 20$$

In the molten salt runs, the typical values are:

$$Q \approx 0.2 \text{ cm}^2/\text{sec} \qquad \sigma \approx 120 \text{ dyne/cm}$$

$$(a + \Delta) \approx 0.15 \text{ cm} \qquad \rho \approx 1.6 \text{ gm/cm}^3$$

$$\nu \approx 0.02 \text{ poise} \qquad g \approx 980 \text{ cm}^2/\text{sec}$$

Therefore, $Re \approx \dfrac{0.2}{2\pi\ (0.15)\ (0.02)} \approx 10$

The amplification in the time for a particle on the surface to travel a distance of $\ell = 10$ cm will be $\approx \exp\ (0.6) \approx 1.8$ for the water experiments, and $\approx \exp\ (0.8) \approx 2.2$ for the molten salt experiments. Thus, an infinitesimal disturbance would only double in amplitude and would remain unnoticeable.

3. Diffusion in the Liquid Film.

(a) Simple Diffusion Case: The equation for simple diffusion in rectangular coordinates is:

$$D \frac{\partial^2 C}{\partial y^2} = u_s \left[1 - \left(\frac{y}{\Delta}\right)^2 \right] \frac{\partial C}{\partial z} \qquad \text{(III-46)}$$

with boundary conditions

$$C\ (y,\ o) = C_o \qquad \text{(III-47)}$$

$$C\ (o,\ z) = C_i \qquad \text{(III-48)}$$

and $\left(\dfrac{\partial C}{\partial y}\right)_\Delta = 0$ (III-49)

Define the dimensionless terms

$$C^* = \frac{C - C_i}{C_o - C_i} \qquad \text{(III-50)}$$

$$z^* = \frac{Dz}{\Delta^2\ u_s} \qquad \text{(III-51)}$$

Equation (III-46) becomes

$$\frac{\partial^2 C^*}{\partial y^{*2}} = (1 - y^{*2})\ \frac{\partial C^*}{\partial z^*} \qquad \text{(III-52)}$$

with boundary conditions

$$C^* (y^*, o) = 1 \qquad \text{(III-53)}$$

$$C^* (o, z^*) = 0 \qquad \text{(III-54)}$$

and

$$\left(\frac{\partial C^*}{\partial y^*}\right)_{y^*=1} = 0 \qquad \text{(III-55)}$$

The average concentration at z can be shown to be:

$$\bar{C}^* = 1 - \frac{3}{2} \int_o^{z^*} \left(\frac{\partial C^*}{\partial y^*}\right) dz^{*\prime} \qquad \text{(III-56)}$$

or the average mass transfer coefficient over a length ℓ is:

$$\frac{\bar{k}\,\Delta}{D} = \frac{2}{3} \; \frac{1 - \bar{C}^*}{\ell^*} \qquad \text{(III-57)}$$

where ℓ^* is given by equation (III-51) with $z = \ell$. The solution given by Pigford[20] is:

$$\bar{C}^* = 0.7857 \exp(-5.121z^*) + 0.1001 \exp(-39.31z^*) + 0.0360 \exp(-105.6z^*) + 0.0181 \exp(-204.7z^*) \qquad \text{(III-58)}$$

For small depths of penetration (short contact time), the diffusion process occurs near the surface, and two simplifications are possible:

(1) The velocity field can be approximated by its constant value at the surface ($u \approx u_s$), especially for the cylindrical case.

(2) The presence of the wall is not felt, thus the gradient boundary conditions at $y = \Delta$ can be replaced by $C = C_o$ at $y \longrightarrow \infty$.

For an infinite depth approximation, equation (III-52) becomes

$$\frac{\partial C^*}{\partial z^*} = \frac{\partial^2 C^*}{\partial y^{*2}} \qquad \text{(III-59)}$$

with boundary conditions,

$$C^* (y^*, o) = 1 \qquad \text{(III-60)}$$

$$C^* (\infty, z^*) = 1 \qquad \text{(III-61)}$$

$$C^* (o, z^*) = 0 \qquad \text{(III-62)}$$

Substitution of the solution for this case[56] into equation (III-56) yields:

$$\bar{C}^* = 1 - \frac{3}{\sqrt{\pi}} \sqrt{z^*} \qquad \text{(III-63)}$$

A comparison of these two solutions is shown in Figure 8. The approximate solution is quite satisfactory up to $(1 - C^*) \approx 0.65$. In terms of directly measurable quantities, equation (III-63) is:

$$1 - \bar{C}^* = [3^{1/3} . 2^{7/6} . \pi^{1/6} . g^{1/6}] \frac{\sqrt{D\ell}\ a^{2/3}}{\nu^{1/6}\ Q^{2/3}} \qquad \text{(III-64)}$$

or

$$1 - \bar{C}^* = \frac{12.35 \sqrt{D\ell}\ a^{2/3}}{\nu^{1/6}\ Q^{2/3}} \qquad \text{(III-65)}$$

where all parameters are in units of cm and sec. The average mass transfer coefficient in the liquid film is obtained from equation (III-57).

$$\bar{k} = \frac{2}{\sqrt{\pi}} \sqrt{\frac{Du_s}{\ell}} \qquad \text{(III-66)}$$

(b) Surface Reaction. Consider a reversible reaction between UCl_4 in the liquid and Cl_2 in the gas phase which occurs only at the gas-liquid interface. UCl_6 is assumed completely soluble in the liquid:

$$UCl_4\ (l) + Cl_2\ (g) \underset{}{\overset{k_r}{\rightleftharpoons}} UCl_6\ (l)$$

with an equilibrium constant

$$K = \frac{C_6}{P\ C_4} \qquad \text{(III-67)}$$

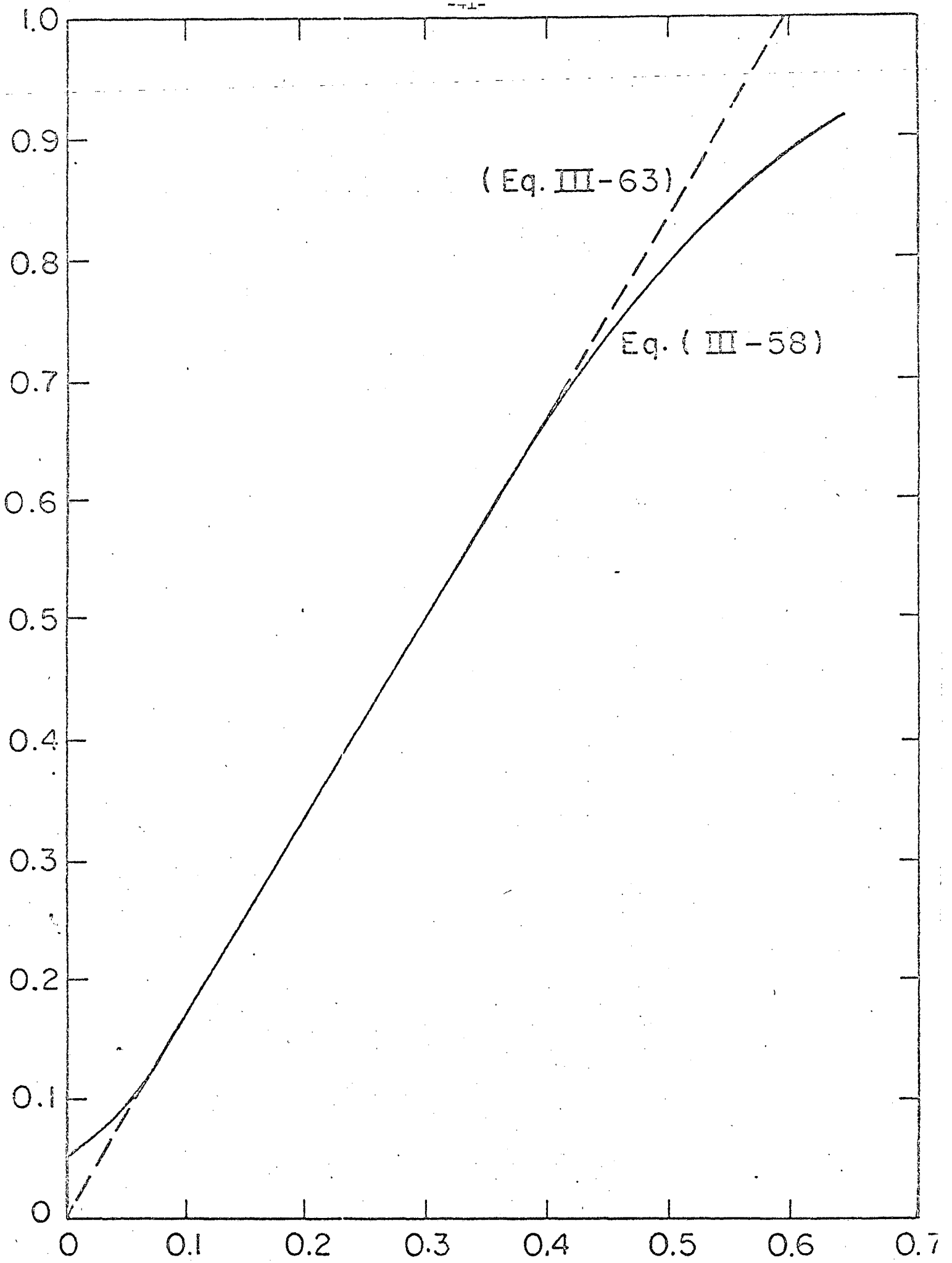
1.0
0.9
0.8
0.7
0.6
0.5
0.4
0.3
0.2
0.1
0
0
0.1
0.2
0.3
0.4
0.5
0.6
0.7
(Eq. III-63)
Eq. (III-58)

Diffusional resistance in the gas phase is neglected, and the partial pressure of Cl_2 at the interface assumed equal to its value in the gas bulk phase. The overall rate of conversion depends upon the diffusional resistance in the liquid film and the surface reaction rate. The transfer of UCl_4 in the liquid is given by:

$$u_s \frac{\partial C_4}{\partial z} = D_4 \frac{\partial^2 C_4}{\partial y^2} \qquad \text{(III-68)}$$

with boundary conditions

$$\begin{aligned} &\text{at } z = 0, \quad C_4 = C_{4o} \\ &\text{at } y = \ , \quad C_4 = C_{4o} \\ &\text{at } y = 0, \quad D_4 \left.\frac{\partial C_4}{\partial y}\right|_o = k_r p \left(C_4 - \frac{C_6}{Kp}\right) \end{aligned} \qquad \text{(III-69)}$$

The reaction is assumed to be first order in UCl_4 concentration and chlorine partial pressure.

For UCl_6 we have

$$u_s \frac{\partial C_6}{\partial z} = D_6 \frac{\partial^2 C_6}{\partial y^2} \qquad \text{(III-70)}$$

with boundary conditions

$$\begin{aligned} &\text{at } z = 0, \quad C_6 = C_{6o} \\ &\text{at } y = \ , \quad C_6 = C_{6o} \\ &\text{at } y = 0, \quad D_6 \left(\frac{\partial C_6}{\partial y}\right)_o = k_r p \left(C_4 - \frac{C_6}{Kp}\right) \end{aligned} \qquad \text{(III-71)}$$

Assuming equal diffusivities, $D_4 = D_6 = D$, and the UCl_6 to be non-volatile, and letting $C = C_4 + C_6$, we have by adding equations (III-68) and (III-70)

$$u_s \frac{\partial C}{\partial z} = D \frac{\partial^2 C}{\partial y^2} \qquad \text{(III-72)}$$

with boundary conditions

$$C\ (y,\ o) = C_o$$

$$C\ (y,\ \infty) = C_o \qquad \text{(III-73)}$$

$$D\left(\frac{\partial C}{\partial y}\right)_{y\ =\ o} = 0$$

The only solution is $C = C_o$ = constant = $C_4 + C_6$. Consequently, the UCl_4 boundary condition at y = o becomes:

$$D\left(\frac{\partial C_4}{\partial y}\right)_o = k_r p\left[C_4\left(1 + \frac{1}{Kp}\right) - \frac{C_o}{Kp}\right]$$

$$= k_r p\ C_4\left[1 - \frac{1}{Kp}\left(\frac{C_o}{C_4} - 1\right)\right] \qquad \text{(III-74)}$$

If equilibrium is assumed at the interface, C_4 is a constant = $C_4^{equil.}$, where at y = o:

$$K = \frac{C_6^{eq.}}{p\ C_4^{eq.}} = \frac{C_o - C_4^{eq.}}{p\ C_4^{eq.}}\ ;\ \frac{C_4^{eq.}}{C_o} = \frac{1}{1 + Kp} \qquad \text{(III-75)}$$

Defining the dimensionless variable

$$C^* = \frac{C_4 - C_4^{eq.}}{C_{4o} - C_{4o}^{eq.}} = \frac{C_4/C_o - C_4^{eq.}/C_o}{C_{4o}/C_o - C_4^{eq.}/C_o} \qquad \text{(III-76)}$$

and using the variables z^* and y^*, we have the same dimensionless equation (III-59). The boundary conditions (III-60) and (III-61) still apply, but at y = o we have

$$\frac{\partial C^*}{\partial y^*}_o = \left(\frac{1 + Kp}{Kp}\right) k_r^*\ C^*(o,\ z^*) = k_r^{*\prime}\ C^*(o,\ z^*) \qquad \text{(III-77)}$$

where $k_r^* = \dfrac{k_r p\ \Delta}{D}$

If $k_r^* \longrightarrow \infty$, $C^*(o, z) = 0$ and the solution reduces to the straight desorption case.

The solution to equation (III-59), subject to equations (III-60), (III-61) and (III-77) can be obtained from the analogous heat conduction problem:[13]

$$C^*(y^*, z^*) = \operatorname{erf}\left(\frac{y^*}{2\sqrt{z^*}}\right) + \exp\left[k_r^{*\prime} y^* + k_r^{*\prime} z^*\right] \operatorname{erfc}\left(\frac{y^*}{2\sqrt{z^*}}\right) + k_r^{*\prime}\sqrt{z^*} \qquad \text{(III-78)}$$

Substititing equation (III-78) into (III-56), the average concentration is:

$$\bar{C}^* = 1 - \frac{3}{\sqrt{\pi}}\sqrt{z^*}\, F\left(k_r^{*\prime}\sqrt{z^*}\right) \qquad \text{(III-79)}$$

where

$$F(k_r^{*\prime}\sqrt{z^*}) = 1 - \frac{\sqrt{\pi}}{2k_r^{*\prime}\sqrt{z^*}}\left[1 - e^{k_r^{*\prime 2} z^*} . \operatorname{erfc}(k_r^{*\prime}\sqrt{z^*})\right] \qquad \text{(III-80)}$$

Equation (III-80) is plotted in Figures 9 and 10.

For diffusion limited reaction ($k_r \longrightarrow \infty$):

$$\lim_{k_r^{*\prime}\sqrt{z^*} \to \infty} F = 1 - \frac{\sqrt{\pi}}{2k_r^{*\prime}\sqrt{z^*}} + \frac{1}{2k_r^{*\prime 2} z^*} + \ldots \qquad \text{(III-81)}$$

For complete diffusional control, F = 1 and equation (III-79) reduces to equation (III-63).

At the other asymptote, for very slow reaction:

$$\lim_{k_r^{*\prime}\sqrt{z^*} \to 0} F = \frac{\sqrt{\pi}}{2} k_r^{*\prime}\sqrt{z^*} \qquad \text{(III-82)}$$

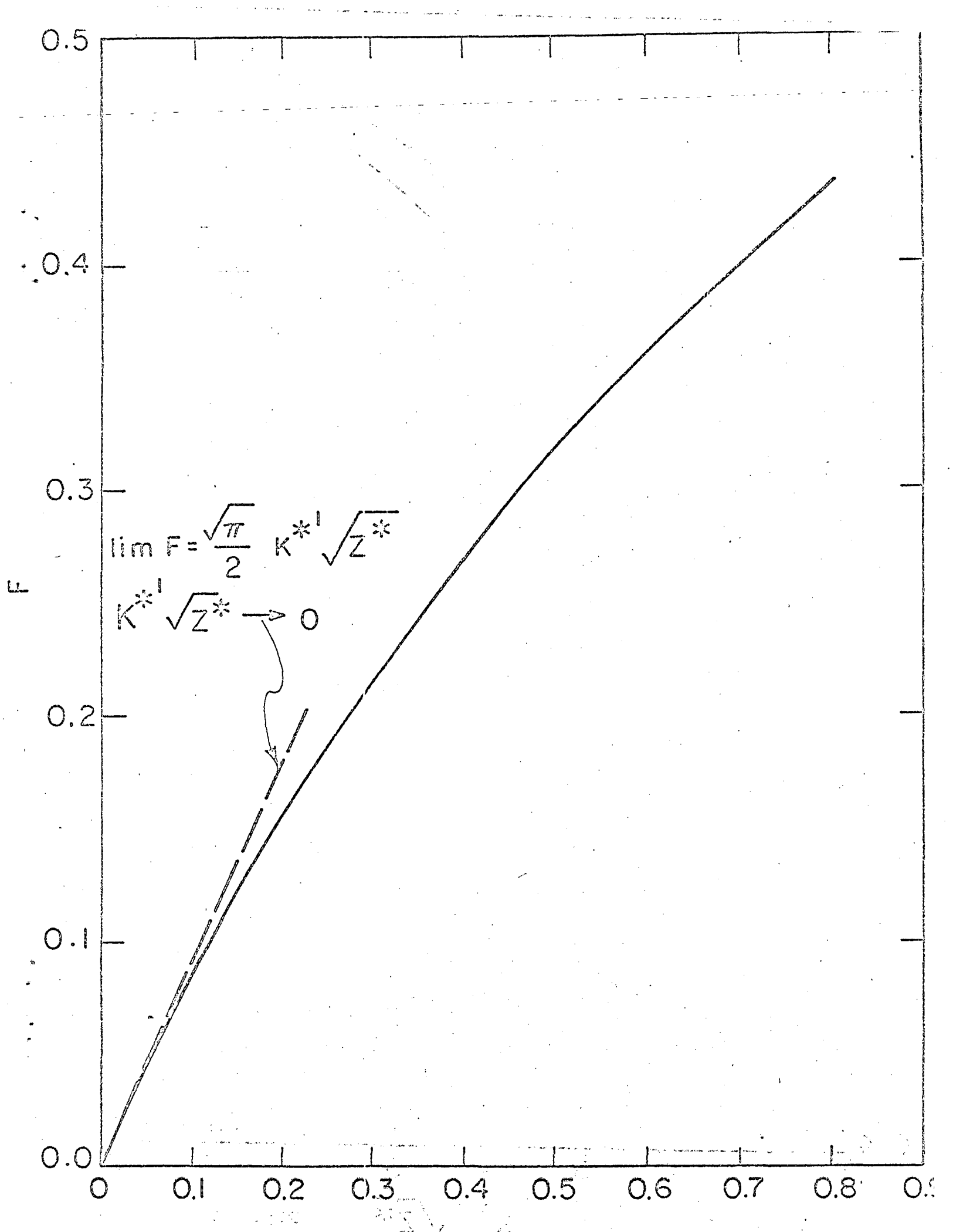
0.5
0.4
0.3
0.2
0.1
0.0
F
$\lim F = \frac{\sqrt{\pi}}{2} K^{*'} \sqrt{Z^*}$
$K^{*'} \sqrt{Z^*} \rightarrow 0$
0
0.1
0.2
0.3
0.4
0.5
0.6
0.7
0.8

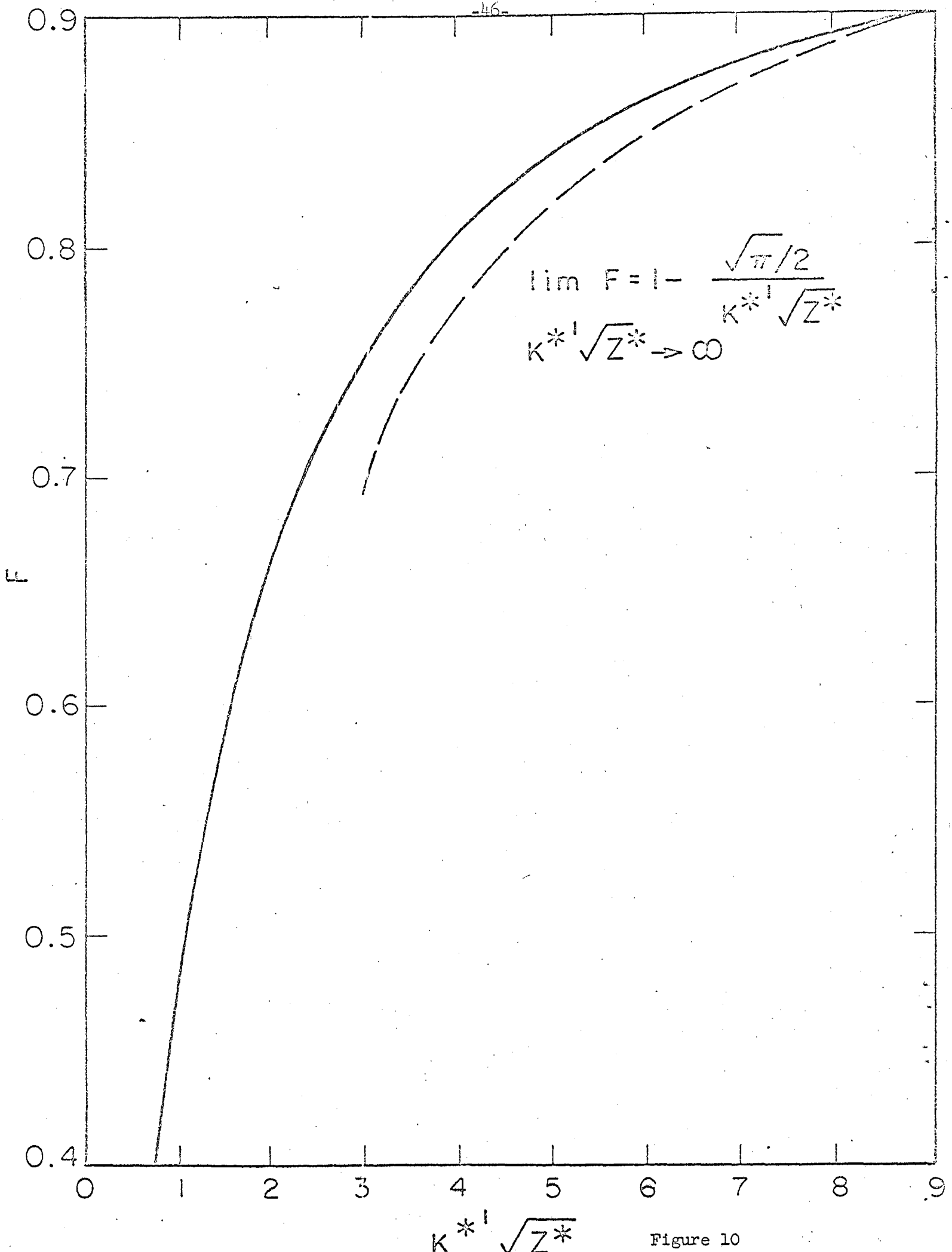
0.9
0.8
0.7
0.6
0.5
0.4
F
0
1
2
3
4
5
6
7
8
9
$K^{*'}\sqrt{Z^*}$
$\lim_{K^{*'}\sqrt{Z^*}\to\infty} F = 1 - \frac{\sqrt{\pi}/2}{K^{*'}\sqrt{Z^*}}$

Figure 10

Inserting equation (III-82) into (III-79):

$$\lim_{k_r^{*\prime}\sqrt{z^*} \to 0} \bar{C}^* = 1 - \frac{3}{2} k_r^{*\prime} z^* = 1 - \left(\frac{1 + Kp}{K}\right) \frac{k_r}{Q} (2\pi a \ell) \qquad \text{(III-83)}$$

In equation (III-83), we have set $z = \ell$, the length of the rod. In the reaction-limited case, $\bar{C}^*$ varies as $^1/Q$, while in the diffusion-limited case [equation (III-65)], $\bar{C}^*$ varies as $^1/Q^{2/3}$.

D. Comparison of Gas and Liquid Phase Resistances

In the previous section, the gas phase resistance was assumed negligible compared to either the surface chemical rate or the liquid phase resistance. While the assumption cannot be precisely assessed, we can estimate the effect for a rapid surface reaction.

Consider a very fast, irreversible chemical reaction occurring at the interface which forms a product completely soluble in the liquid phase. Since the reaction is rapid and irreversible, either the liquid or gas phase concentration must be zero at the interface. That component which exhibits the slowest transfer rate will be depleted at the surface. We will compute the transfer rates of liquid component A from a bulk concentration C_L to a zero interfacial value and of gas phase component B from a bulk partial pressure P_g to zero interfacial partial pressure. The rate will be determined by the smaller of these two rates.

From equation (III-66) the liquid phase rate is:

$$\bar{N}_L = \bar{k}_L C_L = 1.13\, C_L \sqrt{\frac{D_\ell u_s}{\ell}} \qquad \text{(III-84)}$$

where D_ℓ is the diffusivity of A in the liquid.

From equation (III-29), the gas phase transfer rate is:

$$\bar{N}_g = \bar{k}_g \frac{P_g}{RT} = \frac{0.843\ P_g}{RT} \sqrt{\frac{D_g u_s}{\ell}} \qquad \text{(III-85)}$$

where D_g is the diffusivity of B in the gas phase, and Sc has been taken as unity. The ratio is:

$$\frac{\bar{N}_g}{\bar{N}_L} = 0.75 \frac{P_g}{RT\ C_L} \sqrt{\frac{D_g}{D_\ell}} \qquad \text{(III-86)}$$

For comparison, consider the following values typical of our experiments with UCl_4 dissolved in the fused LiCl-KCl eutectic and a 50% Cl_2-Argon gas phase:

P_g = 0.5 atm

T = 873°K

C_L = 0.2 mole/liter (5 wt.%)

D_ℓ = 0.5 x 10^{-5} cm^2/sec

D_g = 0.47 cm^2/sec

The calculated ratio is ~ 8, which indicates that liquid phase diffusion resistance is controlling. The fractional change in gas reactant partial pressure through the gas boundary layer is ≃ 0.12. If the reaction rate also contributes to the overall resistance, the effect of gas phase resistance will be even less.

IV. EXPERIMENTAL WORK

A. Handling of Fused LiCl-KCl Eutectic

Two fused chlorine eutectics, binary LiCl-KCl (59 mole % LiCl, m.p. 351°C) and ternary NaCl-KCl-$MgCl_2$ (30, 20, and 50 mole %, respectively; m.p. 396°C) were used extensively at Brookhaven National Laboratory in connection with the Liquid Metal Fuel Reactor program. The binary eutectic was selected for this work because of its lower melting point.

Corrosion tests on potential materials of construction for the binary eutectic showed that only 347 S.S. was not attacked.[48] Little or no Ni was found in corrodent analysis in the tests of Ni – bearing alloys. This fact suggests that high Ni alloys may be superior to all other materials tested. No cast pipes or fittings can be used for fused salt service because they cannot be made leak-tight. Air and moisture from the atmosphere reacts with the salt to produce extensive corrosion.

An all-welded system is preferred for handling the molten eutectic. Welds should be sound and those in contact with the molten salt should be full-penetration welds. Satisfactory welds can be made on 347 S.S. by the Heliarc process.

Corrosion by the salt is greatly enhanced by the presence of oxidizing impurities. Oxide-free interior surfaces are therefore required on all vessels and process piping. Three methods of cleaning, namely, electropolishing, hydrogen firing, and sandblasting have been used successfully to clean vessels and piping. Sandblasting was found to be the most satisfactory, being applicable to all types of container systems.

The presence of Cl_2 gas at high temperatures compounds the corrosion problems in metal containers (Nickel and 347 S.S.). Quartz and high-

temperature glass systems, however, were found to be quite satisfactory, and were employed in all but the chlorine solubility studies.

B. Solubility Studies

1. Previous Work.

Solubility of gases in molten salts have been the subject of recent investigations. Newton[42] performed some preliminary measurements of the solubility of xenon in molten salt mixtures. The solubility of xenon in the KNO_3-$NaNO_3$ eutectic varied from 8×10^{-8} to 10^{-7} moles Xe/(cm^3 of solvent) (atmosphere) between 260 and 450°C. Burkhard and Corbett[12] determined the solubility of water in molten LiCl-KCl mixtures and presented an approximate value of the solubility of HCl at 480°C in a mixture containing 60% LiCl.

Solubilities of noble gases in molten fluorides have been systematically studied at Oak Ridge.[7,27] The technique consisted in saturating the salt with the test gas, transfer of the solution to an isolated section of the apparatus, recovery of the dissolved gas by sparging with another inert gas, and determination of the recovered gas by mass spectrometry. Henry's Law constants at 600°C in a ZrF_4-NaF mixture (47-53 mole%) were $21.6 \pm 1 \times 10^{-8}$, $11.3 \pm 0.3 \times 10^{-8}$, $5.06 \pm 0.15 \times 10^{-8}$ and $1.94 \pm 0.2 \times 10^{-8}$ moles of solute/(cm^3 of solution) (atmosphere) for He, Ne, Ar and Xe, respectively.

Grimes et al.,[28] using the same technique, recently measured the solubility of hydrogen fluorude in fluoride mixtures. The dissolved HF was stripped from the salt, absorbed in a standard solution of aqueous KOH, and determined by back titration with standard acid

solution. Henry's Law constants in moles HF per cc. of solution per atmosphere at 600, 700 and 800°C are $1.23 \pm 0.04 \times 10^{-5}$, $0.93 \pm 0.02 \times 10^{-5}$, and $0.73 \pm 0.01 \times 10^{-5}$, respectively in $NaF-ZrF_4$ (53 mole % NaF). No information regarding solubilities of chlorine and uranium hexachloride in the molten LiCl-KCl eutectic or of UF_6 and F_2 in fluoride melts appears to have been published.

2. Solubility of Cl_2 in Fused LiCl-KCl Eutectic

(a) Apparatus. The solubility apparatus is shown schematically in Figure 11. It consists of a melt tank where the LiCl-KCl eutectic is prepared and then saturated with chlorine gas, and a stripping section where the dissolved gas is stripped from the melt by argon. The apparatus is placed in a standard chemical fume hood and is operated with the front window almost completely closed.

The melt tank (Figure 12) was fabricated from a 16 inch piece of 3-1/2" Schedule 40 347 S.S. pipe. The bottom was sealed with a 1/2" weld lid and the top with a ring type vacuum flange. Pipe risers for gas connections, a 1" charge port, a movable liquid-level probe, and a thermocouple well are provided at the top of the tank. The stripping section consists of a similar vessel except that the top flange is only provided with gas connections.

The melt tank is connected to the stripping section by a length of 3/8" O.D. 347 S.S. tubing which is welded through the bottoms of both vessels. This transfer tube serves as a simple freeze valve which can be heated by a heating tape wrapped around it or cooled as desired. The entire transfer section is insulated by layers of asbestos tape.

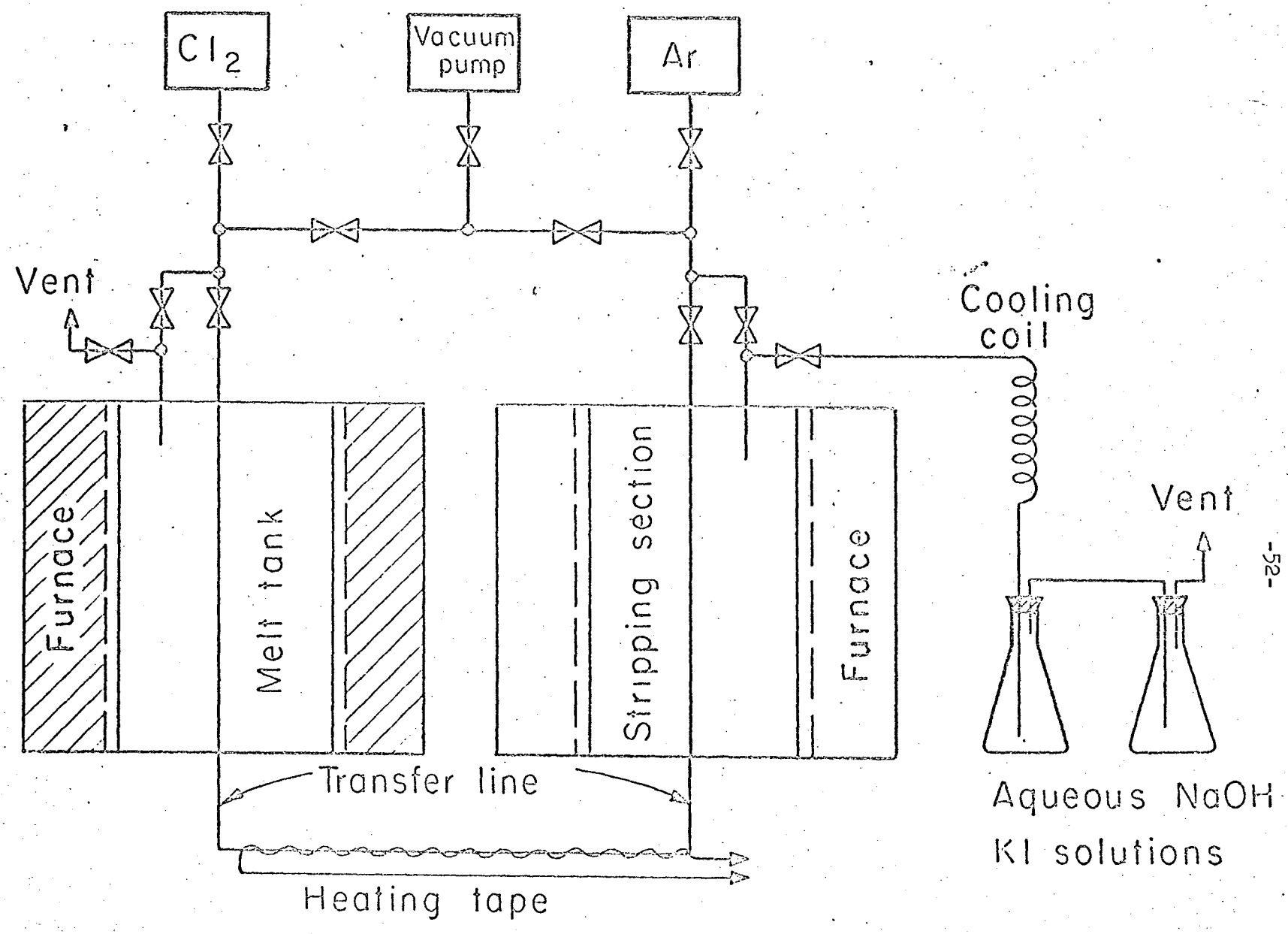
Cl_2
Vacuum pump
Ar
Vent
Cooling coil
Furnace
Melt tank
Stripping section
Furnace
Vent
Transfer line
Heating tape
Aqueous NaOH
KI solutions

Figure 11

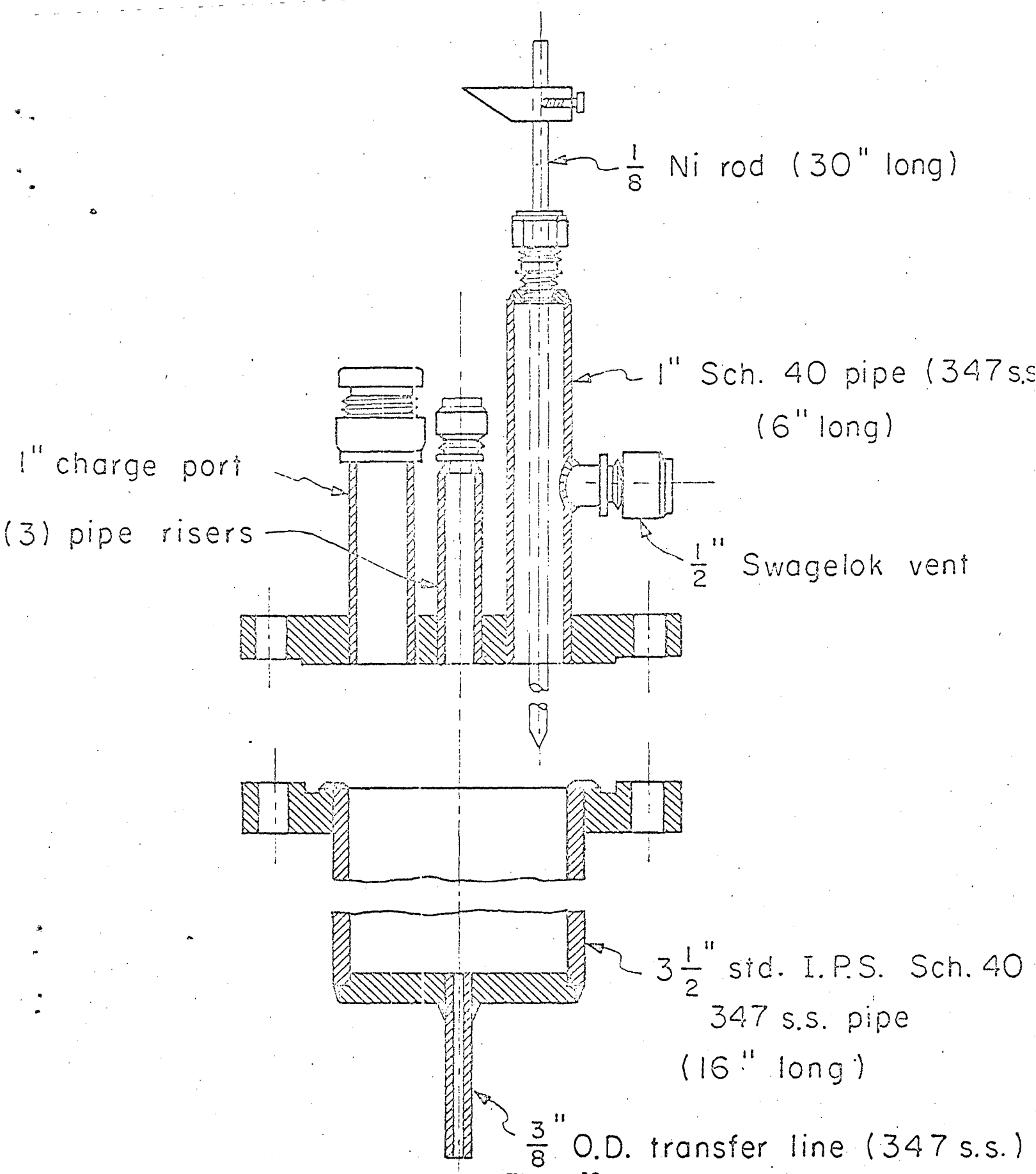
1/8 Ni rod (30" long)
1" Sch. 40 pipe (347 s.s
(6" long)
1" charge port
(3) pipe risers
1/2" Swagelok vent
3 1/2" std. I.P.S. Sch. 40
347 s.s. pipe
(16" long)
3/8" O.D. transfer line (347 s.s.)

Figure 12

Both vessels are surrounded by "Hevi-Duty" resistance furnaces. A chromel-alumel thermocouple in the melt tank activates a Brown electronic recorder to provide temperature measurements of the melt. Temperature control is achieved by means of Brown pyrovane controllers activated by chromel-alumel thermocouples in the furnaces. The temperatures were probably known to ± 5°C.

The liquid-level probe is simply a 30-inch piece of 1/8" polished nickel rod sharpened to a point. The rod protrudes through a swagelok fitting, with a nylon cap and teflon ferrules which act as insulators, and completes an electrical circuit on contact with the liquid surface. This permits measurement of the liquid level in the melt tank before and after transfer. The indicator is a piece of brass cut to a knife edge and drilled to slide over the nickel rod. It is held in place by a set screw and positioned for convenient measurement on a suitable scale.

(b) Materials. Argon was obtained in cylinders from the Linde Air Products Co. The chlorine gas was obtained from the Mathieson Gas Co. The binary eutectic was prepared from reagent grade LiCl and KCl from the Baker Chemical Co.

(c) Experimental Procedure. A batch of the eutectic was loaded into the melt tank through the charge port and melted under vacuum. A 1/2 hp. Kinney Model KC-5 vacuum pump was used to evacuate the vessel. The temperature was kept at 200°C overnight to ensure proper drying of the salts. The melt tank was then isolated from the empty stripping section by establishing the frozen seal. At 400°C the molten charge was mixed thoroughly by sparging with argon. It was then saturated with chlorine gas at the desired temperature and pressure. Chlorine sparge

times varied from one to four hours. After sparging was discontinued, the chlorine gas was maintained at pressure as a covering atmosphere. The liquid level was then measured by use of the electrical probe.

Meanwhile the stripping section, which had continuously been flushed with a stream of argon, was closed and filled with argon at a predetermined pressure such that about half the salt would transfer from the melt tank when the frozen seal was removed. The frozen seal was melted and the melt was allowed to transfer until hydrostatic equilibrium was achieved. The frozen seal was immediately re-established and the final liquid level in the melt tank was determined.

The dissolved chlorine gas was stripped from the salt in the stripping section and absorbed in an aqueous NaOH solution containing KI. This sample was then acidified with HCl and the liberated iodine titrated with sodium thiosulfate to give the amount of dissolved Cl_2. The volume of salt transferred is obtained from the initial and final levels in the melt tank. The solubility of chlorine gas in the molten eutectic is obtained from this volume and the amount of dissolved Cl_2 recovered.

(d) Experimental Results. Severe corrosion of certain components in the melt tank limited the study to four runs, two each at 400 and 500°C. No measureable quantity of chlorine gas was observed in the binary eutectic. The limit of the quantitative determination of chlorine was 2×10^{-6} gmole, therefore, the solubility of Cl_2 in the molten salt at a saturation pressure of about 1 atmosphere is less than 4×10^{-9} g mole/cc. of melt.

The results are shown in Table VI.

Table VI. Solubility of Cl_2 in molten LiCl-KCl

Run	Sparge time, hrs.	Temp. °C	Sat'n Press atm.	Vol. of Salt, cc.	Amt. Cl_2 dissolved gmole	Solubility gmole/cc
1	1	400	1.17	525	$< 2 \times 10^{-6}$	$< 4 \times 10^{-9}$
2	3	400	1.18	530	$< 2 \times 10^{-6}$	$< 4 \times 10^{-9}$
3	2	500	1.12	515	$< 2 \times 10^{-6}$	$< 4 \times 10^{-9}$
4	4	500	1.10	522	$< 2 \times 10^{-6}$	$< 4 \times 10^{-9}$

C. Absorption of CO_2 in Water

1. Apparatus.

The absorption set-up is shown in Figure 13. It consists of an absorption column, a water supply, a gas system and titration apparatus.

The absorption column is shown in Figure 14. It consists of a 1" diameter glass tubing divided into two sections. The constant head section is 6" long and has a ground glass fitting at the bottom. The 4" reaction chamber tapers down to a 45° funnel-like bottom with a 1/2" long tip (3.5 mm I.D.), and is provided with 6 mm O.D. gas inlet and outlet tubes. A 3 mm glass rod, with a ground seat valve, extends through the reaction chamber about 1/8" into its funnel tip. A simple arrangement consisting of a Swagelok fitting and a piece of rubber tubing is used to move the rod up and down the ground fitting to control the film flow down the rod. The apparatus is essentially the same as the one used in the chlorination experiment.

The water supply is simply a 100 ml. burette filled with distilled water. The gas system consists of CO_2 and argon cylinders, and a saturator. The saturation serves a dual purpose. It saturates the CO_2 with H_2O vapor before it is fed into the reaction chamber, and provides samples of water saturated with CO_2,

The titration apparatus consists of $Ba(OH)_2$ solution stored in a burette with an ascarite tube on top to prevent contact with CO_2 in the air, and a microburette with standard HCl solution.

2. Materials.

Standard solutions of $Ba(OH)_2$ and HCl were prepared. HCl was diluted to a concentration of 0.1N from a 1N standard solution.. The

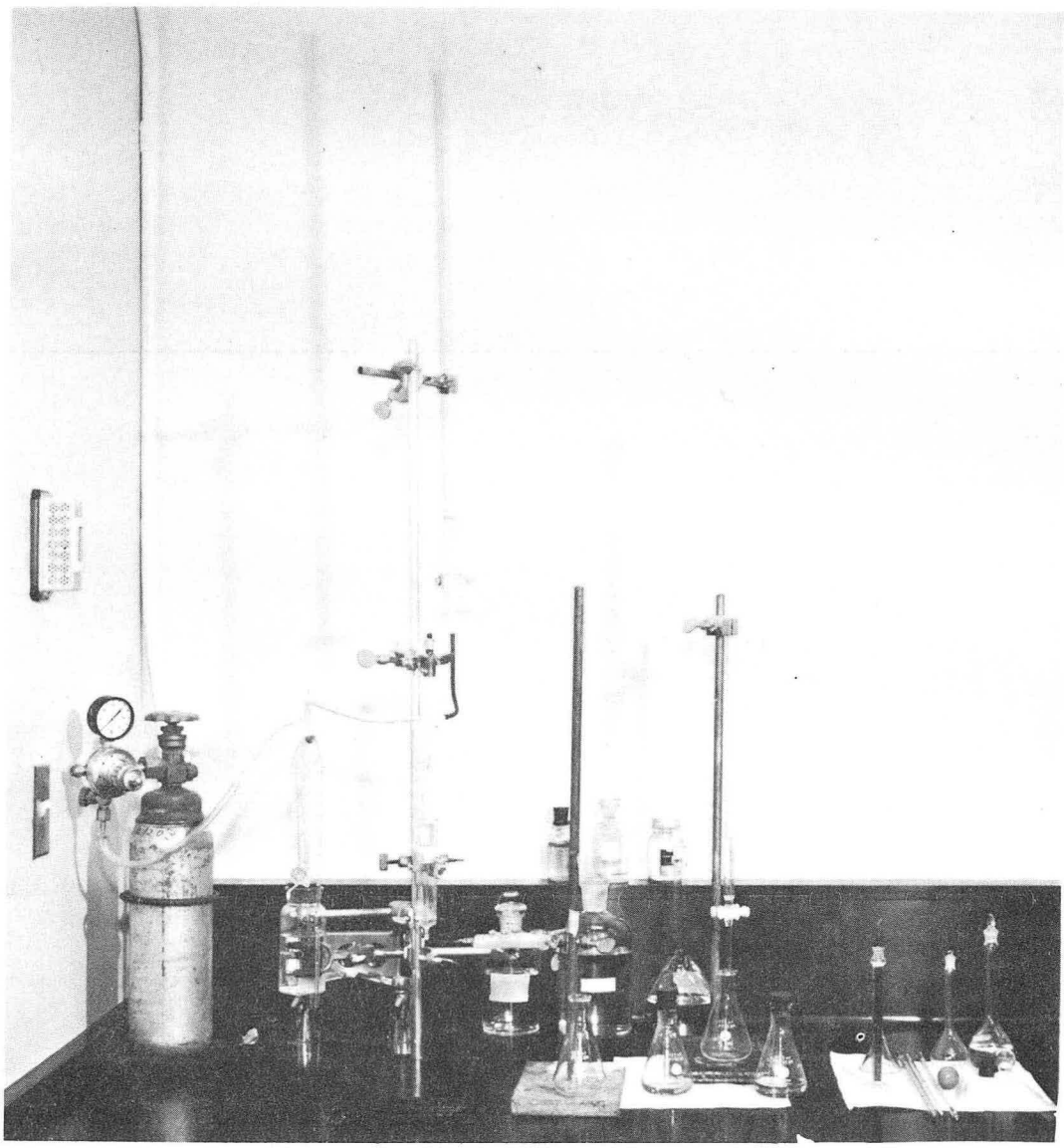

ZN 4982

Fig. 13

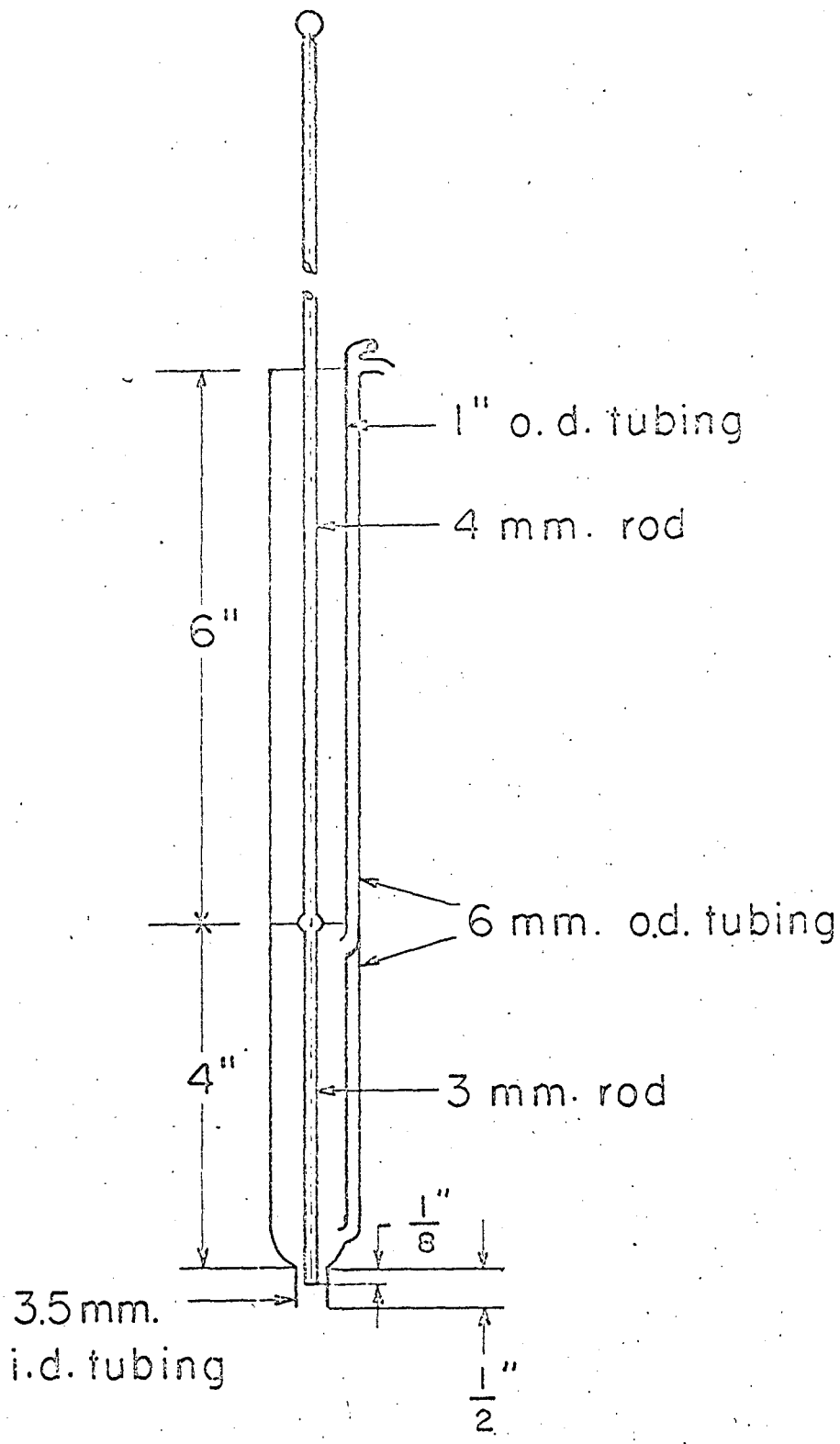
1" o. d. tubing
4 mm. rod
6"
6 mm. o.d. tubing
4"
3 mm. rod
1/8"
3.5 mm.
i.d. tubing
1/2"

Figure 14

concentration $Ba(OH)_2 \cdot 8\ H_2O$ was initially 0.02M. However, before the experiment it was titrated with HCl and found to be 0.0198M.

The CO_2 gas was obtained from the Mathieson Gas Company. Distilled water was used throughout. Phenolphthalein was the indicator used in the titration.

3. Experimental Procedure.

A constant head of H_2O was maintained in the upper section of the absorption column. The reaction chamber was filled with an atmosphere of "H_2O-saturated" CO_2 gas. The ground glass fitting was opened slightly to allow film flow down the rod.

Flow rates of the water film were obtained by collecting the sample in a 1 cc. cup and measuring the time. For each flow rate, two measurements were taken before sampling and one after. The three values were averaged to give the flow rate for each run.

8 cc. samples were collected just inside the funnel tip with a syringe. Extreme care was needed to prevent the effluent from contacting air, which desorbs some of the CO_2. The $Ba(OH)_2$ solution was then transferred into an Erlenmeyer flask from the burette. The amount of $Ba(OH)_2$ solution used depended on the film flow rate. 4 cc. of the sample was then injected under the surface of the $Ba(OH)_2$ solution. Two drops of phenolphthalein were added and the Erlenmeyer flask immediately put under an argon atmosphere to prevent CO_2 absorption from the air. The excess $Ba(OH)_2$ was then titrated with standard HCl. The remaining 4cc. sample was similarly analyzed.

4. Experimental Results.

The absorption of CO_2 in water was measured at different film flow

rates. The conditions used in the measurements were:

CO_2 pressure	= 1 atm.
temperature	= 22.5°C
length of rod(l)	= 8.25 cm
rod radius (a)	= 0.15 cm
film flow rate(Q)	= 1.85 - 31.58 cm^3/min

The results are summarized in Table VII, and plotted in Figure 15. The theoretical plot is given by equation (III-65).

D. The Chlorination of UCl_4

1. Apparatus.

The chlorination equipment is shown in Figures 16, 17 and 18. It consists of a quartz reaction column (Figure 19) enclosed by a resistance furnace, and a gas system.

The reaction column is similar to that used in the CO_2 absorption experiment (Figure 14), except that a short length of 14 mm tubing is fused to the bottom and provided with a 6 mm HCl gas inlet tube. This prevents contact of the UCl_4 solution dropping out of the funnel tip with the surrounding air. The gas system includes drierite columns and flowmeters.

The chemical analysis apparatus (Figure 20) includes Pb columns and a microburette.

2. Materials.

The Cl_2, HCl and mixed gases were obtained from Mathieson Gas Company. Reagent grade LiCl and KCl were used throughout. The UCl_4 salt was supplied by Argonne National Laboratory. Hydrochloric acid, Pb powder, $FeCl_3$ solution, concentrated H_3PO_4, standard $K_2Cr_2O_7$, and diphenylamine sulfonate indicator were used in the chemical analysis of uranium.

Table VII. Absorption of CO_2 in Water Film, t = 22.5°C, P_{CO_2} = 1 atm.

Run	Flow Rate (cc/min)	Concentration (moles CO_2)	$\phi = \frac{\bar{C} - C_o}{C_i - C_o}$	$\frac{1}{Q\ 2/3}$	$\phi\ Q\ 2/3$
1		0.001			
2	Blanks	0.0004			
3		0.00075			
		Ave. = 0.007(C_o)			
4	H_2O	0.13985			
5	Saturated	0.13965			
6	w/CO_2	0.13800			
		Ave. = 0.1393(C_i)			
7	1.85	0.1084	0.777	0.663	1.17
8	2.64	0.0921	0.659	0.524	1.26
9	4.36	0.0680	0.486	0.375	1.30
10	7.50	($\bar{C}$) 0.0450	0.320	0.261	1.23
11	8.18	0.0440	0.312	0.246	1.27
12	10.80	0.0377	0.270	0.205	1.31
13	13.64	0.282	0.198	0.175	1.13
14	31.58	0.0212	0.148	0.100	1.48

Ave. = 1.29 ± 0.08

Theoretical Slope = 1.41

% error = 8.5

% precision = 6.2

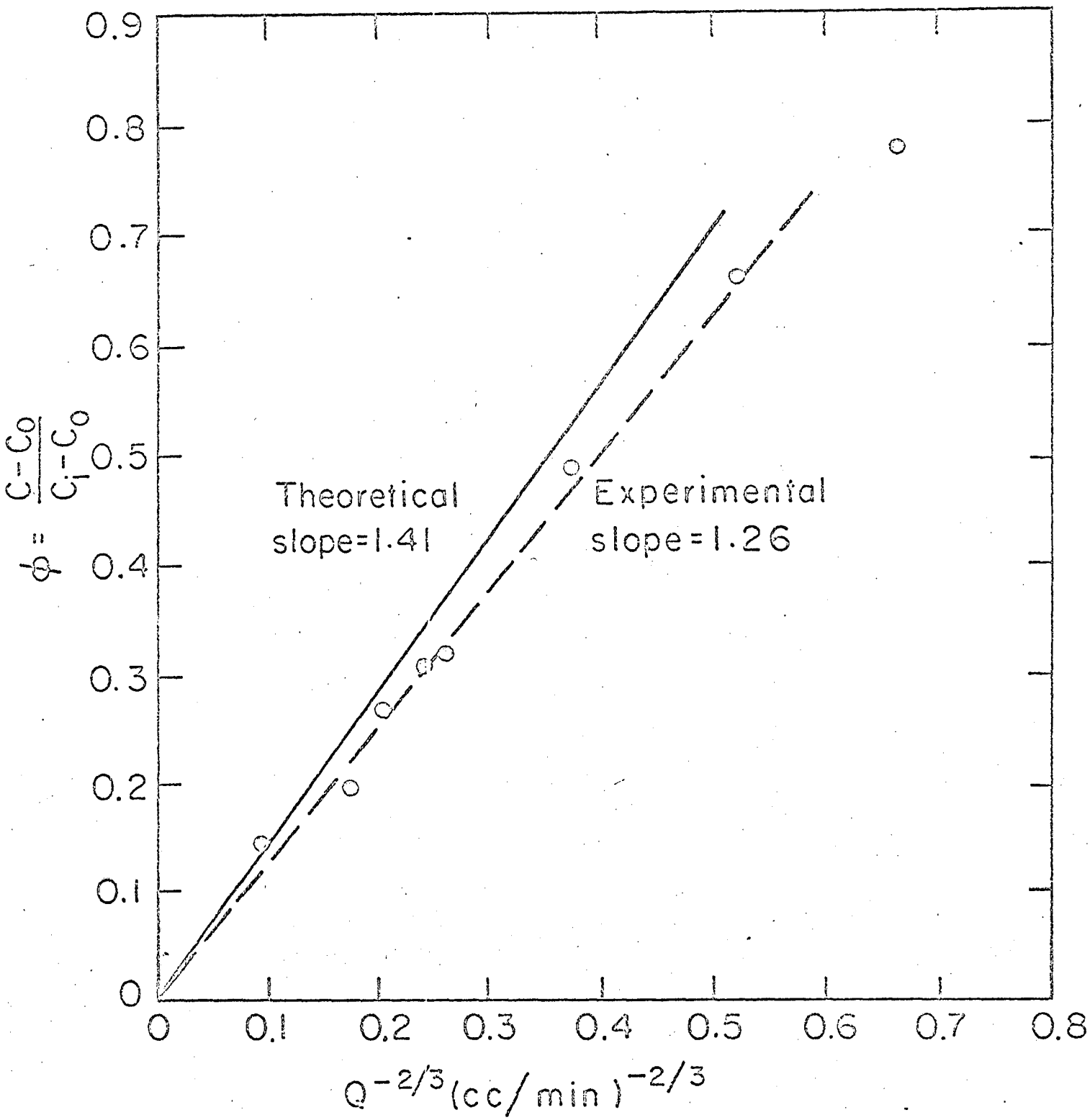
0.9
0.8
0.7
0.6
0.5
0.4
0.3
0.2
0.1
0
$\theta = \frac{C_i - C_o}{C_i - C_o}$
Theoretical
slope=1.41
Experimental
slope=1.26
0
0.1
0.2
0.3
0.4
0.5
0.6
0.7
0.8
$Q^{-2/3}(cc/min)^{-2/3}$

Figure 15

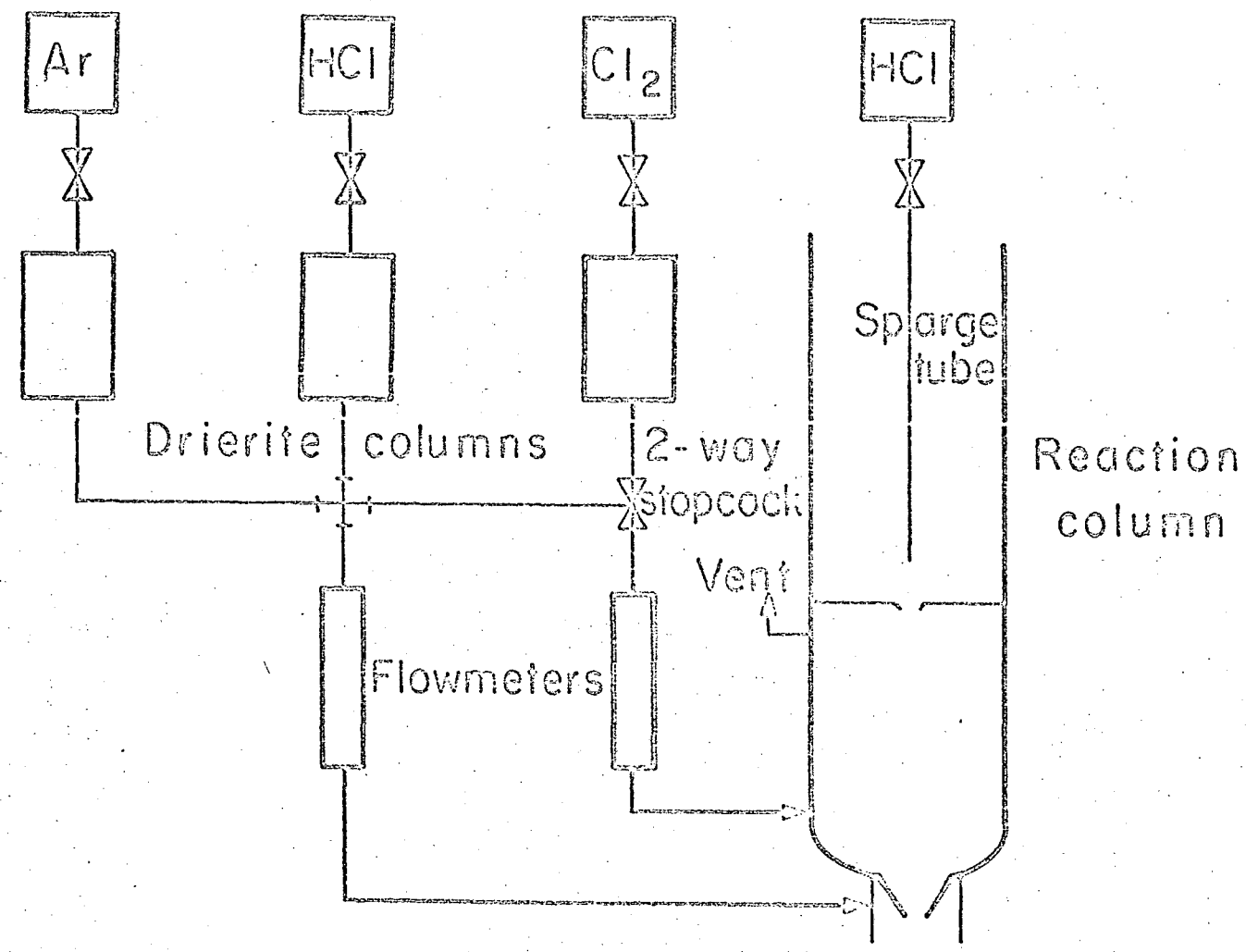
Ar
HCl
Cl_2
HCl
Sparge tube
Drierite columns
2-way stopcock
Reaction column
Vent
Flowmeters

Figure 16

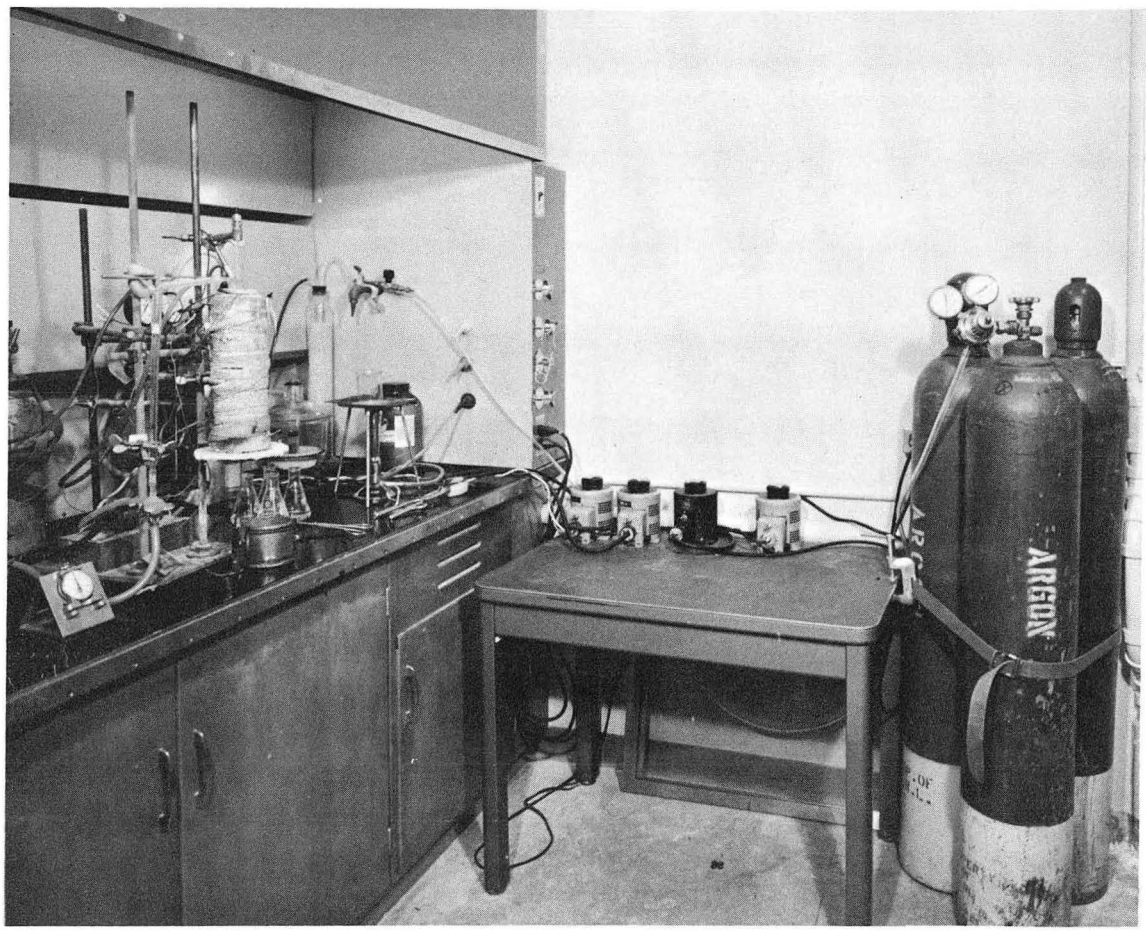

ZN-4983

Fig. 17

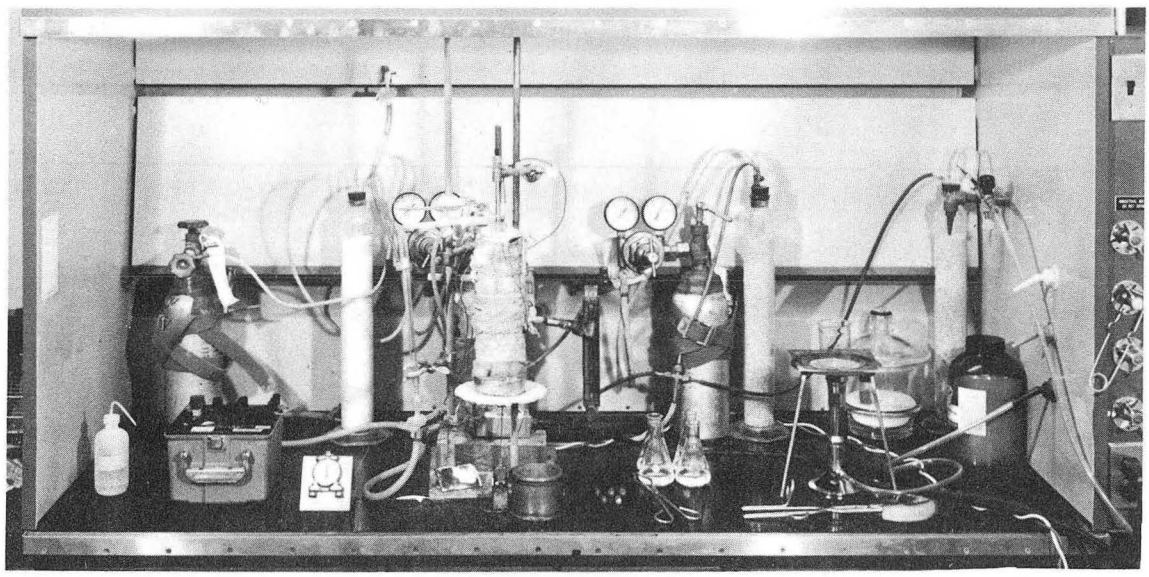

ZN-4984

Fig. 18

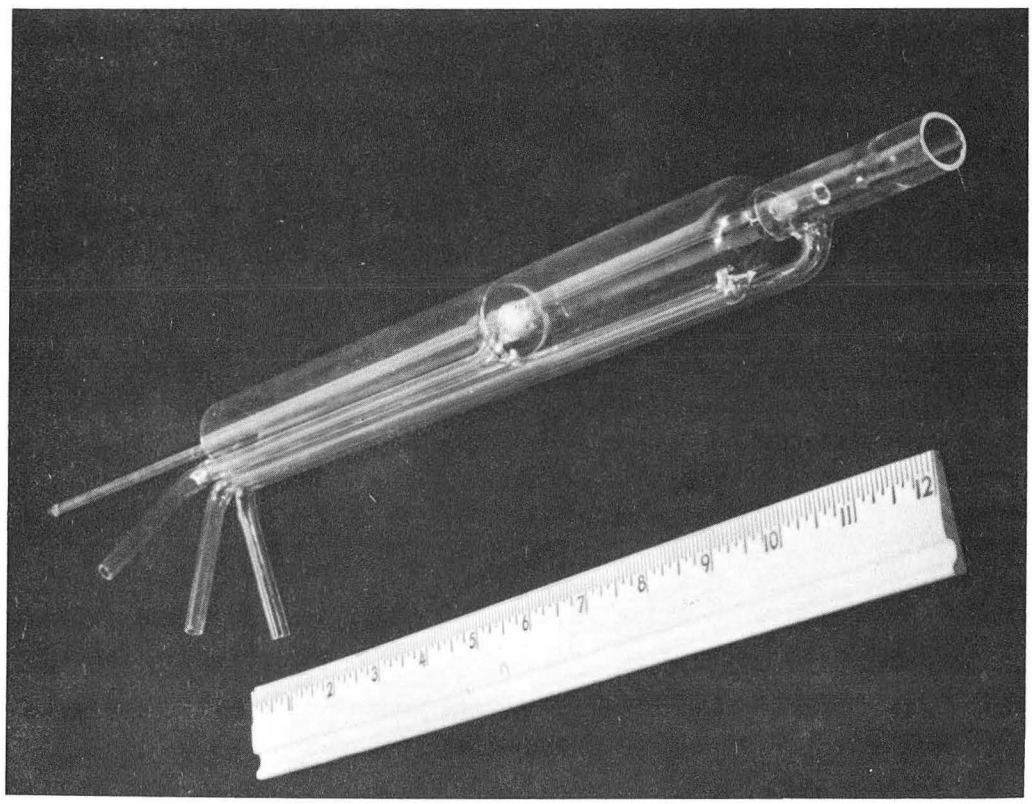

ZN-4985

Fig. 19

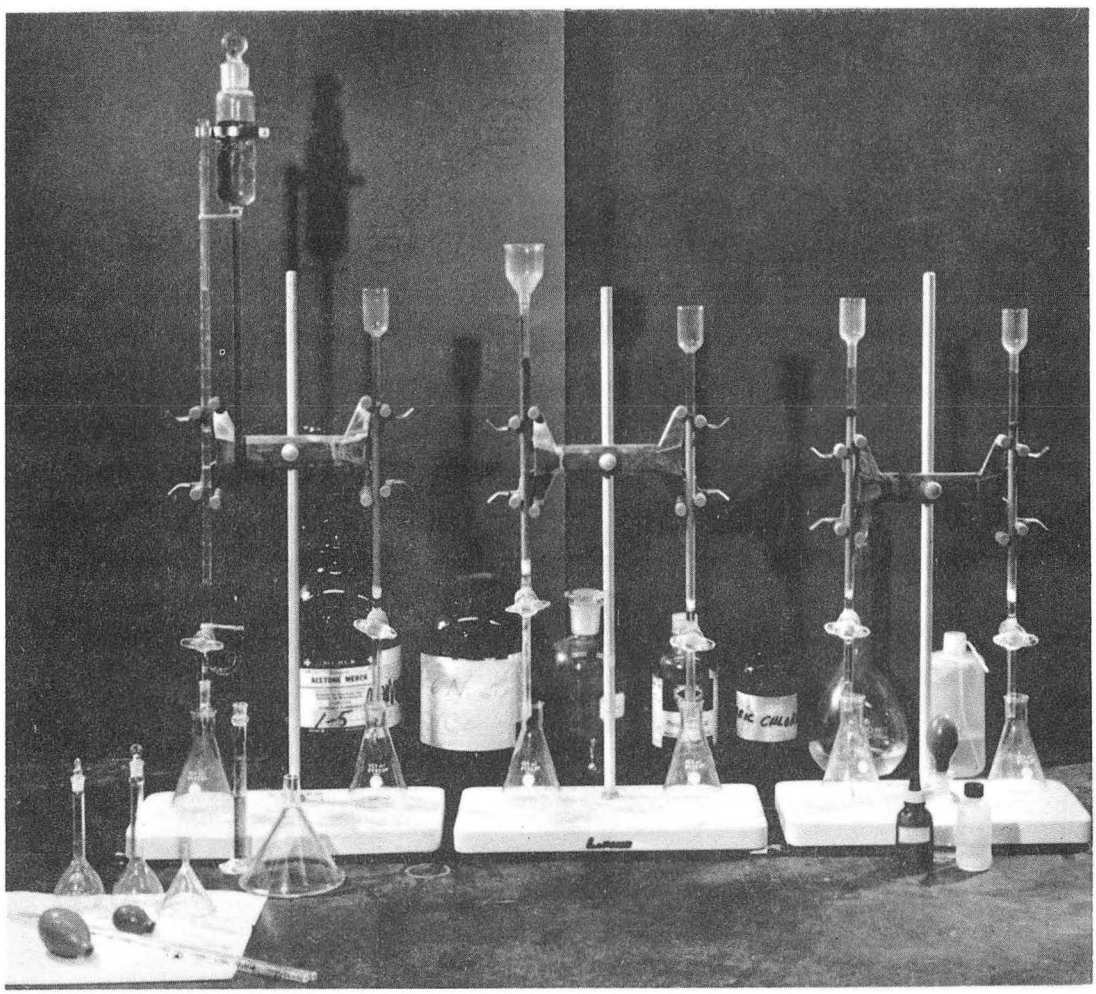

ZN-4986

Fig. 20

3. Experimental Procedure.

A batch of 100-150 grams of LiCl-KCl eutectic mixture (45 wt. % LiCl) was melted in a beaker with a Fisher burner. A small amount of the molten salt was poured into the upper section of the reaction column and allowed to flow down the rod. The rod was then quickly pulled out and inspected for complete wetting (indicated by uniform freezing on the rod). The rest of the melt was then charged into the column and sparged with HCl gas for approximately 10 minutes to remove H_2O vapor and oxidizing impurities. About 2-3 grams of UCl_4 salt was added and dissolved by bubbling with HCl gas for another 10-15 minutes. The reaction chamber and the funnel outlet tube were then flushed with HCl gas and the UCl_4 solution allowed to flow down the rod. Samples were collected and analyzed to determine the initial UCl_4 concentration. The HCl gas in the reaction chamber was replaced with an atmosphere of Cl_2 gas. Samples at different film flow rates were collected in 1 cc. glass cups. The flow rate was determined by measuring the time required to collect 1 cc.

The equilibrium of the reaction was investigated by sparging the UCl_4 solution in a test tube with Cl_2 gas until a constant U^{+4}/U total ratio was observed. The mixture was sampled by dipping a glass cup into the melt.

Kinetic measurements with pure Cl_2 gas were made at 50° intervals from 400 to 700°C. At 600°C, the UCl_4 concentration was varied to determine the order of the reaction in UCl_4. Measurements were also taken at 600°C using Cl_2-Ar and Cl_2-He gas mixtures to investigate the gas phase effect on the kinetics, and a 20% O_2-HCl gas mixture to compare the chlorination and oxidation rates.

The temperature in the reaction chamber was measured with a Conax Chromel-alumel thermocouple and was known to ± 5°. Typical temperature profiles in the chamber are shown in Figure 21.

A sample is prepared for analysis by dissolving it in 50 cc. of HCl solution (1:15). Two 10 cc. aliquots (A and B) are then transferred to flasks. 4 cc. of $FeCl_3$ solution (5%) and a few drops of concentrated H_3PO_4 and diphenylamine sulfonate indicator are added to aliquot A. Titration with 0.02N $K_2Cr_2O_7$ solution with a microburette to a purple endpoint gives the U^{+4} content. Aliquot B is passed through a Pb column (to reduce all U^{+6} to U^{+4}), collected in a flask containing $FeCl_3$, H_3PO_4, and the indicator, and titrated with $K_2Cr_2O_7$ to give the total uranium content.

4. Experimental Results.

The equilibrium constant Kp is obtained from equation (III-75). A plot of ℓnKp vs. $^1/T$ (Figure 22) gives a heat of reaction, $\Delta H = 5.4$ kcal/mole. The conditions used in the kinetic measurements were:

UCl_4 concentration	= 1-3 wt. % or 0.044-0.132 mole/liter
Cl_2 pressure	= 0.25-1 atm.
temperature	= 400-700°C
length of rod (ℓ)	= 9.20 cm
rod radius (a)	= 0.15 cm
film flow rate (Q)	= 2.4-12.0 cc./min

The initial ratio of U^{+4}/U^{total} was found to be consistently about 0.941 throughout this work. The results are summarized in Tables VIII to X and plotted in Figures 23 to 31. The theoretical slopes are computed by equation (III-65) (equilibrium of the surface reaction is assumed).

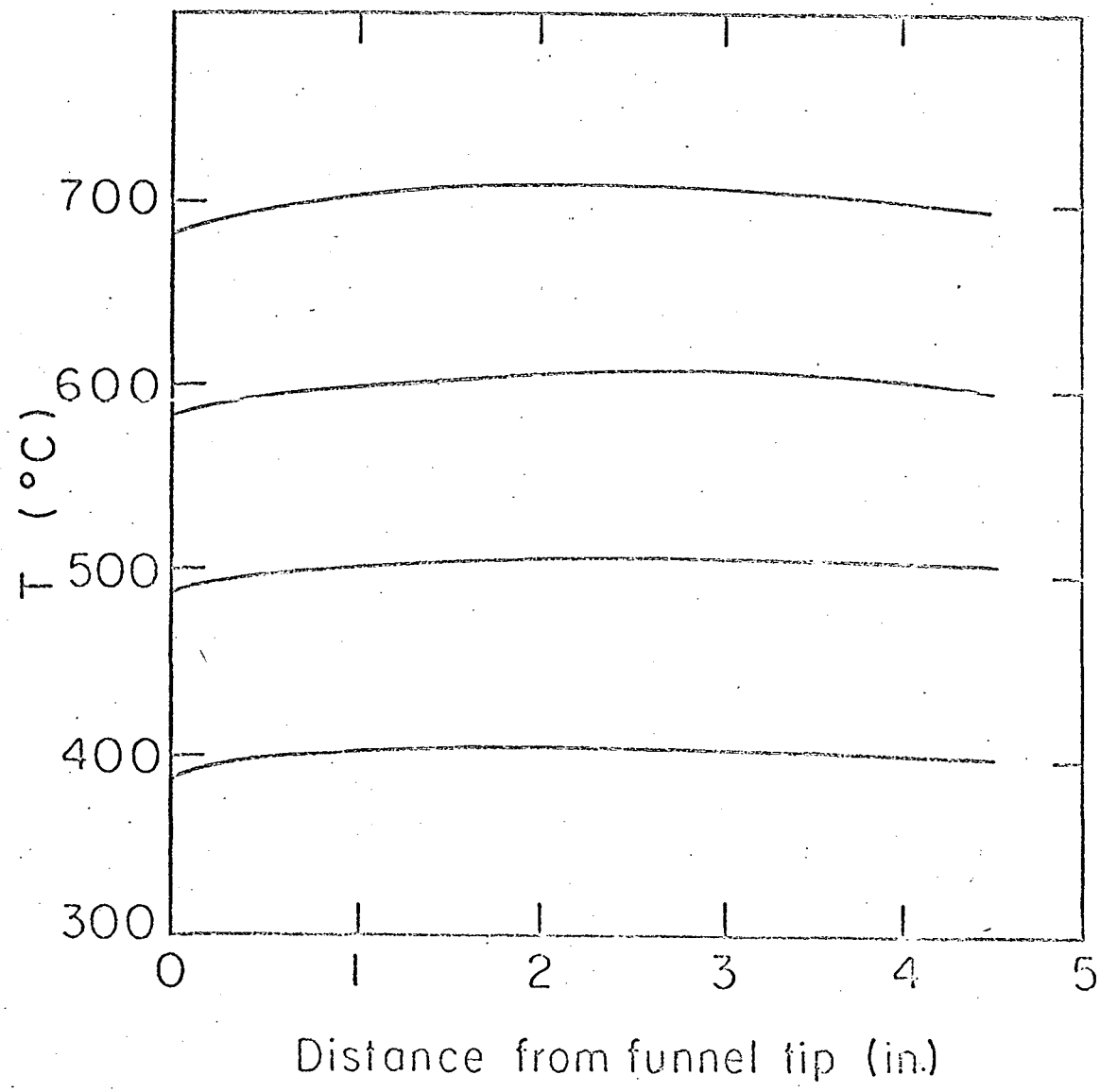

Figure 21

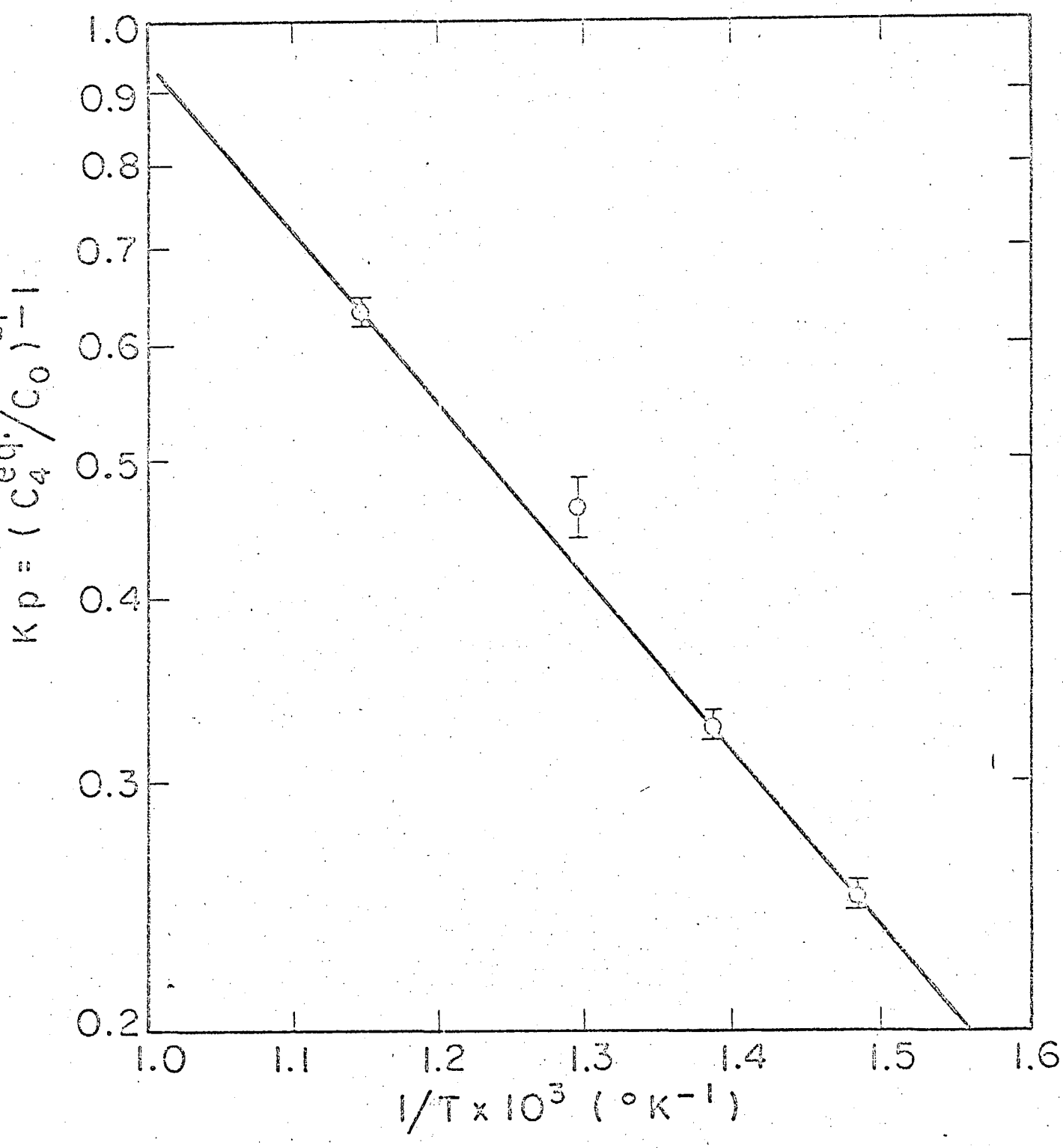
1.0
0.9
0.8
0.7
0.6
0.5
0.4
0.3
0.2
$Kp = (C_4^{eq.}/C_0)^{\frac{1}{2}} - 1$
1.0
1.1
1.2
1.3
1.4
1.5
1.6
$1/T \times 10^3$ ($^\circ K^{-1}$)

Figure 22

Table VIII. Equilibrium determination in pure Cl_2
(Initial U concentration = 2 w/o)

Temperature (°C)	Sparge Time (min)	U Total (C_o)	$\frac{C_4^{eq.}}{C_o}$	$Kp = \frac{C_4^{eq.}}{C_o}^{-1}$
400	15	2.75	0.800	0.250
	30	2.55	0.804	
	60	2.52	0.794	
			Ave. 0.800 + 0.004	
450	15	2.50	0.752	0.328
	25	2.30	0.761	
	35	2.08	0.745	
			Ave. 0.753 ± 0.006	
500	60	1.80	0.695	0.465
	75	1.50	0.667	
	90	1.00	0.700	
			Ave. 0.687 ± 0.013	
600	25	2.45	0.612	0.635
	40	1.70	0.617	
	60	1.40	0.607	
			Ave. 0.612 ± 0.003	

TABLE IX. Kinetics of the chlorination of UCl_4 by pure Cl_2, $P_{c/2}$ = 1 atm, $\frac{C_{4o}}{C_o}$ = 0.942 (except as noted, C_o = 2 w/o U)

Temp. (°C)	$\frac{C_4^{eq.}}{C_o}$	Q (cc./sec)	U Total (C_o)	$\frac{C_4}{C_o}$	$C^* = \frac{C_4/C_o - C_4^{eq}/C_o}{C_{4o}/C_o - C_4^{eq}/C_o}$	Exptal slope
400	0.800	0.133	3.75	0.907	0.755	5.46×10^{-2}
		0.100	3.80	0.908	0.760	
		0.080	3.75	0.893	0.655	
		0.040	3.80	0.882	0.578	
450	0.753	0.125	1.80	0.900	0.778	6.32×10^{-2}
		0.112	2.15	0.884	0.693	
		0.097	1.76	0.881	0.667	
		0.090	2.07	0.879	0.667	
		0.067	1.90	0.874	0.640	
		0.048	2.00	0.855	0.540	
500	0.687	0.182	2.32	0.905	0.855	5.35×10^{-2}
		0.167	2.50	0.904	0.851	
		0.130	2.47	0.898	0.828	
		0.112	2.15	0.879	0.753	
		0.803	2.50	0.868	0.710	
		0.083	2.42	0.876	0.741	
		0.068	2.60	0.846	0.624	
		0.067	2.48	0.867	0.706	
		0.052	2.55	0.839	0.596	
550	0.653	0.095	1.75	0.886	0.806	5.00×10^{-2}
		0.080	1.67	0.868	0.744	
		0.072	1.64	0.860	0.716	
		0.063	1.65	0.848	0.675	
		0.062	1.70	0.841	0.650	

Table IX, Cont.

Temp. (°C)	$\frac{C_4^{eq.}}{C_o}$	Q (cc./sec)	U Total (C_o)	$\frac{C_4}{C_o}$	$C^* = \frac{C_4/C_o - C_4^{eq}/C_o}{C_{4o}/C_o - C_4^{eq}/C_o}$	Exptal slope
600 (2 w/o U)	0.612	0.113	2.20	0.882	0.825	5.90×10^{-2}
		0.129	2.25	0.867	0.773	
		0.095	2.24	0.857	0.742	
		0.072	2.30	0.826	0.648	
		0.064	2.24	0.804	0.582	
600 (1 w/o U)	0.612	0.200	1.27	0.898	0.867	5.67×10^{-2}
		0.133	1.21	0.876	0.800	
		0.100	1.22	0.852	0.727	
		0.070	1.21	0.826	0.648	
600 (3 w/o U)	0.612	0.143	3.02	0.884	0.836	6.00×10^{-2}
		0.111	3.20	0.853	0.730	
		0.100	3.07	0.863	0.761	
		0.080	3.25	0.846	0.709	
		0.070	3.33	0.810	0.600	
		0.060	3.62	0.801	0.573	
650	0.568	0.200	2.55	0.894	0.872	5.46×10^{-2}
		0.143	2.47	0.874	0.818	
		0.111	2.60	0.865	0.794	
		0.095	2.55	0.847	0.746	
		0.083	2.70	0.833	0.708	
		0.069	2.64	0.803	0.628	
		0.062	2.45	0.812	0.652	
700	0.535	0.167	2.25	0.889	0.870	4.90×10^{-2}
		0.118	2.30	0.861	0.801	
		0.100	2.32	0.854	0.784	
		0.078	2.24	0.817	0.701	

Table X. Effect of gas composition on the kinetics, $t = 600°C$, $\frac{C_{4o}}{C_o} = 0.942$

Gas Mixture	$\frac{C_4^{eq}}{C_o}$	Q (cc./sec)	$\frac{C_4}{C_o}$	C^*	Exptal slope
		0.100	0.900	0.693	
		0.077	0.894	0.663	
		0.067	0.881	0.600	
		0.200	0.920	0.792	
50% Cl_2-Ar	0.76	0.142	0.910	0.742	6.78×10^{-2}
		0.111	0.903	0.700	
		0.091	0.898	0.680	
		0.080	0.890	0.643	
		0.074	0.873	0.560	
		0.167	0.930	0.852	
		0.133	0.923	0.765	
		0.118	0.924	0.778	
		0.100	0.921	0.747	
		0.083	0.918	0.704	
25% Cl_2-Ar	0.861	0.200	0.936	0.926	5.14×10^{-2}
		0.167	0.931	0.864	
		0.155	0.925	0.790	
		0.133	0.929	0.840	
		0.118	0.926	0.803	
		0.100	0.920	0.728	
		0.167	0.919	0.787	
		0.155	0.917	0.777	
		0.133	0.913	0.757	
		0.111	0.902	0.703	
		0.100	0.902	0.703	
50% Cl_2-He	0.76	0.087	0.893	0.658	6.70×10^{-2}
		0.200	0.916	0.772	
		0.155	0.911	0.747	
		0.111	0.907	0.727	
		0.100	0.900	0.693	
		0.083	0.892	0.653	
		0.167	0.873		
		0.154	0.867		
20% O_2-HCl		0.125	0.848		
		0.100	0.834		
		0.091	0.833		

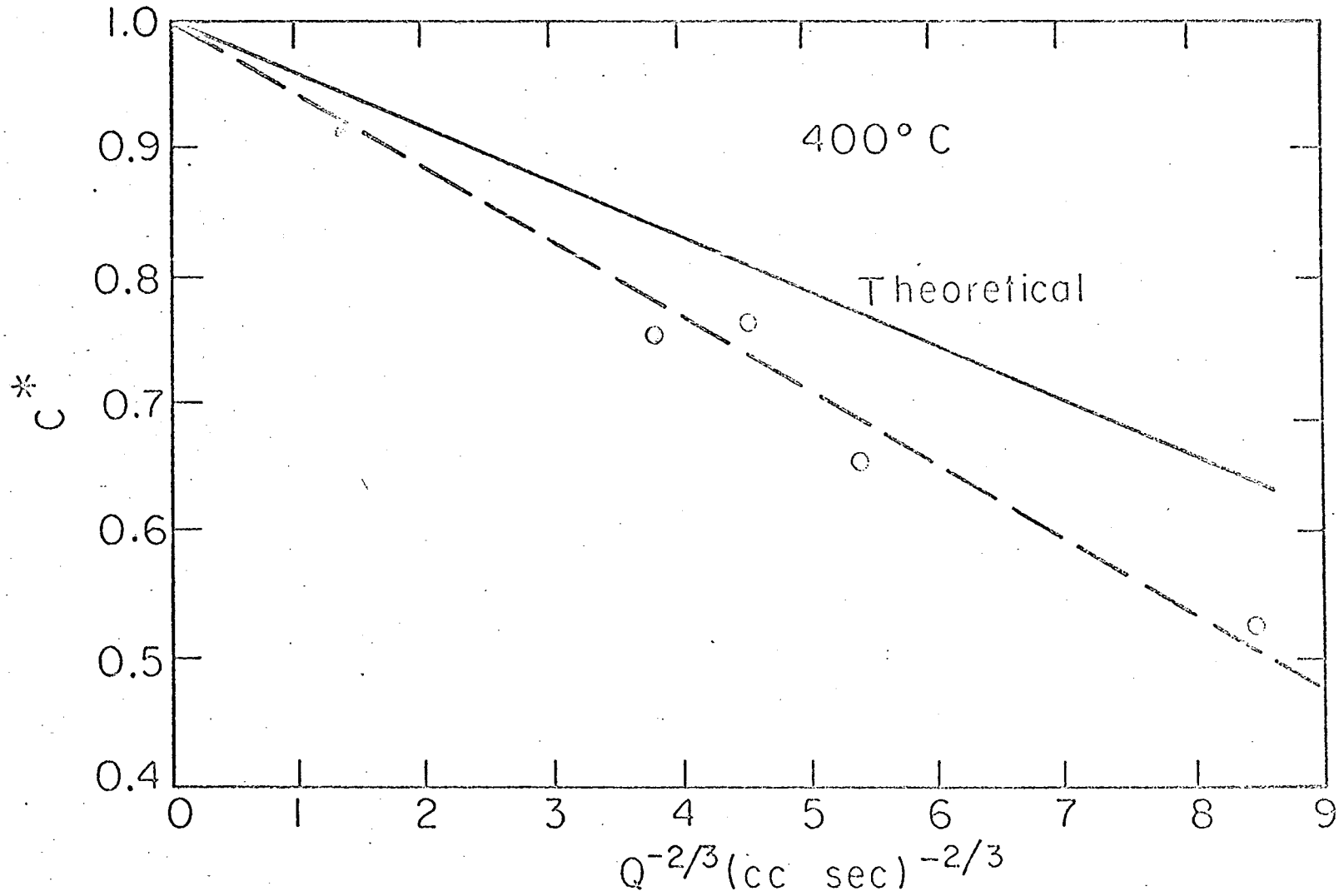
1.0
0.9
0.8
0.7
0.6
0.5
0.4
C^*
400° C
Theoretical
0
1
2
3
4
5
6
7
8
9
$Q^{-2/3}$ (cc sec)$^{-2/3}$

Figure 23

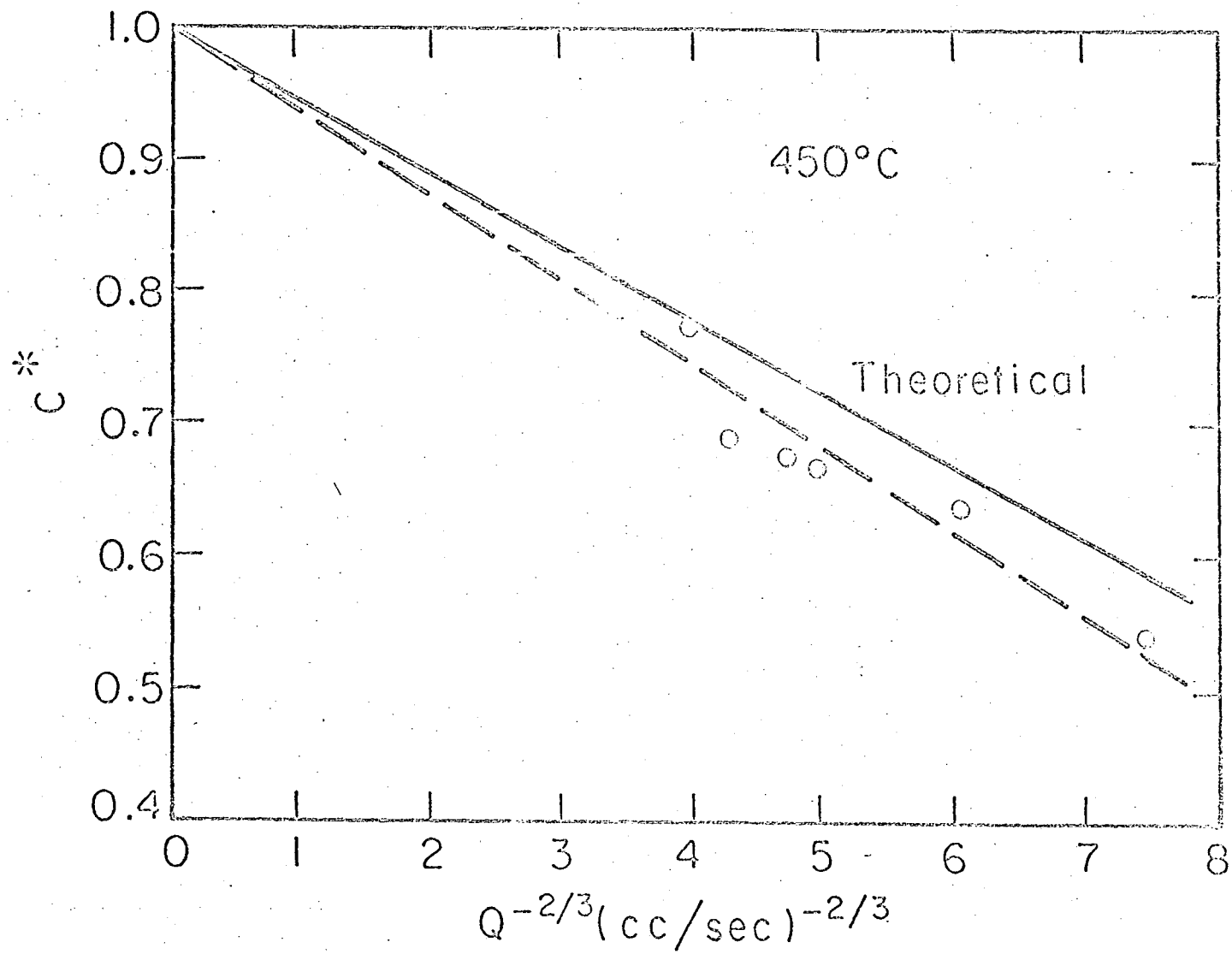

Figure 24

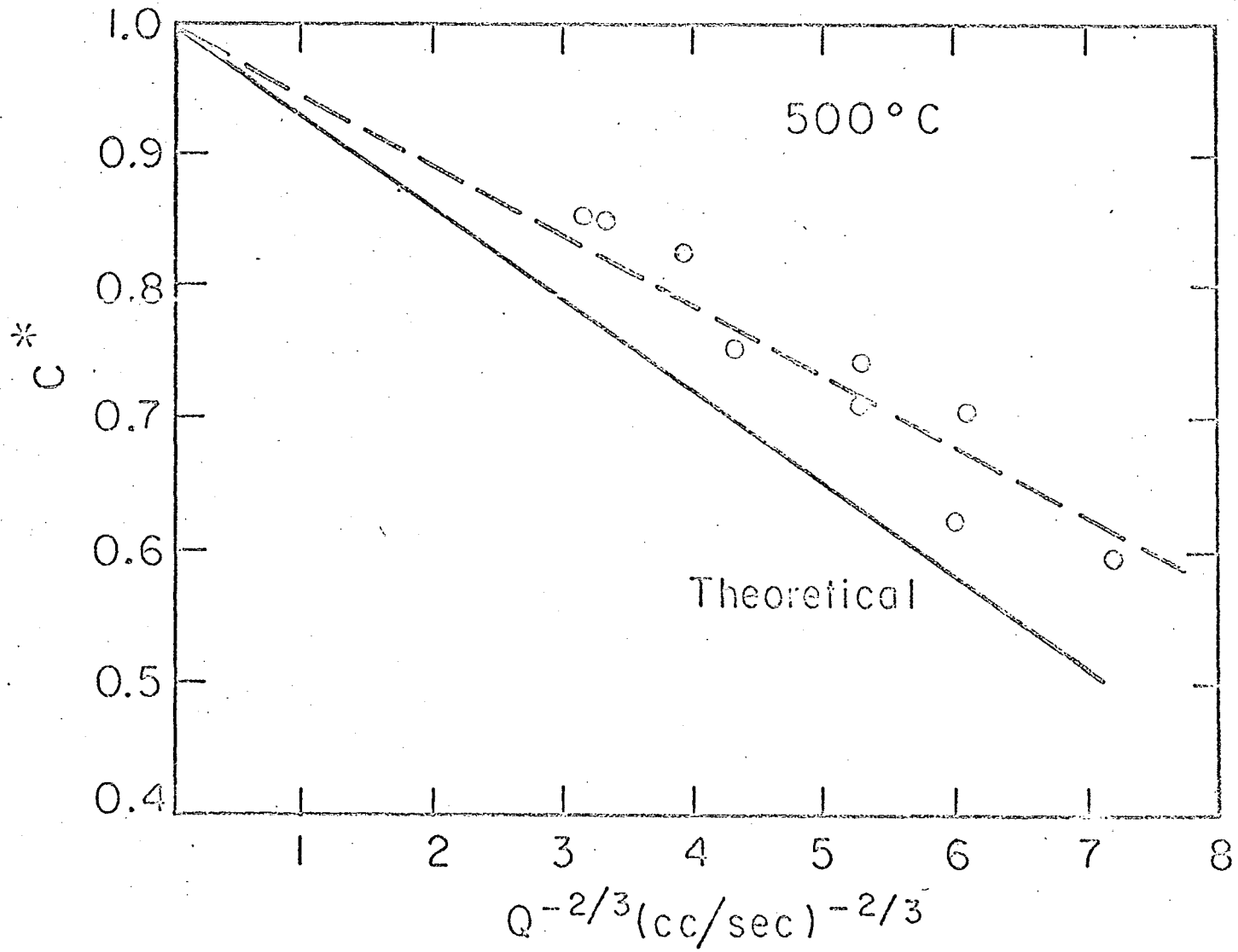

Figure 25

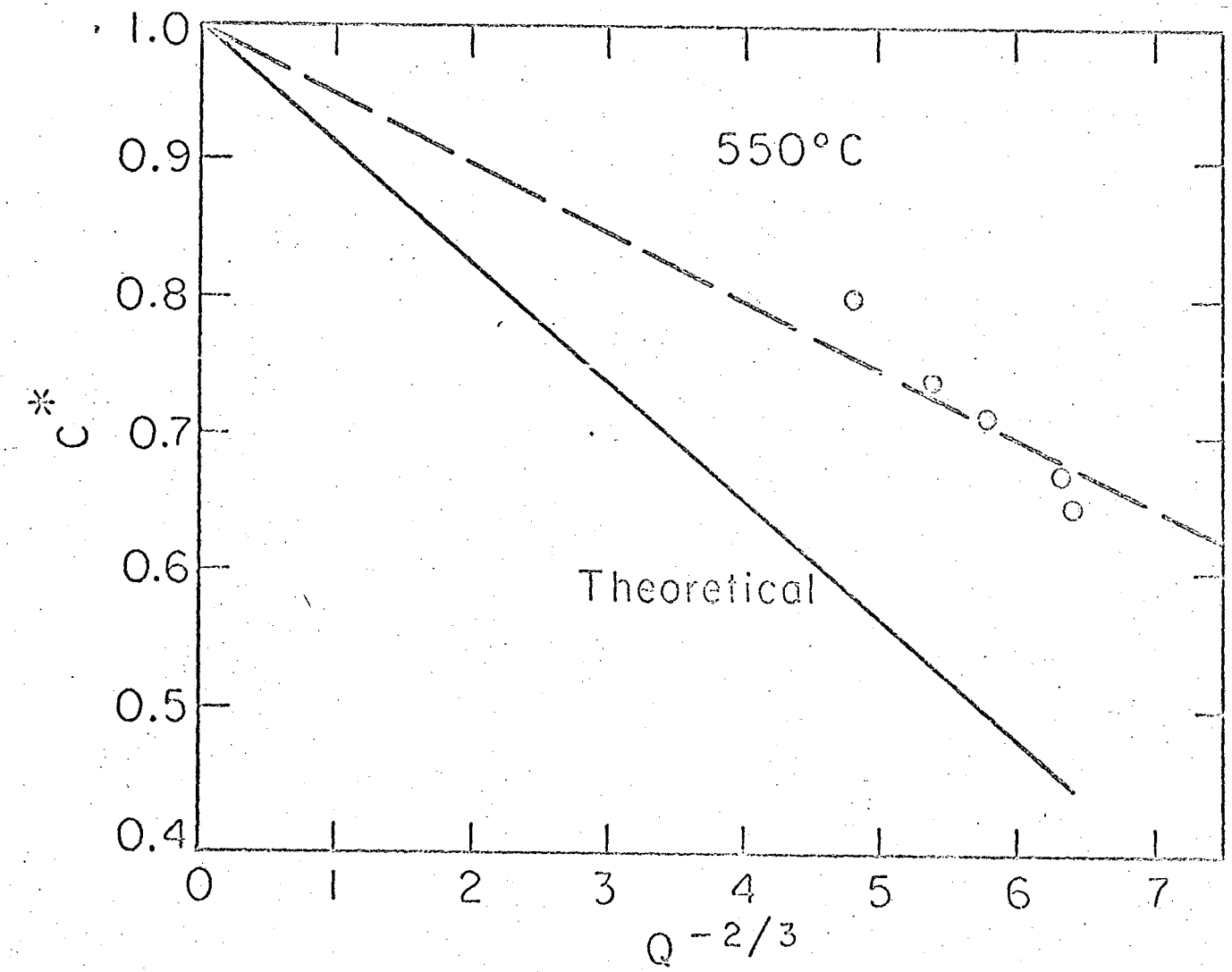

Figure 26

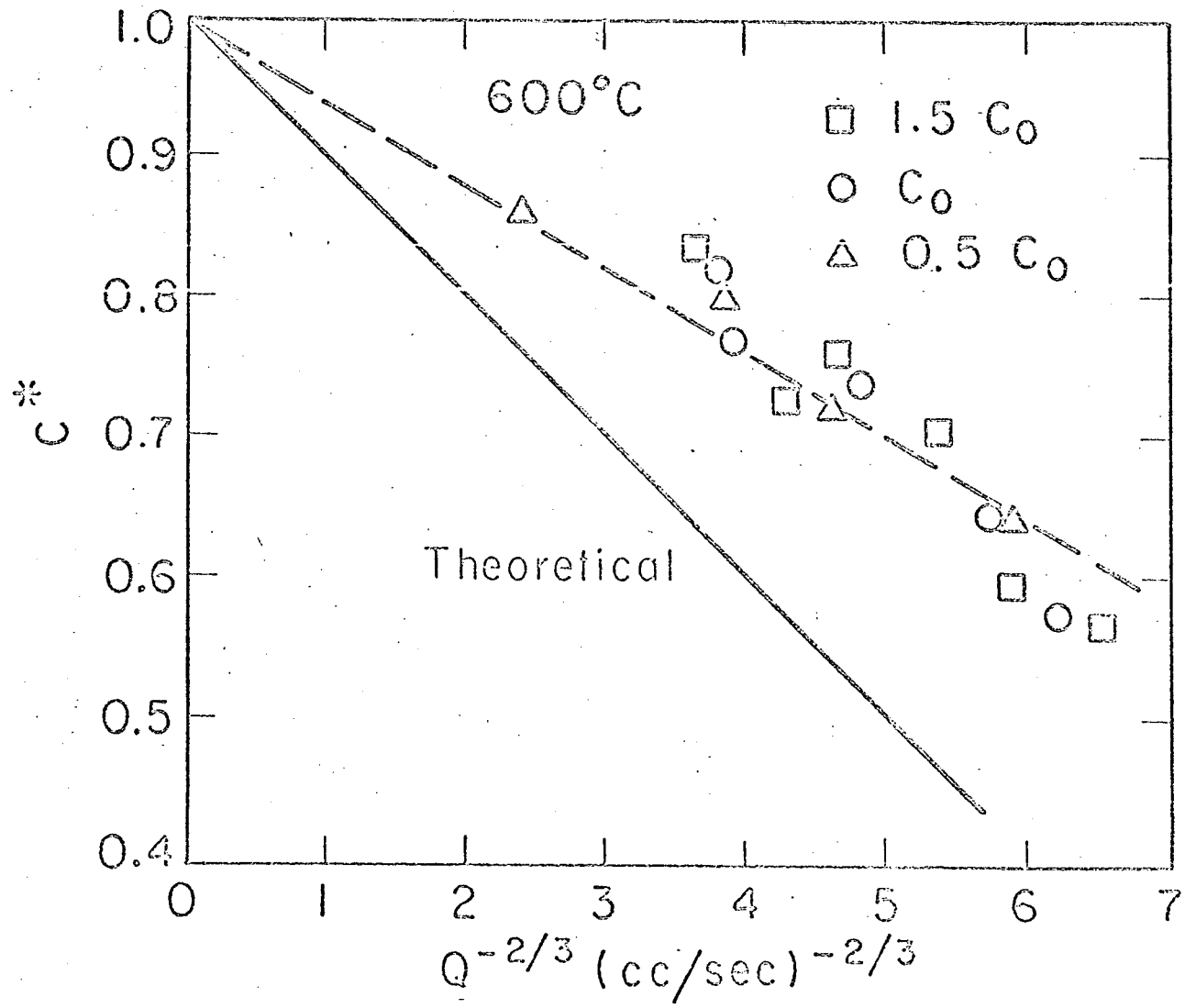
600°C
1.5 C_0
C_0
0.5 C_0
Theoretical
C^*
1.0
0.9
0.8
0.7
0.6
0.5
0.4
0
1
2
3
4
5
6
7
$Q^{-2/3}$ (cc/sec)$^{-2/3}$

Figure 27

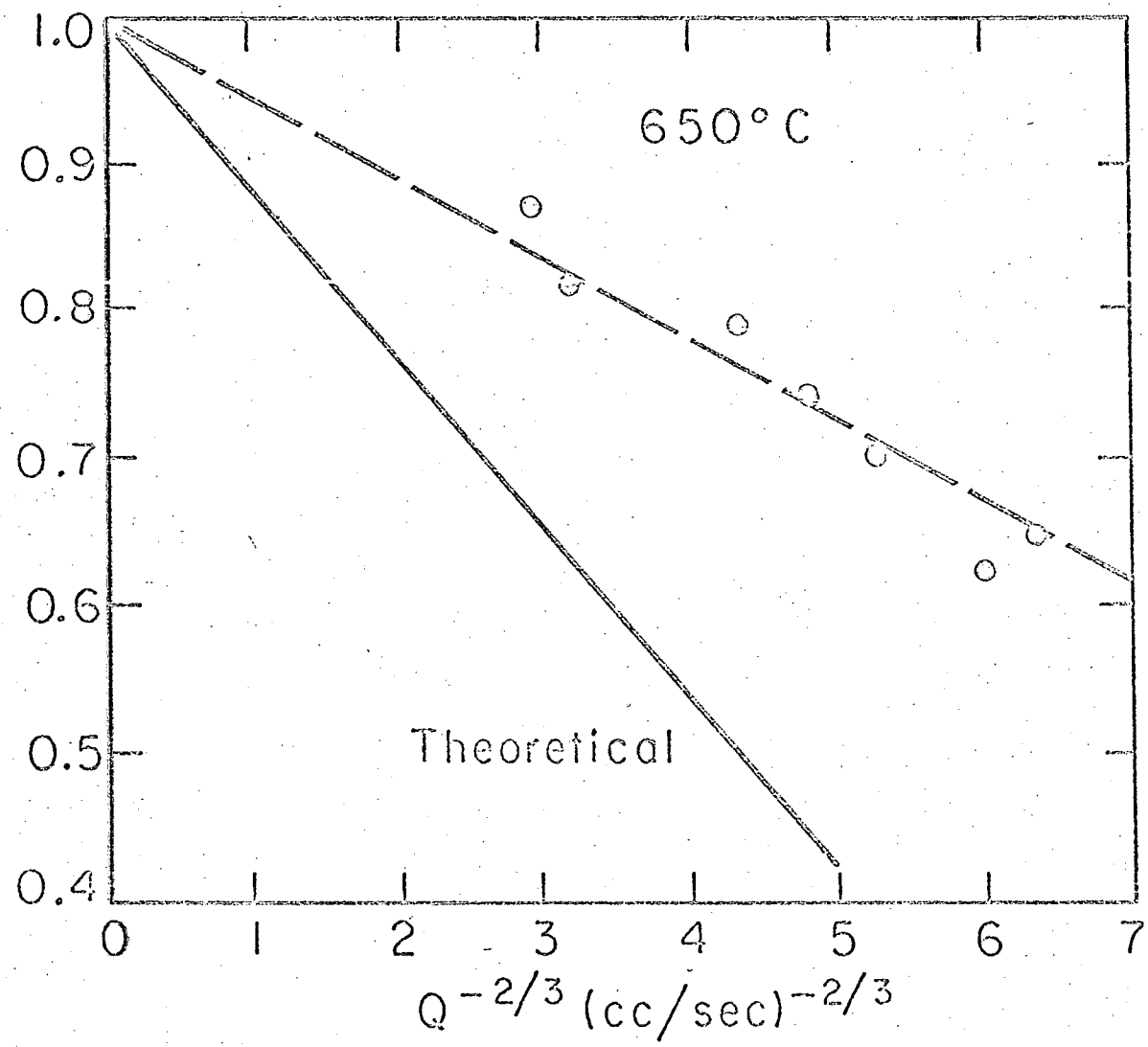

Figure 28

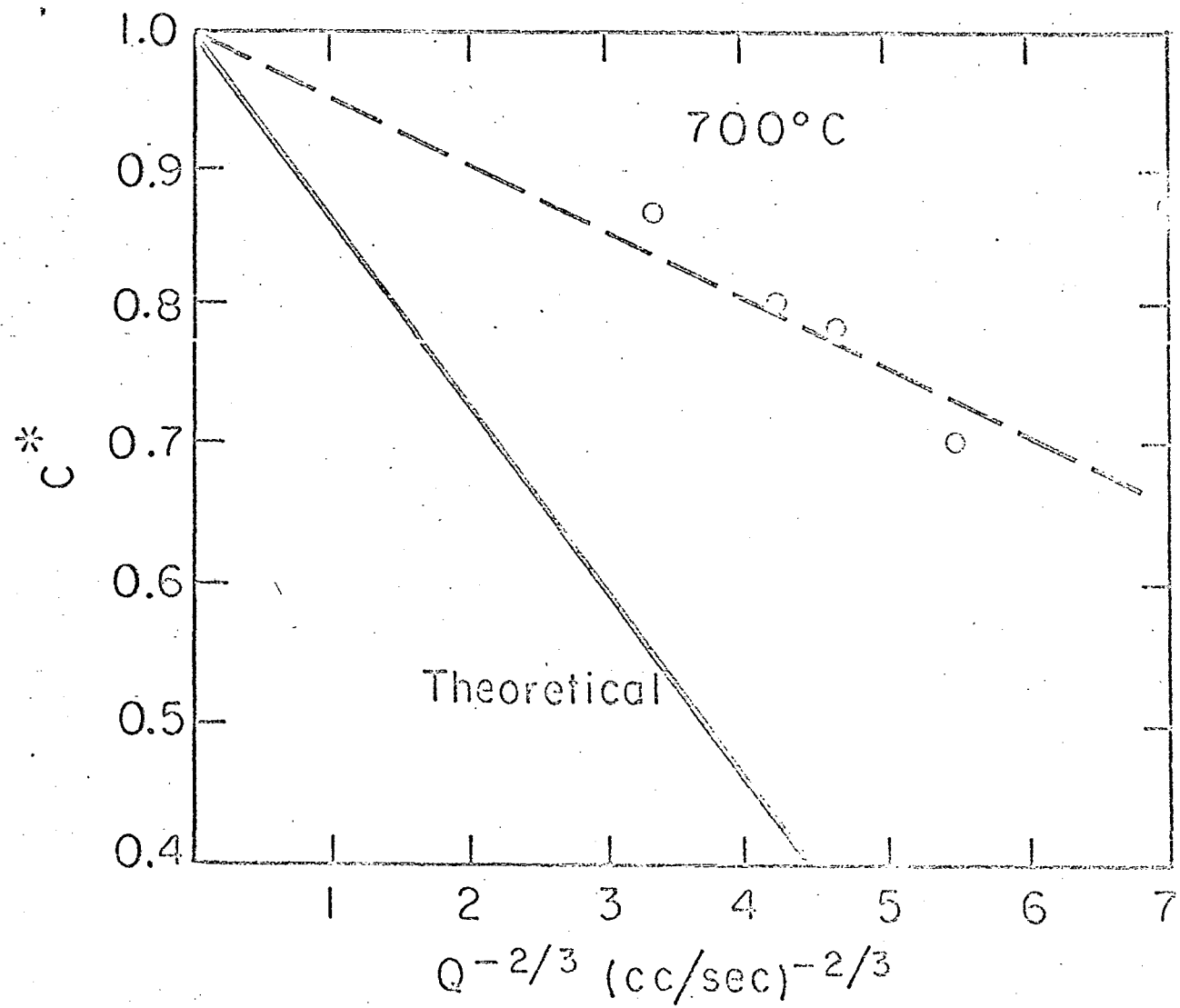

Figure 29

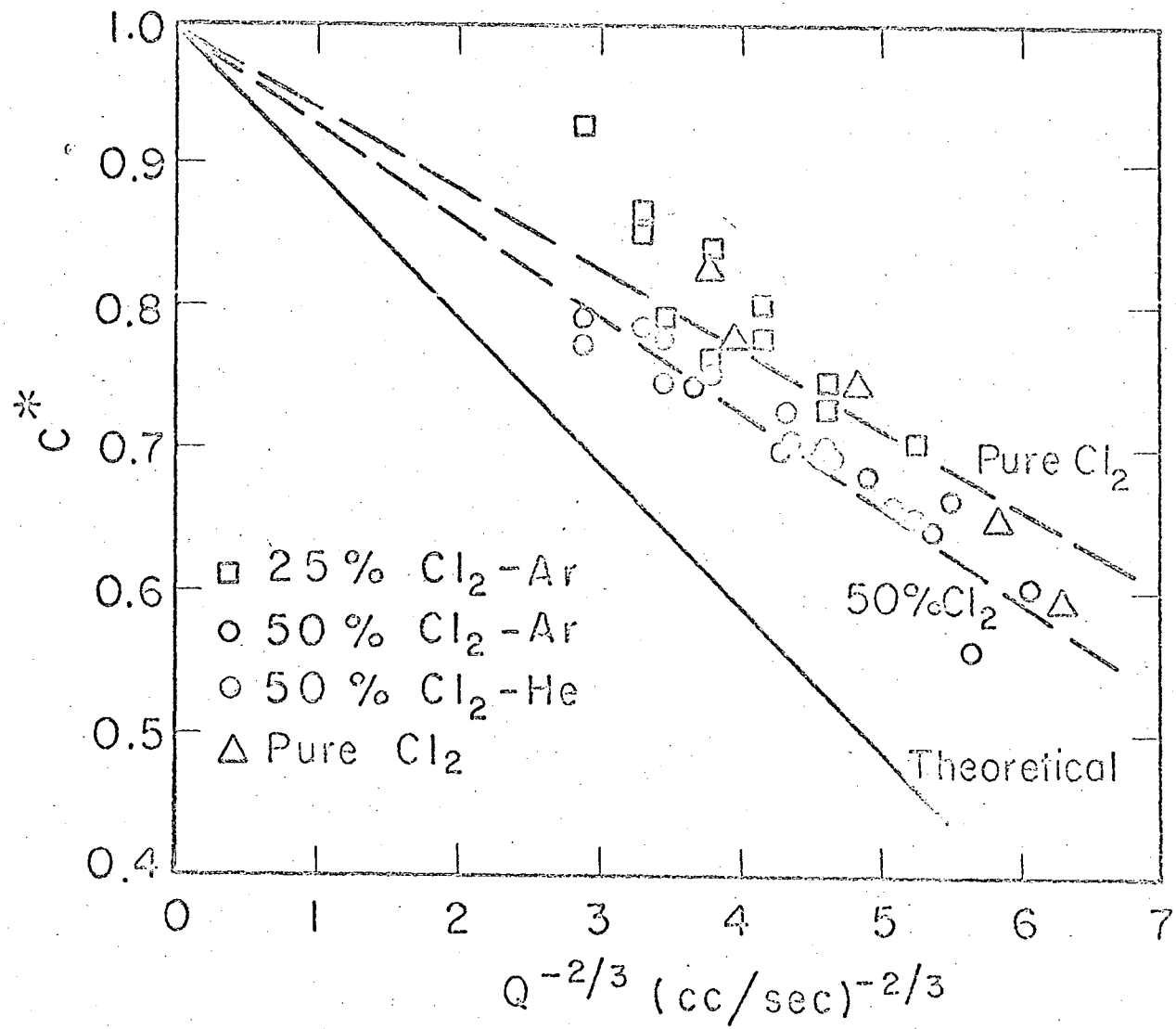
1.0
0.9
0.8
0.7
0.6
0.5
0.4
C^*
0
1
2
3
4
5
6
7
$Q^{-2/3}$ (cc/sec)$^{-2/3}$
25 % Cl_2-Ar
50 % Cl_2-Ar
50 % Cl_2-He
Pure Cl_2
Pure Cl_2
50% Cl_2
Theoretical

Figure 30

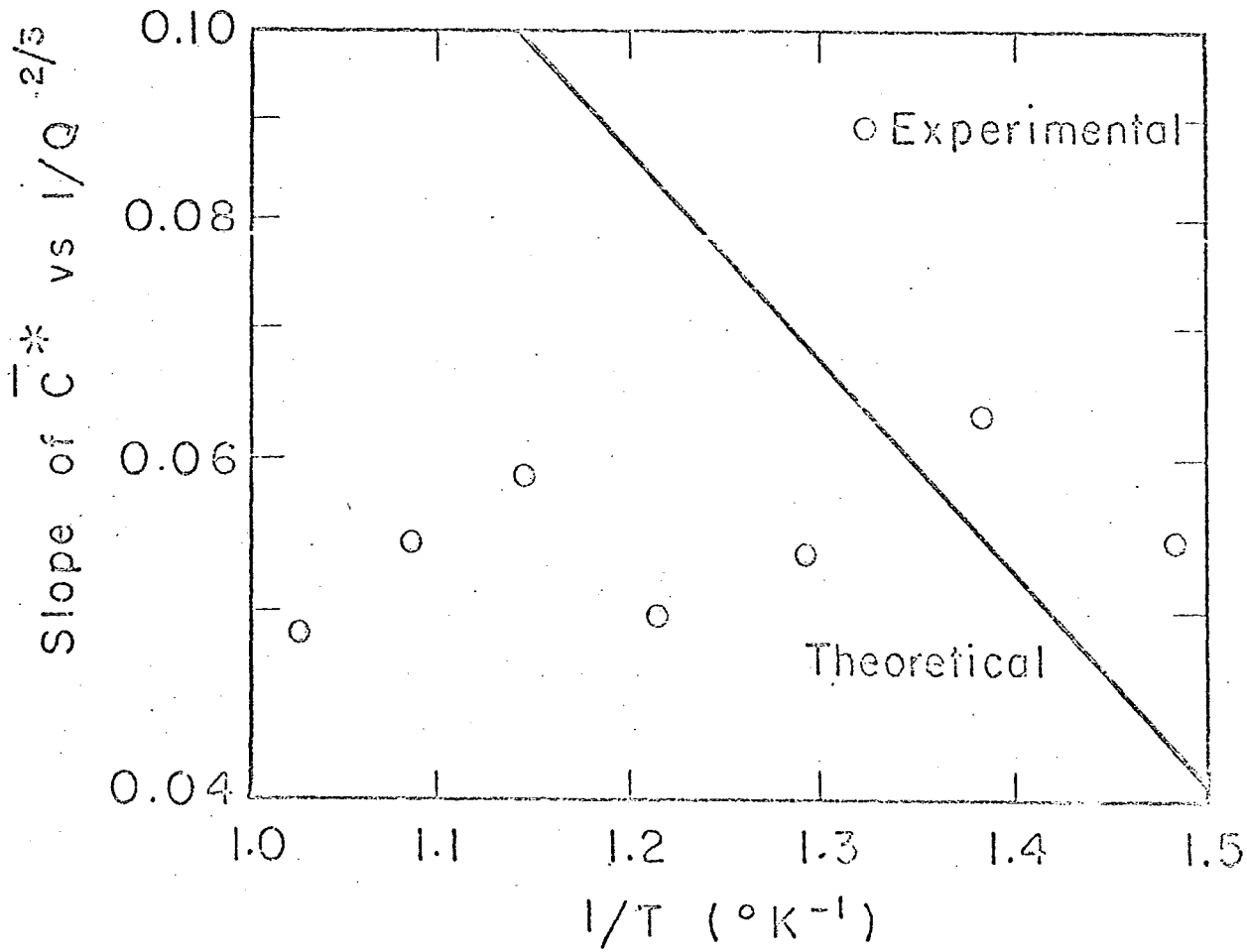
0.10
0.08
0.06
0.04
1.0
1.1
1.2
1.3
1.4
1.5
Slope of $\bar{C}^*$ vs $1/Q^{2/3}$
$1/T$ ($°K^{-1}$)
Experimental
Theoretical

Figure 31

The experimental slopes (s) defined by:

$$C^{*} = \frac{C_4/C_o - C_4^{eq.}/C_o}{C_{4o}/C_o - C_4^{eq.}/C_o} = s\ (1/Q^{2/3})$$

are compared in Figure 31.

V. DISCUSSION OF RESULTS

The performance of the reaction column was found to be satisfactory after preliminary runs with the well-known CO_2-water system. The CO_2 absorption data obtained were consistently about 10 percent lower than the predicted values. This may be due to a stagnant length of film at the end of the wetted-rod. Nijsing et al.[43] observed a similar stagnant surface effect in their falling-film experiments. The use of a syringe for sampling purposes effectively reduces the desorption of dissolved CO_2 to a minimum.

The low solubility of Cl_2 gas in the uranium-free LiCl-KCl eutectic melt indicates that the reaction zone lies at the gas-liquid interface. This was expected from similar measurements at Oak Ridge of the solubilities of HF and inert gases in ZrF_4-NaF melts. Some of the stripped Cl_2 gas probably reacted with its nickel and stainless steel surroundings before it was absorbed by the NaOH-KI solution for chemical analysis. The solubility of Cl_2 was still sufficiently low to insure that the overall process consisted of UCl_4 diffusion in the salt and surface reaction.

The equilibrium studies show that a constant U^{+4}/U total ratio was reached after prolonged sparging of the UCl_4 solution with pure Cl_2 gas. This indicates a reversible reaction. The equilibrium ratio $C_4^{eq.}/C_o$ decreased with increasing temperatures. This means that the reaction is endothermic (equilibrium shifts to the right upon application of heat). The plot of lnKp vs. 1/T gives a heat of reaction of 5.4 kcal/mole.

Kinetic measurements at 600°C showed no appreciable change in the experimental slope at different solution concentrations (1-3 wt.% UCl_4).

This indicates that the reaction is first-order in UCl_4. Using 50% Cl_2-Ar and 25% Cl_2-Ar gas mixtures gave no marked change in experimental slopes. The reaction is therefore also first-order in Cl_2 concentration. This is expected for a diffusion-chemical equilibrium limited process.

The assumption of a negligible gas phase resistance was confirmed when no marked difference was found at 600°C between the experimental slopes obtained with 50% Cl_2-Ar and 50% Cl_2-He atmospheres.

No systematic loss of total uranium was observed during the short contact times of the kinetic studies. This validates the assumption made in the theoretical analysis, i.e. UCl_6 is non-volatile. Volatilization of UCl_6 at the longer contact times of the equilibrium studies was, however, observed. This suggests an induction period where no volatilization of UCl_6 occurs, similar to that found in the fluorination of UF_4.

The results of the kinetic studies with pure Cl_2 at 400-700°C agree reasonably well with the predicted values for an infinitely fast reaction. The experimental rates at 400 and 450°C are greater than the theoretical line but at increasing temperatures (≥ 500°C) they become less than the predicted rates. This behavior rules out the possibility of a chemical rate limitation. Among possible explanations for these findings are:

(a) <u>An unknown interfacial resistance exists and increases with temperature</u>. This is not likely to occur at such high temperatures.

(b) <u>The diffusivity of UCl_6 is much lower than that of UCl_4</u>. This essentially will cause the rapid flooding of the liquid surface with UCl_6, thus preventing more UCl_4 from reaching the reaction zone. This will produce a lower than expected rise in absolute

conversion with increasing temperature and invalidate the assumption used in the theoretical analysis, i.e. $D_4 = D_6$.

(c) <u>The reaction of $UCl_6 \longrightarrow UCl_4 + Cl_2\uparrow$ occurs before the sample is collected.</u> The equilibrium may shift to the left (i.e. the UCl_6 may decompose back to UCl_4) in an HCl atmosphere. The sample dropping through an HCl atmosphere will lose increasing amounts of UCl_6 at higher temperatures due to this thermal decomposition.

(d) <u>Stagnant surface effect at the end of the rod.</u> An end effect similar to that observed in CO_2 absorption may occur in the molten salt experiments. This would not explain however, the high experimental values at 400 and 450°C.

VI. CONCLUSIONS

It can be concluded that the chlorination of UCl_4 was a diffusion-chemical equilibrium limited process, endothermic to the extent of 5.4 kcal/mole. The reaction zone lies at the gas-liquid interface. The effect of the gas phase resistance is negligible, the UCl_6 is essentially non-volatile, and there is no reaction rate control.

ACKNOWLEDGMENTS

The author wishes to express his gratitude to Professor Donald R. Olander for his guidance and help with supervising this work and to Professors T. Vermeulen and E. E. Petersen for their helpful comments.

The author is also indebted to Mr. Mo Rajan for his assistance in the experimental work and Mmes. Margie Janzen and Joan Forney for their generous contributions in preparing the manuscript.

This work was done under the auspices of the U. S. Atomic Energy Commission.

APPENDICES

A. PHYSICAL PROPERTIES OF FUSED LiCl-KCl EUTECTIC

Several of the more important physical properties of the LiCl-KCl eutectic have been determined at the Brookhaven National Laboratory and elsewhere. These include the density, viscosity, surface tension, specific heat, thermal conductivity, and enthalpy. Accurate measurements on these corrosive substances are difficult to obtain.

(1) Density. The density of the binary salt was measured at Oak Ridge[47] and Brookhaven.[2] The ORNL data ranged from 1.67 gm/cc. at 400°C to 1.57 gm/cc. at 600°C. The results are summarized by the equation.

$$\rho = 1.8885 - 0.527 \times 10^{-3}\ t \qquad \text{(A-1)}$$

for the range 380° to 600°, where ρ is the density in gm/cc. and t is the temperature in °C. The BNL data differed slightly (a maximum of 1%) from these results.

(2) Viscosity. Viscosity measurements by Weisman[62] and by Bonilla,[11] using capillary viscometers, appear to be in fairly good agreement. The viscosity measured at BNL ranged from 2.4 Cp. at 510°C to 5.3 Cp. at 385°C. Over this temperature range the data can best be described by

$$\log_{10}\mu = (1500/T) - 1.56 \qquad \text{(A-2)}$$

where μ is the viscosity in centipoises and T is the temperature in °K. Bonilla's data were 5% lower and ranged from 2.25 Cp. at 510°C to 5.22 Cp. at 384°C. The kinematic viscosity is shown in Figure 32 as a function of temperature.

(3) Surface tension. Bonilla and co-worker[53] measured the surface tension of the binary eutectic against air in a capillary apparatus at 432.2° ± 5.5°C. They obtained a value of 118.2 dynes/cm.

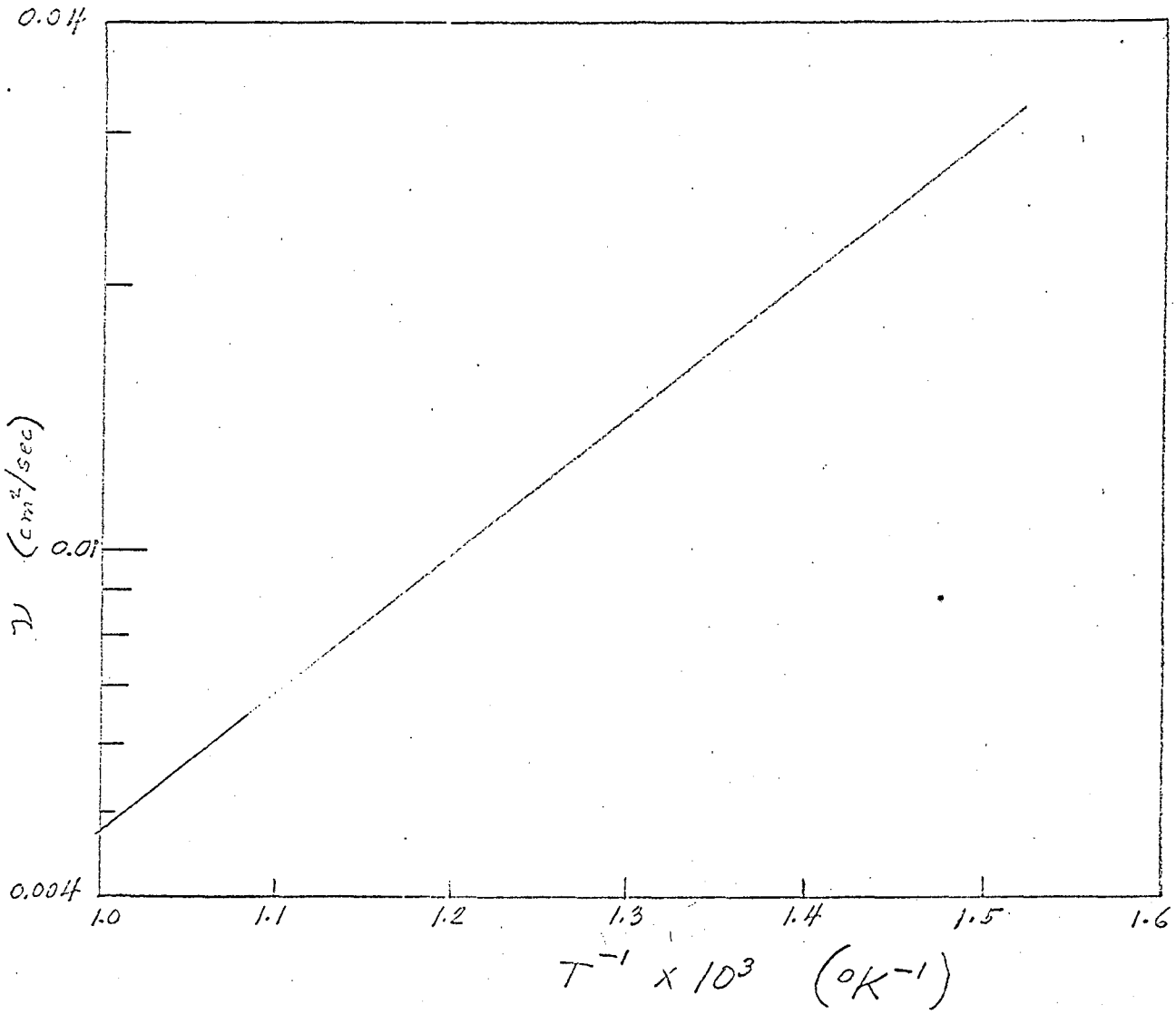

Figure 32

(4) Thermal conductivity. Deem[17] measured the thermal conductivity of the binary salt by using the steady-heat-flow method. Only two values, 0.0060 and 0.0063 cal/sec-cm-°C were obtained at a mean temperature of 510°C. An absolute error of as much as 25% was estimated.

(5) Enthalpy. The enthalpy of the binary eutectic was determined by the ice-calorimeter method at ORNL[47] and the Bureau of Standards[18] - the Oak Ridge data can be represented by the equations:

$$H_t(\text{liq}) - H_o{}^\circ\text{C (solid)} = 30 + 0.32(5)\ t \qquad \text{(A-3)}$$

between 351° and 840°C, and

$$H_t(\text{solid}) - H_o{}^\circ\text{C (solid)} = 4 + 0.23(6)\ t \qquad \text{(A-4)}$$

between 97° and 351°C; where H is the enthalpy in cal/gm and t is the temperature in °C. The heat of fusion was approximately 64 cal/cm.

The Bureau of Standards' work was more precise and a smoothed enthalpy equation was derived for the liquid binary:

$$H_t(\text{liq}) - H_o{}^\circ\text{C (solid)} = 1.4653t - 1.89 \times 10^{-4}t^2 + 0.56 \times 10^{-7}t^3 \qquad \text{(A-5)}$$

between 351° and 800°C, where H is the enthalpy in absolute joules/gm and t is the temperature in °C. The heat capacity and its variation with temperature can be represented by:

$$Cp = 1.4653 - 3.77 \times 10^{-4}t + 1.69 \times 10^{-7}t^2 \qquad \text{(A-6)}$$

between 351° and 800°C, where Cp is the heat capacity in absolute joules/gm - °C and t is the temperature in °C.

B. CHEMISTRY OF URANIUM CHLORIDES[33]

There are four uranium chlorides known: UCl_3, UCl_4, UCl_5 and UCl_6. The first three were prepared and studied by the earliest workers in the chemistry of uranium. Uranium hexachloride was discovered only recently at UCRL.

A summary of the physical properties of the uranium chlorides is given in Table XI. The free energy of formation of uranium chlorides is shown in Figure 33.

1. Preparation.

(a) Uranium tetrachloride. Uranium tetrachloride is prepared in many different ways from both UO_2 and UCl_3. It can be purified either by direct sublimation in vacuum or by sublimation as a higher chloride in a chlorine atmosphere (275 to 700°C) and subsequent reconversion to UCl_4. It can also be sublimed in a stream of inert gas, such as nitrogen or helium. In a nitrogen stream, sublimation is rapid at 600 to 650°C. At a pressure of 3 to 5 mm Hg, the UCl_4 sublimes without melting. At atmospheric pressure, addition of carbon tetrachloride to the nitrogen stream can greatly reduce the non-volatile residue. The purity of UCl_4 can be evaluated by several criteria, the most important being solubility in selected solvents and its volatility.

(b) Uranium pentachloride. UCl_4 can be converted to UCl_5 by the action of Cl_2 at 520 to 555°C:

$$2\ UCl_4 + Cl_2 \longrightarrow 2\ UCl_5$$

The Cl/U ratio in the product obtained depends on the rate of cooling and may be as high as 5.5. This indicates the possibility that compounds of the type $xUCl_6 \cdot yUCl_4$ are formed, where the ratio x/y may be greater than one.

Table XI. Physical properties of the uranium chlorides

Physical Property	UCl_3	UCl_4	UCl_5	UCl_6
Formula weight (gm/mole)	344.44	379.90	415.36	450.81
Color of solid	olive-green	green	red-brown	black, dark green
Melting point (°C)	842 ± 5	590 ± 1	300 †	177.5 †
Density (gm/cc.)*	5.51	4.87	3.81 ††	3.59
Vapor pressure solid, log Pmm	10.0-(12,000/T)	13.3995-(10427/T)	.....	6.6337-(2422/T)
liquid, log Pmm	10.0-(12,000/T)	9.65-(7205/T)	.....	.....
Boiling point(°C)	1410 †	792	.....	372 †
$H_{sublimation}$ (kcal/mole)	55.0	47.7	.....	11.12
$H°_{298}$(kcal/mole)	-212	-251	-262	-273
$F°_{298}$(kcal/mole)	-196.2	-229.0	-235.7	-241.4
$S°_{298}$(e.u.)	40.0	47.14	57.0 †	68.26

*From X-ray data † these quantities estimated ††direct measurement by immersion in benzene

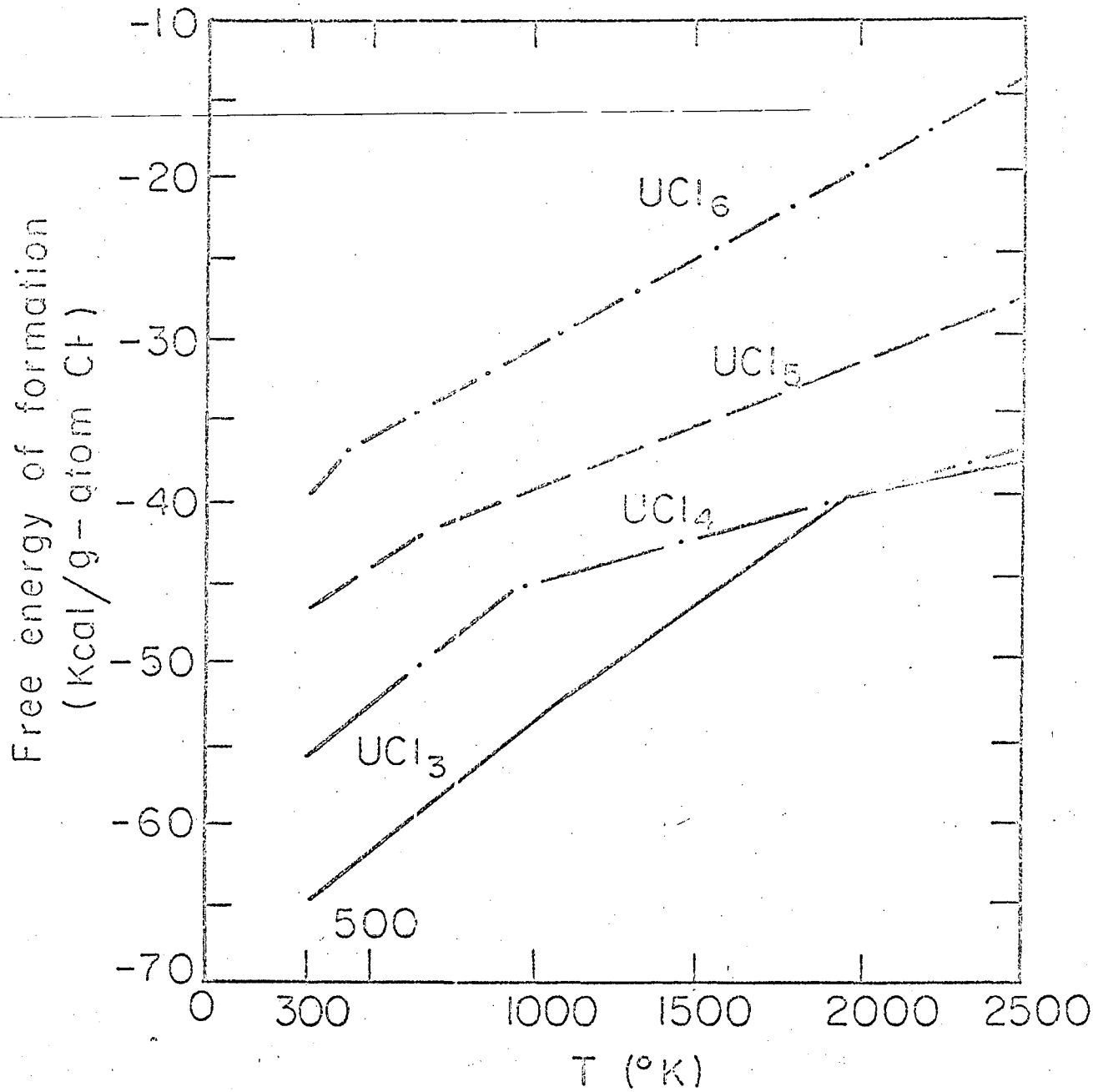
-10
-20
-30
-40
-50
-60
-70
Free energy of formation
(Kcal/g-atom Cl)
UCl6
UCl5
UCl4
UCl3
500
0
300
1000
1500
2000
2500
T (°K)

Figure 33

$$S - S_{0°C} = 0.15706 \log T + 2.88 \times 10^{-5} T - 0.39602 + \frac{0.0056}{T-232}$$

$$+ 5.6 \times 10^{-5} \log \left(\frac{T-232}{T}\right) \text{ cal/gm-°C} \qquad \text{(A-10)}$$

The enthalpy is given by:

$$H-H_{0°C} = 0.07608t + 1.44 \times 10^{-5} t^2 - 0.03 + 1.3/(t + 41) \text{ cal/gm} \qquad \text{(A-11)}$$

The heat capacity is then:

$$C_p = 0.07608 + 2.88 \times 10^{-5} t - \frac{1.3}{(t + 41)^2} \qquad \text{(A-12)}$$

where t is the temperature in °C (0 to 427°C) and T is the temperature in °K. At temperatures above 100°C, the last terms of the enthalpy and heat capacity equations, and the last two terms of the entropy equation are negligible.

The heat of formation of UCl_4 is:

$$U(\text{solid}) + 2\ Cl_2(\text{gas}) \longrightarrow UCl_4(\text{solid})$$

$$\Delta H°\ 273°K = -250.9 \pm 0.6 \text{ kcal/mole}$$

the free energy and entropy are:

$$\Delta F°_{298°K} = -229.65 \text{ kcal/mole and}$$

$$\Delta S°_{298°K} = 71.5 \text{ e.u.}$$

The variation of $\Delta H°$ and $\Delta F°$ with temperatures are given by:

$$\Delta H° = -252{,}600 + 5.70T - 7.79 \times 10^{-4} T^2 \qquad \text{(A-13)}$$

$$\Delta F° = -252{,}600 - 13.13T \log T + 7.79 \times 10^{-4} T^2 \qquad \text{(A-14)}$$

where T is the temperature in °K.

(b) Uranium pentachloride. As prepared by reaction of UCl_4 with chlorine, UCl_5 is a red-brown micro crystalline powder. The difficulties in handling UCl_5 account for the few studies of its physical properties.

1) Density. A density measurement by direct displacement in benzene gave a value of 3.81 gm/cc.

2) Melting point and volatility. No accurate measurement of the melting point or volatility of UCl_5 are available because of its thermal instability. The vapor pressure has been estimated as 10^{-7} mm Hg at 50°C. Doubts have been expressed concerning the existence of UCl_5 vapor above 60°C because it undergoes disproportionation. The difficulty in separating UCl_5 and UCl_6 by sublimation indicates a rather high volatility of the pentachloride. UCl_5 can be distilled in an atmosphere of chlorine containing some carbon tetrachloride; but the sublimate contains UCl_6.

3) Molecular weight. The molecular weight of UCl_5 was determined by ebullioscopy in carbon tetrachloride solution. It was found to correspond quite closely to a dimer, $(UCl_5)_2$. It is then possible to formulate UCl_5, as U_2Cl_{10} in solution.

4) Thermochemistry. The heat of formation of UCl_5 was determined by measuring the difference in the heats of solution of UCl_4 and UCl_5 in water containing excess $FeCl_3$:

$$\Delta H^\circ_{273°K} = -262.1 \pm 0.6 \text{ kcal/mole}$$

the free energy of formation is

$$\Delta F^\circ_{298°K} = -235.7 \pm 2.0 \text{ kcal/mole}$$

(c) Uranium hexachloride. UCl_6 forms fine black or dark green crystals depending on the method of purification or rate at which crystals are grown.

1) Melting point. The melting point of UCl_6 has been determined despite its thermal instability. Thin-walled tubes containing UCl_6 were immersed in an oil bath at various temperatures. At atmospheric pressure, a liquid phase is formed temporarily at 177.5 ± 2.5°C.

2) Density. The density calculated from X-ray data is 3.59 gm/cc. A direct determination by immersion in benzene has given a value of 1.56 gm/cc., but measurements in tetrahydronaphthalene yielded 3.36 ± 0.17 gm/cc.

3) Vapor pressure. Two different methods were used to measure the vapor pressure of UCl_6. An all-glass clicker gauge gave:

$$\log P_{mm\ Hg} = -\frac{2422}{T} + 6.634 \text{ (0 to 200°C)} \qquad \text{(A-15)}$$

$$\Delta H_{sublimation} = 11{,}120 \text{ cal/mole}$$

$$\Delta F^\circ = 17.500 + 36.85T \log T - 129.0T \qquad \text{(A-16)}$$

A transpiration method (using purified helium) gave the following results:

$$\log P = -\frac{3788}{T} + 9.52 \qquad \text{(A-17)}$$

$$\Delta H_{sublimation} = -17{,}300 \text{ cal/mole}$$

4) Thermochemical data. The heat of formation of UCl_6 has been determined to be:

$$\Delta H^\circ_{273°K} = -272.3 \pm 0.7 \text{ kcal/mole}$$

The free energy of formation is

$$\Delta F^\circ_{298°K} = -241.4 \pm 1.0 \text{ kcal/mole}$$

3. Chemical Properties.

(a) Uranium tetrachloride.

1) Reaction with water. UCl_4 is very hygroscopic and will react when the partial pressure of water vapor exceeds 2mm Hg. It first forms hydrates but reacts further to form $UOCl_2$ and hydrogen chloride until completely decomposed. Brown University observers found, however, that very little hydrogen chloride is produced before enough water is absorbed to form $UCl_4 \cdot 2H_2O$.

2) Non-aqueous solvents. UCl_4 is generally soluble in strongly polar solvents and insoluble in non-polar solvents. It is soluble in some oxygen-bearing organic solvents.

3) Complex compounds of UCl_4. UCl_4 forms double salts of the form M_2UCl_6, where M may be Li, Na, K or R_4N. UCl_4 vapors react with KCl at red heat to form K_2UCl_6. This compound is a dark green crystalline material, somewhat hygroscopic in air which melts at 350°C.

(b) Uranium pentachloride.

1) Effect of solvents. UCl_5 is highly hygroscopic and is sensitive to moisture with a partial pressure of 0.007 mm Hg or more. Liquid water decomposes it instantaneously:

$$2\ UCl_5 + 2H_2O \longrightarrow UCl_4 + UO_2Cl_2 + 4\ HCl$$

2) Oxidation reactions. UCl_5 reacts with oxygen to give a mixture of uranium oxychlorides. At elevated temperatures, it is partly converted to UCl_6 by chlorine. The reaction $2\ UCl_5 + Cl_2 \rightleftharpoons 2\ UCl_6$ is reversible, but the addition of CCl_4 vapors can produce practically complete conversion to the hexachloride.

3) Disproportionation and thermal decomposition. When UCl_5 is heated it decomposes as follows:

$$2\ UCl_5 \longrightarrow 2\ UCl_4 + Cl_2$$

Some decomposition occurs below 100°C, but at 250°C it becomes rapid. The rate is about the same in atmospheres of chlorine and pure nitrogen. This indicates that the reaction is not very reversible.

The kinetics of the thermal decomposition of UCl_5 have been investigated. The reaction appears to be first order with respect to UCl_5 and the reaction rate constant in the order of 10^{-3} min^{-1} for the

temperature range 100-152°C. The activation energy was computed to be about 28 kcal/mole.

UCl_5 also undergoes the disproportionation:

$2UCl_5 \longrightarrow UCl_4 + UCl_6$ at 100 to 175°C in a high vacuum.

(c) Uranium hexachloride. UCl_6 is extremely unstable in the presence of moist air and reacts violently with water to form UO_2Cl_2.

1) Solubility. UCl_6 dissolves in carbon tetrachloride to give a stable brown solution. It appears to react with tetrachloroethylene and naphthenic hydrocarbons, and is slightly soluble in the fluorocarbon C_7F_{16} and in isobutyl bromide.

2) Thermal decomposition. UCl_6 is probably stable up to temperatures of 120 to 150°C. The rate of decomposition in the vapor phase is negligible compared to that in the solid phase. In the range 130-180°C, the reaction rate constant of $2UCl_6(g) \longrightarrow 2\ UCl_5(s) + Cl_2(g)$ is between 10^{-3} and 10^{-1} min^{-1}. An energy of activation equivalent to 40 kcal/mole is needed.

C. CHEMICAL REACTIONS AND EQUILIBRIA OF ANALYTICAL METHODS[46]

1. Cl_2 analysis.

The Cl_2 gas absorbed in the NaOH-KI solution displaces the I^- ion and releases iodine (I_2) into the solution. The solution is then slightly acidified with HCl and titrated with sodium thiosulfate. The reaction of thiosulfate ion with iodine in slightly acid or neutral solutions is given by the equation,

$$2S_2O_3^{=} + I_2 \longrightarrow S_4O_6^{=} + 2I^-$$

This reaction is essentially complete at the stoichiometric point. In basic solutions the oxidation may proceed further according to the reaction,

$$S_2O_3^{=} + 4I_2 + 5H_2O \longrightarrow 2SO_4^{=} + 8I^- + 10H^+$$

This reaction is not quantitative, since the one above may also occur. The titration of iodine by thiosulfate must therefore be made in slightly acid or neutral solutions.

2. CO_2 determination.

The analysis of CO_2 simply involves the precipitation of $BaCO_3$ and the neutralization of excess $Ba(OH)_2$ with standard HCl, according to the equations,

$$Ba(OH)_2 + CO_2 \longrightarrow BaCO_3 + H_2O$$

$$\text{xs } Ba(OH)_2 + 2HCl \longrightarrow BaCl_2 + H_2O$$

3. Uranium analysis.

The U^{+4} ion is oxidized by $FeCl_3$ according to the equation,

$$U^{+4} + 2Fe^{+3} \longrightarrow U^{+6} + 2Fe^{++}$$

The Fe^{++} ion is then oxidized by the $Cr_2O_7^{=}$ ion during the titration in an acidic medium,

$$6Fe^{++} + Cr_2O_7^{=} + 14H^{+} \text{———} 6Fe^{+3} + 2Cr^{+3} + 7H_2O$$

REFERENCES

1. J. H. Arnold, J. Am. Chem. Soc. 52, 3937 (1930).

2. J. Berkowitz, Memorandum, BNL (March, 1952).

3. J. D. Bernal, Nature 183, 141 (1959).

4. J. D. Bernal, Nature 185, 68 (1960).

5. J. D. Bernal and J. Mason, Nature 188, 910 (1960).

6. L. L. Bircumshaw and A. C. Riddiford, Quart. Rev. Chem. Soc. (London), 6, 157 (1952).

7. M. Blander, W. R. Grimes, N. V. Smith, and G. M. Watson, J. Phys. Chem., 63, 1164 (1952).

8. H. Bloom, Disc. Farad. Soc., 32, 53 (1961).

9. J. O'M. Bockris and C. Richards, Proc. Roy. Soc., A 241, 44 (1957).

10. J. Bockris, R. Crook, H. Bloom and C. Richards, Proc. Roy. Soc. A 255, 558 (1960).

11. C. F. Bonilla, Columbia Univ. Progress Report, Sept. 1, 1953 (NYO-3094).

12. W. J. Burkhard and J. D. Corbett, J. Am. Chem. Soc., 79, 6361 (1957).

13. H. S. Carslaw and J. C. Jaeger, Heat Conduction in Solids, Clarendon, Oxford (1947).

14. G. I. Cathers, "Fluoride Volatility Processes for High Alloy Fuels", Symposium on the Reprocessing of Irradiated Fuels, Brussels (1957), Book 2, pp. 560-573 (TID-7534).

15. P. V. Danckwerts, Trans. Farad. Soc., 46, 300 (1950).

16. P. V. Danckwerts and A. M. Kennedy, Trans. Instn. Chem. Engrs. (London), 32, 549 (1954).

17. H. W. Deem, Batelle Memorial Institute, Private Communication to O. E. Dweyer, Dec. 10, 1953.

18. W. D. Douglas and J. L. Dever, NBS Report 2303 (Feb. 20, 1953).

19. A. S. Dworkin, F. J. Miller, D. J. Sasmor, I. S. Yaffe and E. R. Van Artsdalen, ORNL-1674, 21.

20. R. L. Emmert and R. L. Pigford, Chem. Eng. Prog., 50, 87 (1954).

21. H. Eyring, S. Glasstone and K. J. Laidler, The Theory of Rate Processes, McGraw-Hill, N.Y., (1941).

22. H. Eyring F. H. Ree and T. Ree, Ind. Eng. Chem., 50, 1036 (1958).

23. J. Frenkel, Kinetic Theory of Liquids, Oxford (1946).

24. K. Furukawa, Disc. Farad. Soc., 32, 53 (1961).

25. T. A. Gens, "Chloride Volatility Processing of Nuclear Fuels", Symposium on Volatility Reprocessing of Nuclear Reactor Fuels: Part II, New York, N.Y. (2-7 December, 1961).

26. S. Goren, Univ. of Calif., Private Communication to D. R. Olander, Oct. 13, 1964.

27. W. R. Grimes, N. V. Smith and G. M. Watson, J. Phys. Chem., 62, 862 (1958).

28. W. R. Grimes, J. H. Shaffer and G. M. Watson, J. Phys. Chem., 63, 1999 (1959).

29. W. R. Grimes, J. H. Shaffer, A. I. Ch. E. Symposium, 55, No. 27, pp. 65-71 (1959).

30. T. Hatta, Tohoku Imp. Univ. Tech. Report, 8, 1 (1928-29).

31. R. Higbie, Trans. A.I. Ch. E., 31, 365 (1935).

32. J. Hildebrand, Disc. Farad. Soc., 15, 9 (1953).

33. J. J. Katz and E. Rabinowitch, The Chemistry of Uranium, Part I, McGraw-Hill, N.Y. (1951).

34. E. Kordes, Z. Elektrochem., 59, 551 (1955).

35. R. W. Laity, J. Chem. Phys., 30, 682 (1959).

36. G. J. Landon and A. R. Ubbelohde, Trans. Farad. Soc., 52, 647 (1956).

37. J. Li and Pin Chang, J. Chem. Phys., 23, 518 (1955).

38. J. Lumsden, Disc. Farad. Soc., 32, 138 (1961).

39. B. F. Markov and I. U. K. Delimarskyi, Electrochemistry of Fused Salts, Sigma Press Publ. (1961).

40. J. E. Mayer, J. Chem. Phys., 1, 270 (1933).

41. E. A. Moelwyn-Hughes, Physical Chemistry, Pergamon, London (1957).

42. R. F. Newton, ORNL unpublished work (1954).

43. R. A. T. O. Nijsing, R. H. Hendriksz and H. Kramers, Chem. Eng. Sci., 10, 88 (1959).

44. D. R. Olander, A. I. Ch. E. Journal, 9, 207 (1963).

45. D. F. Othmer and N. S. Thaker, Ind. Eng. Chem., 45, 589 (1953).

46. W. C. Pierce and E. L. Haenisch, Quantitative Analysis, 3rd ed., Wiley & Sons, New York (1948).

47. W. D. Powers and G. C. Blalock, ORNL-CF-53-8-30 (Aug. 5, 1953).

48. C. J. Raseman, H. Susskind, G. Farber, W. E. McNulty and F. J. Salzano, BNL 627 (T-192), June 1960.

49. B. C. Sakiadis, A. I. Ch. E. Journal, 7, 26 (1961).

50. B. C. Sakiadis, A. I. Ch. E. Journal, 7, 467 (1961).

51. E. G. Scheibel, Ind. Eng. Chem., 46, 2007 (1954).

52. H. Schlichting, Boundary-Layer Theory, McGraw-Hill, N.Y. (1955).

53. N. S. Shaikhmahmud and C. S. Bonilla, Columbia Univ., NYO-3093, June 1, 1953.

54. T. K. Sherwood and R. L. Pigford, Absorption and Extraction, 2nd Ed., McGraw-Hill, N.Y. (1952).

55. Ph. Spéeckaert, "Reprocessing of Irradiated Uranium and Uranium Compounds by Fractional Sublimation of Their Chlorides", Symposium on Volatility Reprocessing of Nuclear Reactor Fuels: Part II, New York, N.Y. (2-7 December, 1961).

56. W. E. Stewart, R. B. Bird and E. N. Lightfoot, Notes on Transport Phenomena, Wiley & Sons, New York (1958).

57. B. R. Sundheim, "Fused Salts", McGraw-Hill, N.Y. pp. 231 (1964).

58. H. Susskind, F. E. Hill, L. Green, S. Kalish, L. E. Furacka, W. E. McNulty, and E. Wirsing, Jr., BNL 585 (T-164), June 1960.

59. C. E. Thalmayer, S. Bruckenstein and D. M. Gruen, J. Inorg. Nucl. Chem., 26, 347 (1964).

60. A. R. Ubbelohde, Proc. Chem. Soc., 332 (1930).

61. A. F. Voigt, A. H. Danne, E. H. Dewell, R. G. Clark, J. E. Gonser, J. F. Haefling, K. L. Malaby, A. I. Ch. E. Journal, 2, 169 (1956).

62. J. Weisman, Memorandum, BNL, April 17, 1953.

63. C. R. Wilke, Chem. Eng. Prog., 45, 218 (1949).

64. C. R. Wilke and Pin Chang, A. I. Ch. E. Journal, 1, 264 (1955).

65. J. Zimmerman, J. Phys. Chem., 53, 562 (1949).

FIGURE CAPTIONS

Figure 1 Diffusion in molten salts.

Figure 2 Boundary layer behavior on a moving continuous cylindrical surface.

Figure 3 Dimensionless boundary layer thickness.

Figure 4 Velocity profile on cylindrical surface.

Figure 5 Diffusion boundary layer-growth constant.

Figure 6 Film flow down a rod.

Figure 7 Velocity profile in the liquid phase.

Figure 8 Solution of diffusion equation for film flow.

Figure 9 Function F for slow chemical reaction.

Figure 10 Function F for fast chemical reaction.

Figure 11 Solubility apparatus.

Figure 12 Melt tank.

Figure 13 CO_2 absorption set-up.

Figure 14 CO_2 absorber.

Figure 15 Absorption of CO_2 in a water film.

Figure 16 Schematic diagram of kinetic set-up.

Figure 17 Side view of kinetic apparatus.

Figure 18 Front view of kinetic apparatus.

Figure 19 Reaction column.

Figure 20 Chemical analysis of uranium.

Figure 21 Temperature distribution in the reaction chamber.

Figure 22 Equilibrium data.

Figure 23 Kinetic data at 400°C.

Figure 24 Kinetic data at 450°C.

Figure 25 Kinetic data at 500°C.

Figure 26 Kinetic data at 550°C.

Figure 27 Kinetic data at 600°C.

Figure 28 Kinetic data at 650°C.

Figure 29 Kinetic data at 700°C.

Figure 30 Effect of chlorine partial pressure.

Figure 31 Comparison of experimental and theoretical slopes.

Figure 32 Kinematic viscosity of LiCl-KCl eutectic.

Figure 33 Free energy of formation of uranium chlorides.

This report was prepared as an account of Government sponsored work. Neither the United States, nor the Commission, nor any person acting on behalf of the Commission:

A. Makes any warranty or representation, expressed or implied, with respect to the accuracy, completeness, or usefulness of the information contained in this report, or that the use of any information, apparatus, method, or process disclosed in this report may not infringe privately owned rights; or

B. Assumes any liabilities with respect to the use of, or for damages resulting from the use of any information, apparatus, method, or process disclosed in this report.

As used in the above, "person acting on behalf of the Commission" includes any employee or contractor of the Commission, or employee of such contractor, to the extent that such employee or contractor of the Commission, or employee of such contractor prepares, disseminates, or provides access to, any information pursuant to his employment or contract with the Commission, or his employment with such contractor.